

**THE *C. elegans* ROR RECEPTOR TYROSINE KINASE,
CAM-1, REGULATES WNT SIGNALING BY TWO
DISTINCT MECHANISMS**

Thesis by

Jennifer Leigh Green

In Partial Fulfillment of the Requirements for the

degree of

Doctor of Philosophy



CALIFORNIA INSTITUTE OF TECHNOLOGY

Pasadena, California

2008

(Defended May 14, 2008)

© 2008

Jennifer Leigh Green

All Rights Reserved

Acknowledgments

During our first meeting, I told my future advisor, Paul Sternberg, that I had no desire to work on worms for my graduate career. Since that day, I developed a great appreciation for *C. elegans*, and for Paul, who have both been amazing to work with. Paul's support and encouragement have never wavered; even when things seemed bleak, he was there cheering me on. Thank you Paul for giving me the freedom to pursue ROR signaling; this project has been consuming, challenging, frustrating and ultimately fulfilling; and I have loved every minute of it. I am extremely fortunate to have had Paul Sternberg as my thesis advisor. I only hope that through his training and example I can emulate his approach to science, and life.

I owe many thanks to my thesis committee; Marianne Bronner-Fraser, Ray Deshaies and Bruce Hay, who not only offered helpful advice during my committee meetings, but who also had their doors open anytime I came looking for help. Your input and perspective was invaluable.

Thank you to all members of the Sternberg lab, past and present. Paul has amassed a collection of outstanding scientists and I have really enjoyed working with each of you. In particular, I want to thank the girls in room 217. Adeline, Cheryl and Mihoko – thank you for making it a pleasure to come to work every day. Each of you is a dear friend and I treasure getting to know you so well. Another individual in the Sternberg lab who deserves a special mention is Takao Inoue, a brilliant geneticist who patiently taught me several techniques. Takao, it was wonderful to work with you and I'm proud to share authorship with you on two publications.

Thank you to Cindy Wilson, Frank Calzone and Judy Dering for bringing ROR to my attention while I was at UCLA. Cindy, your early mentorship and continued support have been instrumental to my success and I am forever indebted to you. I cherish your friendship as well.

Thank you to Martin Ikkanda, my Biology professor at Pierce College, who instilled in me a love for the subject.

Thank you to Amanda Vincent, my dear friend of fifteen years and to my newer friends from Caltech, especially Ashley, Josh, Cheryl, Dave, Adeline, Mihoko, Eric, Fernanda, Jim and Teresa.

I would like to acknowledge my parents, Rudy and Sue Sanders, and my brother Russell Sanders for always loving me and being proud of me. Mom and Dad, thank you for consistently encouraging me and for making me believe that I can do anything. Even though it took me a little longer to find my calling, you stood behind me every step of the way. You have always been there to share my burden when life is hard, and to share my joy when it's not. I love you dearly.

Last, but not least, thank you to my husband, Jonathan Green. Despite the long hours and hard work, these have been the best years of my life, thanks to you. I am grateful for your steadfast love, friendship and support. Graduate school was the first chapter in our lives together. As I prepare to close the book, I am overjoyed that I will write the remaining chapters by your side.

Abstract of the thesis

The ROR (receptor orphan) family of receptor tyrosine kinase, which is required for human skeletal development and has been implicated in human cancer, is one of the few classes of RTK whose activity remains elusive.

Although the mechanism is unknown, there is evidence that ROR proteins inhibit signaling by Wnts, a conserved class of secreted glycoproteins. We have studied how ROR proteins interact with Wnt signaling during *C. elegans* vulval development, a classic model used to study cell-signaling pathways. Wnt/ β -catenin signaling controls cell-fate decisions of the vulval precursor cells (VPCs). We found that loss and over-expression of the *C. elegans* ROR homolog, *cam-1*, caused reciprocal defects in Wnt-mediated cell-fate specification. Our molecular and genetic analysis revealed that during vulval induction the CAM-1 extracellular domain (ECD) is sufficient to non-autonomously antagonize multiple Wnts, implying that the CAM-1 ECD sequesters Wnts. Our finding that the CAM-1 ECD specifically binds Wnts *in vitro* supports a sequestration model. Thus, CAM-1/ROR regulates Wnt signaling by modifying the spatial profile of Wnt activity.

In addition to regulating cell-fate specification, Wnt signaling also determines VPC polarity. The mirror symmetry of the *C. elegans* vulva is achieved by the opposite division orientation of the VPCs flanking the axis of symmetry. We characterized the molecular mechanisms by which opposing Wnts establish this division pattern and how CAM-1 contributes to VPC orientation. Wnts MOM-2 and LIN-44 are expressed at the axis of symmetry and orient the VPCs towards the center. We show that these Wnts, via Fz/LIN-17 and Ryk/LIN-18, control β -catenin localization and activate gene transcription. In

addition, we found that VPCs on both sides of the axis of symmetry possess a uniform underlying “ground” polarity, established by the instructive activity of Wnt/EGL-20. EGL-20 establishes ground polarity via a novel type of signaling involving CAM-1 and the Planar Cell Polarity component Van Gogh/VANG-1. CAM-1 activity during ground polarity signaling requires the CAM-1 intracellular domain and is thus likely to be a cell-autonomous function. Therefore, CAM-1 interacts with Wnts by two distinct mechanisms: it sequesters Wnts and it transmits directional information from Wnts to individual cells.

Table of contents

Acknowledgements.....	iii
Abstract.....	v
Table of contents.....	vii

Chapter 1: Introduction..... I

Thesis Overview	I-2
References	I-3
Function and signaling of ROR receptor tyrosine kinases	I-5
What is ROR?.....	I-5
Human Phenotypes.....	I-6
ROR in skeletal development.....	I-7
ROR in neuronal development.....	I-9
ROR Signaling I — a Wnt receptor.....	I-11
ROR Signaling II — other interactions.....	I-18
Summary	I-20
References	I-23
Figures.....	I-28

Chapter 2: The *C. elegans* ROR RTK, CAM-1, non-autonomously inhibits the Wnt pathway..... II

Abstract	II-2
Introduction	II-3
Results.....	II-6

CAM-1 negatively regulates vulval induction.....	II-6
Analysis of CAM-1 domains and site-of-action.....	II-7
<i>cam-1</i> interacts with genes required for vulval induction	II-8
CAM-1 antagonizes Wnts.....	II-10
The CAM-1 ECD binds to Wnts CWN-1, EGL-20 and MOM-2.....	II-12
Overexpression of CAM-1 non-autonomously inhibits vulval induction.....	II-13
Discussion	II-15
Acknowledgements.....	II-19
Materials and Methods	II-20
References	II-26
Tables.....	II-30
Figures.....	II-35
Chapter 3: Opposing Wnt signals orient cell polarity during organogenesis.....	III
Abstract	III-2
Introduction	III-3
Results.....	III-6
<i>Wnt/egl-20</i> antagonizes <i>Fz/lin-17</i> and <i>Ryk/lin-18</i> in P7.p	III-6
Wnt/EGL-20 is required for the posterior-facing (ground) orientation of P5.p and P7.p.....	III-7
Default orientation in the absence of Wnts	III-7
The anchor cell is an important Wnt source during VPC orientation.....	III-8

EGL-20 acts instructively	III-9
Wnt/ β -catenin asymmetry pathway components.....	III-10
β -catenin function during VPC orientation	III-12
Fz/LIN-17 and Ryk/LIN-18 regulate POPTOP expression in the VPC progeny	III-14
Van Gogh/VANG-1 functions in ground polarity	III-15
ROR/CAM-1 functions in ground polarity	III-16
Discussion	III-19
Acknowledgements.....	III-24
Materials and Methods	III-25
Supplemental Material	III-27
References	III-34
Tables.....	III-38
Figures.....	III-43
 Chapter 4: Concluding remarks.....	 IV
References	IV-5

CHAPTER 1

Introduction

Thesis Overview

Like any architectural project, building tissues and organs depends on the organized arrangement of component parts. Organization of cells into functional structures is achieved by the coordination of cellular processes such as division and orientation. This organization requires communication between a cell and its neighbors, which often takes the form of intracellular signaling pathways. These molecular relays are initiated when an extracellular molecule, called a ligand, binds to a receptor protein in the plasma membrane. Ligand binding triggers a biochemical response inside the cell, which is interpreted as instructions about whether the cell should divide or which way it should face. There are numerous types of ligands, receptors and signaling mechanisms operating within a cell continuously and what were once considered linear signal transduction pathways are now thought to be vast and integrated networks. Many opportunities exist for signals to get misrouted, which can have dire consequences, such as cancer.

The Ras/MAPK pathway and the Wnt pathway are two intracellular signaling pathways that are known to cause cancer when inappropriately activated (Weinberg, 2006). The Ras/MAPK signaling pathway is initiated when a growth factor (i.e., EGF) binds to a receptor tyrosine kinase (RTK) (i.e., EGFR). The Wnt signaling pathway is initiated when a Wnt ligand binds to a receptor called Frizzled. ROR (receptor orphan), the focus of my thesis, is an RTK that has an extracellular Wnt-binding domain. I was intrigued by ROR because it appeared to bridge the Ras and Wnt pathways, suggesting its potential importance in cancer, and also because it was one of the few RTKs whose ligand and signaling pathway were unknown. The ROR receptor family is conserved in *C. elegans*, a powerful genetic

model organism. I investigated ROR function during *C. elegans* vulva development, which is a classic model used to study cell-signaling pathways.

To place my work in its context, my thesis begins with a review of what is currently known about ROR function, which is considerably more than what was known when I started in 2002. Chapter 2 is a study of ROR function as a regulator of Wnt distribution. Here, I showed that the extracellular domain of ROR proteins can sequester Wnt ligands. In this way, they non-autonomously inhibit Wnt signaling. Incidentally, this is more suggestive of a cancer-preventing agent than a cancer-causing one. Chapter 3 is a study of ROR function during cell polarity, where ROR appears to act autonomously via its intracellular domain. During my study of ROR function in cell polarity, I discovered that opposing Wnt signals orient the vulval precursor cells (VPCs). ROR is the receptor for one of these Wnt signals and acts in the same pathway as Van Gogh, a core component of the Planar Cell Polarity Pathway, which is known to regulate cell polarity in other organisms, but has not been demonstrated to function in *C. elegans*.

In summary, I illustrated two previously unknown and distinct signaling mechanisms used by ROR receptors to regulate cellular communication. Notably, these results coincided with two reports implicating ROR receptors in human cancer (Baskar et al., 2008; Fukuda et al., 2008).

Baskar, S., Kwong, K. Y., Hofer, T., Levy, J. M., Kennedy, M. G., Lee, E., Staudt, L. M., Wilson, W. H., Wiestner, A. and Rader, C. (2008). Unique Cell Surface Expression of Receptor Tyrosine Kinase ROR1 in Human B-Cell Chronic Lymphocytic Leukemia. *Clin Cancer Res* **14**, 396-404.

Fukuda, T., Chen, L., Endo, T., Tang, L., Lu, D., Castro, J. E., F. Widhopf G, n., Rassenti, L. Z., Cantwell, M. J., Prussak, C. E. et al. (2008). Antisera induced by infusions of autologous Ad-CD154-leukemia B cells identify ROR1 as an oncofetal antigen and receptor for Wnt5a. *Proc Natl Acad Sci U S A*.

Weinberg, R. A. (2006). *The Biology of Cancer*: Garland Science.

Function and signaling of ROR receptor tyrosine kinases

What is ROR?

ROR proteins are type I transmembrane receptor tyrosine kinases (Figure 1). The extracellular region of vertebrate RORs contains an immunoglobulin (Ig) domain, a cysteine-rich domain (CRD), and a Kringle (Kr) domain. Intracellularly, RORs possess a tyrosine kinase (TK) domain, a proline-rich domain and, two serine-threonine-rich (S/T) domains (Masiakowski and Carroll, 1992). Like other RTKs, they are predominantly located in the plasma membrane (Matsuda et al., 2001).

Vertebrates have two *ROR* family members: *ROR1* and *ROR2*. These genes were first identified in a human neuroblastoma cell line by a PCR-based search for tyrosine kinases similar to *Trk* neurotrophic receptors (Masiakowski and Carroll, 1992). Overall, ROR1 and ROR2 proteins share 58% amino acid identity. Despite several changes in consensus tyrosine kinase amino acids, mammalian ROR1 and ROR2 each have kinase activity *in vitro* (Masiakowski and Carroll, 1992; Oishi et al., 1999). Unlike other tyrosine kinase receptors, such as FGF receptors and Trks, RORs display higher similarity in the extracellular domain (ECD) than in the kinase domain, suggesting that the ECD may be the more critical end of the protein (discussed below). Also, RORs display unusually high similarity in the transmembrane domain, suggesting that this region is functionally important as well (Masiakowski and Carroll, 1992).

ROR orthologs have been identified in *Drosophila* (*Dror* and *Dnrk*) (Oishi et al., 1997; Wilson et al., 1993), *Caenorhabditis elegans* (*cam-1*) (Forrester et al., 1999; Koga et al., 1999), *Aplysia californica* (sea slug) (McKay et al., 2001), *Danio rerio* (zebrafish) (Kato and Kato, 2005), *Gallus gallus* (chicken) (Rodriguez-Niedenfuhr et al., 2004;

Stricker et al., 2006), *Xenopus laevis* (frog) (Hikasa et al., 2002), and *Mus musculus* (mouse) (Oishi et al., 1999). While the CRD, Kringle, and TK domains are characteristic of all ROR proteins, the architecture of the other domains varies between species (Figure 1).

Human phenotypes

The severe phenotypes caused by mutations in human *ROR2* (*hROR2*) illustrate the crucial function of ROR proteins during development and emphasize the need for their further study. *hROR2* mutations cause well-characterized skeletal defects: Brachydactyly type B (BDB) and recessive Robinow syndrome (RRS). Brachydactyly is a condition of shortened digits and BDB, the most severe type of brachydactyly, is an autosomal dominant disorder caused by heterozygous mutations in *hROR2* (Oldridge et al., 2000; Schwabe et al., 2000). The *hROR2* mutations that cause BDB are thought to result in gain-of-function or dominant-negative *hROR2* activity, a hypothesis supported by the observance of patients heterozygous for *hROR2* deletions that do not display BDB (Oldridge et al., 2000). *hROR2* mutations that cause BDB are restricted to truncation of the protein either just before or just after the intracellular kinase domain (Schwabe et al., 2000); however, the significance of these mutations on *hROR2* activity is unclear. Recessive Robinow syndrome (RRS) is a form of dwarfism associated with mesomelic limb shortening and abnormalities of the head, face, genitals and vertebrae (Robinow et al., 1969) that is caused by presumed loss-of-function mutations in *hROR2* (Afzal et al., 2000; van Bokhoven et al., 2000). In contrast to BDB, mutations causing RRS are found throughout the coding region of *hROR2*, with the exception of mutations that result in a protein with a truncated TK domain (Afzal et al., 2000; van Bokhoven et al., 2000). Instead, all *hROR2* missense mutations known to cause RRS result in

a misfolded protein that is retained in the endoplasmic reticulum (Ali et al., 2007; Chen et al., 2005).

There is an accumulating body of evidence that hROR2 plays a role in skeletal development. The chromosomal location of *hROR2*, 9q22, has been linked to human height (Liu et al., 2006) and recently, a pilot study found that *hROR2* polymorphisms are associated with human bone length and bone mineral density (Ermakov et al., 2007). These studies complement the well-characterized skeletal defects of *hROR2*-associated diseases.

While mutations in *hROR1* have not been linked to any human disease, *hROR1* was recently discovered to be over-expressed in chronic lymphocytic leukemia (CLL). Using gene expression profiling to identify surface antigens unique to B-CLL cells, Baskar et al. found that *hROR1* was highly expressed in malignant cells compared to normal cells (Baskar et al., 2008). Localization of ROR1 on the cell surface and lack of expression in normal adult tissues makes it an attractive candidate for monoclonal antibody therapy. Fukuda et al., who simultaneously identified ROR1 as an oncofetal antigen (an antigen that is normally expressed in the fetus whose expression resurfaces in adults with cancer) present on CLL cells, found that ROR1 enables Wnt5a to confer a survival advantage to CLL cells *in vitro* (Fukuda et al., 2008). Consistent with a role of hROR1 in the pathology of cancer, ROR1 was also identified as a potent survival kinase in an RNAi screen for kinases that prevent apoptosis of HeLa cervical carcinoma cells (MacKeigan et al., 2005).

ROR in skeletal development

During murine development, *ROR* genes are expressed in the skeletal, cardiac, nervous, digestive, urogenital, and pulmonary systems, as well as the limbs and face

(DeChiara et al., 2000; Nomi et al., 2001; Oishi et al., 1999; Oldridge et al., 2000; Schwabe et al., 2004; Takeuchi et al., 2000). *mROR1* and *mROR2* expression patterns mostly overlap, with *mROR2* being more broadly expressed (Al-Shawi et al., 2001; Matsuda et al., 2001).

Several mouse *ROR* mutations have been isolated and phenotypically analyzed. These include deletions of the first exon of *mROR1* (Nomi et al., 2001) and *mROR2* (Schwabe et al., 2004; Takeuchi et al., 2000), which are predicted to eliminate expression, and an insertion into *mROR2* that disrupts the TK domain (DeChiara et al., 2000). Homozygous disruption of either *mROR1* or *mROR2* causes postnatal/perinatal lethality (DeChiara et al., 2000; Nomi et al., 2001; Takeuchi et al., 2000). *mROR2* is required for development of the cartilage and skeletal systems and *mROR2* mutant mice exhibit dwarfism, shortened limbs, brachydactyly, malformed facial structures and other abnormalities reminiscent of RRS (DeChiara et al., 2000; Schwabe et al., 2004; Takeuchi et al., 2000). An allele engineered to resemble a human BDB-causing mutation, *mROR2*^{W749X}, caused recessive defects in skeletal development and joint patterning, but did not cause the dominant effects expected from human phenotypes (Raz et al., 2008). As in humans, *mROR1* mutations do not appear to cause skeletal phenotypes; however, disruption of *mROR1* enhances the skeletal abnormalities of *mROR2* mutant mice, suggesting a partially redundant function (Nomi et al., 2001).

During chick development, *ROR* genes are expressed in the developing face, eyes, lungs, cartilage, limbs, digestive system, and strongly in the nervous system and muscle (Rodriguez-Niedenfuhr et al., 2004; Stricker et al., 2006). Like mice, *cROR1* displays a more restricted expression pattern than *cROR2*. Over-expression of truncated forms of *cROR2* that correspond to human BDB-causing mutations delayed chondrocyte differentiation in

proximal limb elements (Stricker et al., 2006). This phenotype mimics *mROR2* mutant mice, which display mesomelic limb shortening due to defective chondrocyte differentiation (Schwabe et al., 2004). Thus, alleles causing BDB are likely to act in a dominant-negative manner rather than as gain-of-function. Because the phenotype caused by overexpression of truncated *cROR2* is stronger than the phenotype caused by *cROR2* mutation, Stricker et al. (2006) proposed that the dominant-negative activity of *cROR2* also affects *cROR1*. This hypothesis is consistent with observations that mutation of both *mROR1* and *mROR2* causes a phenotype more severe than mutation of *mROR2* alone (Nomi et al., 2001).

ROR2 regulation of skeletogenesis is supported by *in vitro* studies of osteoblast differentiation. *hROR2* mRNA, not detectable in pluripotent stem cells, is dramatically upregulated as the cells differentiate into preosteoblasts (Billiard et al., 2005). Similarly, in human mesenchymal stem cells (hMSCs), ROR2 can initiate commitment to osteoblastic lineages (Liu et al., 2007a). Over-expression of *hROR2* in hMSCs induces expression of osteogenic transcription factors (osterix) and causes formation of mineralized extracellular matrix. Conversely, *hROR2* knockdown by shRNA prevents mineralization induced by an osteogenic agent (Liu et al., 2007a). These *in vitro* studies are complemented by *ex vivo* organ culture experiments where ROR2 over-expression causes increased bone formation (Liu et al., 2007a).

ROR in neuronal development

Although the largely non-overlapping expression patterns of *mROR1* and *mROR2* in the developing mouse nervous system makes redundancy unlikely, *mROR2* knockout mice do not display obvious neurological defects (Al-Shawi et al., 2001; Oishi et al., 1999).

However, it is possible that a subtle phenotype is masked by the early lethality of these mice. Suggestive of ROR function in neuronal development, *ROR* expression has also been observed in the developing nervous systems of chick (Stricker et al., 2006), *Xenopus* (Hikasa et al., 2002), *Aplysia* (McKay et al., 2001), *C. elegans* (Forrester et al., 1999; Koga et al., 1999), and *Drosophila*. While the *Drosophila* homologs, *Dror* and *Dnrk*, are expressed exclusively in the developing nervous system (Oishi et al., 1997; Wilson et al., 1993), their mutant phenotypes have not been described.

Expression of *ROR* in neurons agrees with a role of ROR proteins in neuronal development. In cultured murine hippocampal neurons, *mROR1* and *mROR2* expression is concentrated in growth cones of immature neurons and in the somatodendritic domain of mature neurons (Paganoni and Ferreira, 2003). Additionally, knockdown of *mROR1* and *mROR2* in these cells inhibits neurite elongation and branching (Paganoni and Ferreira, 2005).

Much of what is known about the function of ROR proteins in the nervous system comes from studies of the sole *C. elegans* *ROR* family member, *cam-1*, which was isolated in two separate screens: a genetic screen for canal-associated neuron (CAN) migration defects (Forrester and Garriga, 1997) and by a hybridization screen for tyrosine kinases (Koga et al., 1999). CAM-1, equally similar to ROR1 and ROR2, regulates the migration of several neurons along the anterior-posterior axis (see *ROR signaling I*, below) and also functions in axon outgrowth and guidance (Forrester, 2002; Forrester et al., 1999). CAM-1 additionally regulates the asymmetric division of some *C. elegans* neurons (Forrester et al., 1999). Unlike mouse *ROR* mutants, *C. elegans cam-1* mutants are viable and have locomotion defects, a phenotype that often reflects a defect in synaptic transmission (Forrester et al., 1999; Francis

et al., 2005). These studies suggest that the functions of ROR proteins in axon outgrowth and synaptic development are conserved between *C. elegans* and vertebrates. Interestingly, *cam-1* is the closest *C. elegans* homolog of both *ROR* and the gene encoding Muscle-Specific Kinase, *MuSK*. MuSK is a member of the Trk superfamily of RTKs and, similar to ROR, contains extracellular cysteine-rich, and Ig domains. Furthermore, in some species – *Xenopus*, chick, Torpedo (ray) — MuSK also contains a Kringle domain (Fu et al., 2001). Like MuSK, which is involved in organizing the neuromuscular junction (NMJ) and stimulates clustering of acetylcholine receptors (DeChiara et al., 1996; Lin et al., 2001), CAM-1 also organizes the NMJ and regulates the distribution of acetylcholine receptors (Francis et al., 2005). Therefore, *cam-1* might fulfill the role of both genes, *ROR* and *MuSK*, in *C. elegans*.

ROR signaling I — a Wnt Receptor

The extracellular cysteine-rich domain (CRD) of ROR is similar to the Wnt-binding domain found in Frizzled receptors (Roszmusz et al., 2001; Saldanha et al., 1998; Xu and Nusse, 1998), suggesting that ROR also binds to Wnt ligands. This was later shown (see below). Wnts are a family of secreted glycoproteins that play critical roles in development and disease (reviewed by Clevers, 2006; Logan and Nusse, 2004). Wnt signals are transduced by a variety of mechanisms, which are separated into two categories based on the involvement of beta-catenin. Wnt/beta-catenin signaling, or canonical Wnt signaling, is initiated when Wnt binds to a Frizzled (Fz) receptor and the Lrp5/6 co-receptor. This signaling prevents beta-catenin degradation, allowing beta-catenin to accumulate, translocate to the nucleus, and act as a transcriptional co-activator with TCF, a DNA-binding protein.

Wnt pathways that are independent of beta-catenin, non-canonical Wnt pathways, include diverse mechanisms such as Wnt/calcium signaling, Wnt/JNK signaling and Planar Cell Polarity (PCP) (reviewed by Veeman et al., 2003). The degree to which these beta-catenin-independent pathways overlap is presently unclear.

Several studies in various systems report diverse, and sometimes conflicting, interactions of ROR with Wnt signaling. It is likely that the discrepancies reflect the diversity of systems tested and ROR proteins in fact haveing multiple functions depending on the cellular context (the co-existence of other Wnt pathway components operating in a given cell). We have attempted to cluster compatible descriptions into a handful of signaling mechanisms (Figure 2).

A series of studies, led by Wayne Forrester, demonstrated that *cam-1*, the *C. elegans* ROR ortholog, inhibits the function of a *C. elegans* Wnt, EGL-20. In one of the first publications on a ROR gene, Forrester et al. showed that *cam-1* mutations cause defects in the migration of several cells along the anterior-posterior axis (Forrester et al., 1999). This migration phenotype was later determined to be reciprocal to the phenotype caused by loss of the Wnt *egl-20*. Further investigation revealed that CAM-1 over-expression mimics the *egl-20* mutant phenotype and that EGL-20 over-expression mimics the *cam-1* mutant phenotype. Thus, CAM-1 and Wnt/EGL-20 appeared to have an antagonistic relationship (Forrester et al., 2004). Experiments using engineered *cam-1* deletions showed the membrane-anchored CAM-1 CRD was sufficient to rescue cell migration, leading to the proposal that CAM-1 might function to regulate the spatial distribution of Wnt/EGL-20 (Figure 2A) (Kim and Forrester, 2003). The hypothesis that CAM-1 can sequester Wnt proteins was recently confirmed in our study of CAM-1 function in *C. elegans* vulva development. We found that

cam-1 mutations result in elevated Wnt pathway activity in the vulval precursor cells (VPCs) and that CAM-1 over-expression between the source of Wnt expression and the VPCs acts as a barrier and reduces Wnt pathway activity in the VPCs (Green et al., 2007). Additionally, we showed that the CAM-1 CRD is sufficient to bind Wnts and to non-autonomously inhibit their activity. The function of ROR in other systems is also consistent with Wnt sequestration. For example, in U20S human osteosarcoma cells, ROR2 binds Wnt1 and Wnt3 and antagonizes Wnt1 and Wnt3-mediated stabilization of cytosolic beta-catenin by a mechanism that does not require the ROR2 kinase domain (Billiard et al., 2005).

There also exist examples where the influence of ROR proteins on Wnt signaling cannot be explained by simple sequestration of Wnts, indicating that ROR function includes additional mechanisms. Studies of *Xenopus* convergent extension (CE), which were the first to show that ROR binds Wnts (Hikasa et al., 2002), indicate that ROR2 transmits a Wnt5a signal via JNK (Schambony and Wedlich, 2007). *XWnt5a* and *XROR2* regulate constriction by activating a JNK pathway, which upregulates expression of paraxial protocadherin, *XPAPC* (Figure 2B). By measuring constriction in Keller explants, Schambony and Wedlich showed that knockdown of *XWnt5a*, *XROR2* or *XJNK* phenocopies the constriction defect caused by *XPAPC* loss-of-function. Conversely, *XWnt5a* over-expression upregulates *XPAPC* expression and this activity requires the *XROR2* kinase domain. Activated *XJNK* similarly upregulates *XPAPC* expression and *XJNK* activity is stimulated by *XWnt5a* over-expression and is reduced by *XWnt5a* depletion. This report suggests that Wnt5a/ROR2/JNK constitutes a distinct functional pathway *in vivo*.

These *Xenopus* studies revealed that *XROR2* and *XWnt5a* physically interact and have a common effect on convergent extension (Hikasa et al., 2002; Moon et al., 1993;

Schambony and Wedlich, 2007). Additional evidence linking ROR and Wnt5a comes from studies in mice, where the *mWnt5a* expression pattern is highly similar to that of *mROR2* and includes expression in the developing face, limbs, lungs and genitals (Li et al., 2002; Yamaguchi et al., 1999). The gross morphological phenotypes of *mROR2* and *mWnt5a* mutants are also similar; both display dwarfism, facial abnormalities and shortened limbs (Takeuchi et al., 2000; Yamaguchi et al., 1999). For these reasons, Oishi et al. investigated whether there existed a functional relationship between the two genes (Oishi et al., 2003). They found that mROR2 physically interacts with Wnt5a, but not Wnt3a *in vitro*, and that mROR2 and Wnt5a synergistically activate JNK, supporting the existence of a Wnt5a/ROR2/JNK pathway (Figure 2B).

Wnt5a/ROR2 interactions where JNK involvement has not been demonstrated also exist. Wnt5a, a non-canonical Wnt, acts via ROR2 to inhibit canonical signaling by Wnt3a (Figure 2C). Wnt/beta-catenin pathway activity is commonly measured by a reporter called TOPFLASH (or Super-TOPFLASH, STF), that has multiple TCF binding sites driving expression of luciferase (Molenaar et al., 1996; van de Wetering et al., 1997). In human 293 cells, Wnt5a inhibits Wnt3a-induced STF expression, not by influencing beta-catenin levels, but by down-regulating gene expression downstream of beta-catenin (Mikels and Nusse, 2006). This Wnt5a signal is mediated by ROR2 and does not involve Ca^{2+} signaling. Over-expression of ROR2 enhances the ability of Wnt5a to block Wnt3a activation of STF and the ROR2 intracellular domain is required for this function, which argues against a sequestration function of ROR2. Contrary to U2OS cells (Billiard et al., 2005), ROR2 does not bind Wnt3a in this system, possibly because 293 cells do not express a co-factor necessary for binding. The ROR2 CRD physically interacts with several Frizzled receptors, raising the possibility

that Fz may function as a co-receptor; however, the biological significance of these interactions has not been tested (Li et al., 2008; Oishi et al., 2003). ROR2 also inhibits canonical Wnt signaling in the H441 human lung carcinoma cell line, in which Wnt5a antagonizes Wnt3a-induced STF expression in the presence of ROR2 (Li et al., 2008). The effectors that act downstream of ROR2 during the inhibition of canonical Wnt signaling are unknown. One candidate is Src kinase, which is activated when ROR2 expressing cells (T/C28a2 human chondrocytes) are treated with Wnt5a (Akbarzadeh et al., 2008). In these cells, activation by Wnt5a caused robust tyrosine phosphorylation of ROR2 followed by rapid internalization of ROR2 via Rab5-positive endosomes. Another potential mechanism is activation of NF- κ B. While most functional studies of mammalian ROR proteins have focused on ROR2, a recent study shows that Wnt5a also binds ROR1 and that co-transfection of these two proteins in 293 cells causes NF- κ B activation (Fukuda et al., 2008).

While these studies indicate that ROR2 antagonizes Wnt/beta-catenin signaling, other studies indicate that ROR2 potentiates Wnt/beta-catenin signaling. In U2OS osteosarcoma cells, ROR2 potentiates Wnt1-induced TOPFLASH expression by a mechanism requiring the ROR2 kinase domain. (Billiard et al., 2005). That ROR2 antagonizes Wnt1-mediated stabilization of beta-catenin, yet potentiates the transcriptional response to Wnt1 in the same cell line is an enigma and presents a challenge to current views of Wnt signaling. One possibility is that the interactions between ROR2 and Wnt1 can be separated into two distinct ROR2 functions. Perhaps ROR2 antagonizes Wnt1-mediated stabilization of beta-catenin by sequestering Wnt1 (Figure 2A) and ROR2 potentiates Wnt1-induced reporter activation by a signaling mechanism involving the ROR2 kinase domain (Figure 2D). ROR2 also potentiates Wnt/beta-catenin signaling in other cell types. In H441 lung carcinoma cells, ROR2

cooperates with Fzd2 to activate STF in response to Wnt3a (Li et al., 2008). This activity requires the ROR2 intracellular domain, but not ROR2 kinase activity (Figure 2E).

Wnt5a and ROR2 also appear to act together during cell migration. Wnt5a-induced migration of mouse embryonic fibroblasts (MEFs) requires ROR2 and the CRD and proline-rich domains are required for this ROR2 function (Figure 2F) (Nishita et al., 2006). In NIH3T3 mouse cells, treatment with Wnt5a causes glycogen synthase kinase-3 (GSK-3)-mediated phosphorylation of ROR2 on serine/threonine residues and GSK-3 is required for Wnt5a to mobilize these cells, suggesting that phosphorylation of ROR2 by GSK-3 may be required for ROR2 function in cell migration (Yamamoto et al., 2007). *ROR2* over-expression also induces filopodia formation in MEFs and this effect is independent of the ROR2 CRD and of Wnt5a (see Figure 3A) (Nishita et al., 2006). In MEF filopodia, ROR2 co-localizes with actin and the cytoplasmic domain of ROR2 associates with the actin-binding protein filamin A. ROR2-induced filopodia formation is not sufficient to stimulate motility; however, it is possible that Wnt5a acts as a cue and stimulates the cells to move and that ROR2, associated with filopodia, enables MEFs to respond to that cue. While ROR2 appears to positively regulate filopodia in MEFs, it has a different effect on filopodia in Keller open-face explants, in which knockdown of *XRor2* or *XWnt5a* results in an increase in transient filopodia (Schambony and Wedlich, 2007). One explanation that would reconcile these observations is that ROR2 functions to stabilize filopodia. In this case, *ROR2* over-expression may cause increased filopodia, as seen in MEFs, and *ROR2* knockdown may cause more transient filopodia, instead of stable filopodia, as seen in Keller open-face explants. ROR proteins interact with the cytoskeleton in several other cell types as well. For example, transfection of *ROR2* in T/C28a2 human chondrocytes causes extensive filopodia

formation (Akbarzadeh et al., 2008). Also, in cultured hippocampal neurons, ROR proteins mobilize the cytoskeleton and regulate neurite and axon extension and branching (Paganoni and Ferreira, 2005).

A final context in which Wnts and ROR interact is in the regulation of cell polarity. In addition to regulating neuronal migration in *C. elegans*, which can be considered a function of cell polarity, Wnts and ROR regulate the polarity of the *C. elegans* vulval precursor cells (VPCs) (Green et al., 2008). The VPCs are epithelial cells that divide asymmetrically along the anterior-posterior axis of the worm. Several Wnts, including Wnt/EGL-20, determine the orientation of VPC division. During VPC orientation, *cam-1*, the *C. elegans* ROR ortholog, mediates EGL-20 activity by a mechanism that requires the CAM-1 intracellular domain and that is independent of JNK (Figure 2G). EGL-20 acts as a directional cue in this process and CAM-1 conveys directional information to the cell. VPC orientation resembles planar cell polarity, which is a process wherein cells, or groups of cells, are polarized along the plane of the epithelium, perpendicular to the apical-basal axis (reviewed by Seifert and Mlodzik, 2007). During VPC orientation, Van Gogh, a core component of the Planar Cell Polarity (PCP) pathway acts in the same pathway as CAM-1 and EGL-20, suggesting that ROR proteins interact with the PCP pathway. CAM-1 also regulates neuronal polarity and the asymmetric division of several neurons (Forrester et al., 1999); however, whether *cam-1* interacts with Wnts in these processes is unknown.

In addition to the interactions with Wnt signaling described above, there also exist ROR activities that are not obviously related to Wnt signaling, although a connection to Wnt signaling may become clear upon further investigation.

ROR signaling II — other interactions

Like many other RTKs, ROR proteins may function as homodimers (Figure 3B). Homodimerization of ROR2, which occurs naturally, can be enhanced by treatment with a bivalent ROR2 antibody (Liu et al., 2007b), or by fusion to the dimeric Fc portion of human Ig (Akbarzadeh et al., 2008). Frizzled receptors can also form dimers, which may be ligand-independent (Carron et al., 2003); therefore, it is unclear whether Wnts promote dimerization of ROR receptors. ROR2 homodimerization results in tyrosine phosphorylation of the receptor (Akbarzadeh et al., 2008; Liu et al., 2007b) and in this regard, ROR2 appears to function as a typical RTK. While the signaling cascade downstream of activated ROR is poorly understood, some of the components that interact with the ROR intracellular domain are beginning to be elucidated.

Forced dimerization causes autophosphorylation of the receptor and activates ROR2 signaling, as seen by increased bone formation in organ culture and increased osteogenesis in hMSCs (Liu et al., 2007b). Immunoprecipitation followed by mass spectrometric analysis of FLAG-tagged ROR2 revealed that the 14-3-3-beta scaffold protein is a ROR2 binding partner (Figure 3B). In U2OS osteosarcoma cells, the ROR2 intracellular domain directly interacts with and phosphorylates 14-3-3-beta. Interestingly, 14-3-3-beta exhibits stronger binding to kinase-inactivated ROR2 (ROR2-KD) than to wild type ROR2, suggesting that 14-3-3-beta may be released by ROR2 phosphorylation. Because 14-3-3-beta proteins inhibit osteogenesis, these authors proposed that ROR2 might promote osteogenic differentiation in part by antagonizing 14-3-3-beta.

Matsuda et al. used a different method to identify proteins that interact with ROR. A yeast-two-hybrid (Y2H) screen using the mROR1 and mROR2 C-termini as bait identified

Dlxin-1 as a protein that interacts with ROR2, but not ROR1 (Figure 3D) (Matsuda et al., 2003). Dlxin-1 is a melanoma-associated-antigen (MAGE) family member and was confirmed to bind ROR2, but not ROR1, by co-immunoprecipitation. ROR2 kinase activity is not required for this association. Dlxin-1 also associates with homeodomain proteins Msx2 and Dlx5 and affects their transcriptional activity. ROR2, via its C-terminal proline-rich and S/T2 domains, recruits Dlxin-1 to the plasma membrane and Dlxin-1 is localized in the nucleus in the absence of ROR2. ROR2 thus indirectly affects Msx2 transcriptional activity by regulating the subcellular distribution of Dlxin-1. Consistent with an interaction between ROR2 and Dlxin-1, their expression significantly overlaps in the developing mouse face and lung.

This Y2H screen also identified casein kinase I epsilon (CKI ϵ) as a ROR2 binding partner and the two proteins co-immunoprecipitated when over-expressed in 293 cells (Figure 3E) (Kani et al., 2004). CKI ϵ phosphorylates the S/T2 domain of ROR2 and induces autophosphorylation of tyrosine residues in the ROR2 proline-rich domain. After activation by CKI ϵ , ROR2 associates with and tyrosine phosphorylates G protein-coupled receptor kinase 2 (GRK2). The expression pattern of GRK2 is similar to that of ROR2 and Dlxin-1 in mice (Kani et al., 2004). Association of ROR2 with Dlxin-1 and CKI ϵ may be specific to vertebrates, as invertebrate ROR proteins do not have the proline-rich domain. It will be interesting to learn the biological function of these interactions and whether the single S/T domain of invertebrate ROR proteins is sufficient to recapitulate these interactions.

Taking a candidate-driven approach, Sammar et al. (2004) identified GDF5 and BMPR1b as ROR-interacting proteins (Sammar et al., 2004). They hypothesized that the molecular mechanisms responsible for Brachydactyly type B (BDB), caused by ROR2

mutation, might be shared among other forms of brachydactyly. Brachydactyly type C (BDC) and brachydactyly type A2 (BDA2) are caused by mutation in GDF5, which is a TGF-beta/BMP family member, and its receptor, BMPR1b, respectively. Sammar et al. describe a genetic and physical interaction between ROR2, BMPR1b, and GDF5, in which BMPR1b binds to and phosphorylates ROR2 and activated ROR2 inhibits the GDF5/BMPR1b pathway (Figure 3E). All three of these components regulate chondrogenesis. A relationship between ROR2 and BMP signaling was reproduced in a second study where Lehmann et al. (2007) detected mutations in the GDF5 antagonist, NOGGIN, in patients with BDB who did not have ROR2 mutations (Lehmann et al., 2007). The signaling events that take place following these interactions and the mechanism by which they cause the brachydactyly phenotype are presently unclear. It remains to be shown whether GDF5 directly binds to ROR2 and if so, which domains are involved.

Summary

ROR proteins are involved in a multitude of cellular processes and signaling events. As predicted, there is now substantial evidence that ROR proteins act as Wnt receptors. There is great consensus that Wnt5a binds to and activates ROR2; therefore, Wnt5a can be considered a bona fide ROR2 ligand. While much progress has been made in understanding ROR2 function as a Wnt receptor, several key questions remain unanswered. What is the mechanism by which ROR2 transduces a Wnt signal? How does ROR2 toggle between activating and repressing Wnt/beta-catenin signaling; is this simply a matter of which Wnt binds ROR2? Are there cofactors involved in creating specificity of response? What

determines whether ROR2 will transduce a Wnt signal versus sequester the Wnt? Are these exclusive functions or do both occur at once?

The ability of ROR proteins to efficiently sequester Wnts has potential therapeutic value. Several types of human cancer are caused by elevated Wnt signaling and introduction of a membrane-tethered ROR CRD could dampen this activity. The sequestration capability of ROR can also be used to control the distribution of Wnts in other contexts. For example, during basic research, inducible ROR over-expression allows the scientist to conditionally and simultaneously inhibit multiple Wnts (Green et al., 2008), which would otherwise be technically challenging in any system. The ability to create local environments of reduced Wnt activity could also be used in tissue engineering to create regions of distinct cell fate or cell polarity in multicellular tissues and organs.

While there is abundant evidence in many systems that ROR proteins act as Wnt receptors, most of these functions depend on the CRD. To date, there is no knowledge of the function of the other extracellular domains; Kringle and Ig. These domains could be required to interact with a co-receptor, or be involved in receptor localization, or they could be required for binding to unidentified non-Wnt ligands. Similarly, the function of the intracellular domain remains ambiguous. Studies involving yeast-two-hybrid (Y2H) assays and mass-spectrometry, as well as candidate-driven approaches, have identified multiple binding partners; however the biological significance of many of these interactions remains to be determined.

ROR2 has been the focus of many studies because of its involvement in human disease; in contrast, ROR1 function has been less rigorously studied. In light of its implication in human cancer, it will be important to also decipher the signaling properties of

ROR1. The unique domain architecture of these RTKs and the variety of processes in which they are involved hold promise for exciting revelations about ROR signaling. While great progress has been made in placing these orphan receptors into the cellular signaling network, ROR signaling remains rich with mystery.

- Afzal, A. R., Rajab, A., Fenske, C. D., Oldridge, M., Elanko, N., Ternes-Pereira, E., Tuysuz, B., Murday, V. A., Patton, M. A., Wilkie, A. O. et al.** (2000). Recessive Robinow syndrome, allelic to dominant brachydactyly type B, is caused by mutation of ROR2. *Nat Genet* **25**, 419-22.
- Akbarzadeh, S., Wheldon, L. M., Sweet, S. M., Talma, S., Mardakheh, F. K. and Heath, J. K.** (2008). The deleted in brachydactyly B domain of ROR2 is required for receptor activation by recruitment of Src. *PLoS ONE* **3**, e1873.
- Al-Shawi, R., Ashton, S. V., Underwood, C. and Simons, J. P.** (2001). Expression of the Ror1 and Ror2 receptor tyrosine kinase genes during mouse development. *Dev Genes Evol* **211**, 161-71.
- Ali, B. R., Jeffery, S., Patel, N., Tinworth, L. E., Meguid, N., Patton, M. A. and Afzal, A. R.** (2007). Novel Robinow syndrome causing mutations in the proximal region of the frizzled-like domain of ROR2 are retained in the endoplasmic reticulum. *Hum Genet*.
- Baskar, S., Kwong, K. Y., Hofer, T., Levy, J. M., Kennedy, M. G., Lee, E., Staudt, L. M., Wilson, W. H., Wiestner, A. and Rader, C.** (2008). Unique Cell Surface Expression of Receptor Tyrosine Kinase ROR1 in Human B-Cell Chronic Lymphocytic Leukemia. *Clin Cancer Res* **14**, 396-404.
- Billiard, J., Way, D. S., Seestaller-Wehr, L. M., Moran, R. A., Mangine, A. and Bodine, P. V.** (2005). The orphan receptor tyrosine kinase Ror2 modulates canonical Wnt signaling in osteoblastic cells. *Mol Endocrinol* **19**, 90-101.
- Carron, C., Pascal, A., Djiane, A., Boucaut, J. C., Shi, D. L. and Umbhauer, M.** (2003). Frizzled receptor dimerization is sufficient to activate the Wnt/beta-catenin pathway. *J Cell Sci* **116**, 2541-50.
- Chen, Y., Bellamy, W. P., Seabra, M. C., Field, M. C. and Ali, B. R.** (2005). ER-associated protein degradation is a common mechanism underpinning numerous monogenic diseases including Robinow syndrome. *Hum Mol Genet* **14**, 2559-69.
- Clevers, H.** (2006). Wnt/beta-catenin signaling in development and disease. *Cell* **127**, 469-80.
- DeChiara, T. M., Bowen, D. C., Valenzuela, D. M., Simmons, M. V., Poueymirou, W. T., Thomas, S., Kinetz, E., Compton, D. L., Rojas, E., Park, J. S. et al.** (1996). The receptor tyrosine kinase MuSK is required for neuromuscular junction formation in vivo. *Cell* **85**, 501-12.
- DeChiara, T. M., Kimble, R. B., Poueymirou, W. T., Rojas, J., Masiakowski, P., Valenzuela, D. M. and Yancopoulos, G. D.** (2000). Ror2, encoding a receptor-like tyrosine kinase, is required for cartilage and growth plate development. *Nat Genet* **24**, 271-4.
- Ermakov, S., Malkin, I., Keter, M., Kobylansky, E. and Livshits, G.** (2007). Family-based association study of ROR2 polymorphisms with an array of radiographic hand bone strength phenotypes. *Osteoporos Int*.
- Forrester, W. C.** (2002). The Ror receptor tyrosine kinase family. *Cell Mol Life Sci* **59**, 83-96.
- Forrester, W. C., Dell, M., Perens, E. and Garriga, G.** (1999). A *C. elegans* Ror receptor tyrosine kinase regulates cell motility and asymmetric cell division. *Nature* **400**, 881-5.
- Forrester, W. C. and Garriga, G.** (1997). Genes necessary for *C. elegans* cell and growth cone migrations. *Development* **124**, 1831-43.
- Forrester, W. C., Kim, C. and Garriga, G.** (2004). The *Caenorhabditis elegans* Ror RTK CAM-1 inhibits EGL-20/Wnt signaling in cell migration. *Genetics* **168**, 1951-62.

- Francis, M. M., Evans, S. P., Jensen, M., Madsen, D. M., Mancuso, J., Norman, K. R. and Maricq, A. V.** (2005). The Ror receptor tyrosine kinase CAM-1 is required for ACR-16-mediated synaptic transmission at the *C. elegans* neuromuscular junction. *Neuron* **46**, 581-94.
- Fu, A. K., Cheung, J., Smith, F. D., Ip, F. C. and Ip, N. Y.** (2001). Overexpression of muscle specific kinase increases the transcription and aggregation of acetylcholine receptors in *Xenopus* embryos. *Brain Res Mol Brain Res* **96**, 21-9.
- Fukuda, T., Chen, L., Endo, T., Tang, L., Lu, D., Castro, J. E., F. Widhopf G, n., Rassenti, L. Z., Cantwell, M. J., Prussak, C. E. et al.** (2008). Antisera induced by infusions of autologous Ad-CD154-leukemia B cells identify ROR1 as an oncofetal antigen and receptor for Wnt5a. *Proc Natl Acad Sci U S A*.
- Green, J. L., Inoue, T. and Sternberg, P. W.** (2007). The *C. elegans* ROR receptor tyrosine kinase, CAM-1, non-autonomously inhibits the Wnt pathway. *Development* **134**, 4053-62.
- Hikasa, H., Shibata, M., Hiratani, I. and Taira, M.** (2002). The *Xenopus* receptor tyrosine kinase Xror2 modulates morphogenetic movements of the axial mesoderm and neuroectoderm via Wnt signaling. *Development* **129**, 5227-39.
- Kani, S., Oishi, I., Yamamoto, H., Yoda, A., Suzuki, H., Nomachi, A., Iozumi, K., Nishita, M., Kikuchi, A., Takumi, T. et al.** (2004). The receptor tyrosine kinase Ror2 associates with and is activated by casein kinase Iepsilon. *J Biol Chem* **279**, 50102-9.
- Katoh, M. and Katoh, M.** (2005). Comparative genomics on ROR1 and ROR2 orthologs. *Oncol Rep* **14**, 1381-4.
- Kim, C. and Forrester, W. C.** (2003). Functional analysis of the domains of the *C. elegans* Ror receptor tyrosine kinase CAM-1. *Dev Biol* **264**, 376-90.
- Koga, M., Take-uchi, M., Tameishi, T. and Ohshima, Y.** (1999). Control of DAF-7 TGF-(alpha) expression and neuronal process development by a receptor tyrosine kinase KIN-8 in *Caenorhabditis elegans*. *Development* **126**, 5387-98.
- Lehmann, K., Seemann, P., Silan, F., Goecke, T. O., Irgang, S., Kjaer, K. W., Kjaergaard, S., Mahoney, M. J., Morlot, S., Reissner, C. et al.** (2007). A new subtype of brachydactyly type B caused by point mutations in the bone morphogenetic protein antagonist NOGGIN. *Am J Hum Genet* **81**, 388-96.
- Li, C., Chen, H., Hu, L., Xing, Y., Sasaki, T., Villosis, M. F., Li, J., Nishita, M., Minami, Y. and Minoo, P.** (2008). Ror2 modulates the canonical Wnt signaling in lung epithelial cells through cooperation with Fzd2. *BMC Mol Biol* **9**, 11.
- Li, C., Xiao, J., Hormi, K., Borok, Z. and Minoo, P.** (2002). Wnt5a participates in distal lung morphogenesis. *Dev Biol* **248**, 68-81.
- Lin, W., Burgess, R. W., Dominguez, B., Pfaff, S. L., Sanes, J. R. and Lee, K. F.** (2001). Distinct roles of nerve and muscle in postsynaptic differentiation of the neuromuscular synapse. *Nature* **410**, 1057-64.
- Liu, Y., Bhat, R. A., Seestaller-Wehr, L. M., Fukayama, S., Mangine, A., Moran, R. A., Komm, B. S., Bodine, P. V. and Billiard, J.** (2007a). The orphan receptor tyrosine kinase Ror2 promotes osteoblast differentiation and enhances ex vivo bone formation. *Mol Endocrinol* **21**, 376-87.
- Liu, Y., Ross, J. F., Bodine, P. V. and Billiard, J.** (2007b). Homo-dimerization of Ror2 Tyrosine Kinase Receptor Induces 14-3-3{beta} Phosphorylation and Promotes Osteoblast Differentiation and Bone Formation. *Mol Endocrinol*.

- Liu, Y. Z., Xiao, P., Guo, Y. F., Xiong, D. H., Zhao, L. J., Shen, H., Liu, Y. J., Dvornyk, V., Long, J. R., Deng, H. Y. et al.** (2006). Genetic linkage of human height is confirmed to 9q22 and Xq24. *Hum Genet* **119**, 295-304.
- Logan, C. Y. and Nusse, R.** (2004). The Wnt signaling pathway in development and disease. *Annu Rev Cell Dev Biol* **20**, 781-810.
- MacKeigan, J. P., Murphy, L. O. and Blenis, J.** (2005). Sensitized RNAi screen of human kinases and phosphatases identifies new regulators of apoptosis and chemoresistance. *Nat Cell Biol* **7**, 591-600.
- Masiakowski, P. and Carroll, R. D.** (1992). A novel family of cell surface receptors with tyrosine kinase-like domain. *J Biol Chem* **267**, 26181-90.
- Matsuda, T., Nomi, M., Ikeya, M., Kani, S., Oishi, I., Terashima, T., Takada, S. and Minami, Y.** (2001). Expression of the receptor tyrosine kinase genes, Ror1 and Ror2, during mouse development. *Mech Dev* **105**, 153-6.
- Matsuda, T., Suzuki, H., Oishi, I., Kani, S., Kuroda, Y., Komori, T., Sasaki, A., Watanabe, K. and Minami, Y.** (2003). The receptor tyrosine kinase Ror2 associates with the melanoma-associated antigen (MAGE) family protein Dlxin-1 and regulates its intracellular distribution. *J Biol Chem* **278**, 29057-64.
- McKay, S. E., Hislop, J., Scott, D., Bulloch, A. G., Kaczmarek, L. K., Carew, T. J. and Sossin, W. S.** (2001). Aplysia ror forms clusters on the surface of identified neuroendocrine cells. *Mol Cell Neurosci* **17**, 821-41.
- Mikels, A. J. and Nusse, R.** (2006). Purified Wnt5a protein activates or inhibits beta-catenin-TCF signaling depending on receptor context. *PLoS Biol* **4**, e115.
- Molenaar, M., van de Wetering, M., Oosterwegel, M., Peterson-Maduro, J., Godsave, S., Korinek, V., Roose, J., Destree, O. and Clevers, H.** (1996). XTcf-3 transcription factor mediates beta-catenin-induced axis formation in *Xenopus* embryos. *Cell* **86**, 391-9.
- Moon, R. T., Campbell, R. M., Christian, J. L., McGrew, L. L., Shih, J. and Fraser, S.** (1993). Xwnt-5A: a maternal Wnt that affects morphogenetic movements after overexpression in embryos of *Xenopus laevis*. *Development* **119**, 97-111.
- Nishita, M., Yoo, S. K., Nomachi, A., Kani, S., Sougawa, N., Ohta, Y., Takada, S., Kikuchi, A. and Minami, Y.** (2006). Filopodia formation mediated by receptor tyrosine kinase Ror2 is required for Wnt5a-induced cell migration. *J Cell Biol* **175**, 555-62.
- Nomi, M., Oishi, I., Kani, S., Suzuki, H., Matsuda, T., Yoda, A., Kitamura, M., Itoh, K., Takeuchi, S., Takeda, K. et al.** (2001). Loss of mRor1 enhances the heart and skeletal abnormalities in mRor2-deficient mice: redundant and pleiotropic functions of mRor1 and mRor2 receptor tyrosine kinases. *Mol Cell Biol* **21**, 8329-35.
- Oishi, I., Sugiyama, S., Liu, Z. J., Yamamura, H., Nishida, Y. and Minami, Y.** (1997). A novel *Drosophila* receptor tyrosine kinase expressed specifically in the nervous system. Unique structural features and implication in developmental signaling. *J Biol Chem* **272**, 11916-23.
- Oishi, I., Suzuki, H., Onishi, N., Takada, R., Kani, S., Ohkawara, B., Koshida, I., Suzuki, K., Yamada, G., Schwabe, G. C. et al.** (2003). The receptor tyrosine kinase Ror2 is involved in non-canonical Wnt5a/JNK signalling pathway. *Genes Cells* **8**, 645-54.
- Oishi, I., Takeuchi, S., Hashimoto, R., Nagabukuro, A., Ueda, T., Liu, Z. J., Hatta, T., Akira, S., Matsuda, Y., Yamamura, H. et al.** (1999). Spatio-temporally regulated expression of receptor tyrosine kinases, mRor1, mRor2, during mouse development: implications in development and function of the nervous system. *Genes Cells* **4**, 41-56.

- Oldridge, M., Fortuna, A. M., Maringa, M., Propping, P., Mansour, S., Pollitt, C., DeChiara, T. M., Kimble, R. B., Valenzuela, D. M., Yancopoulos, G. D. et al.** (2000). Dominant mutations in ROR2, encoding an orphan receptor tyrosine kinase, cause brachydactyly type B. *Nat Genet* **24**, 275-8.
- Paganoni, S. and Ferreira, A.** (2003). Expression and subcellular localization of Ror tyrosine kinase receptors are developmentally regulated in cultured hippocampal neurons. *J Neurosci Res* **73**, 429-40.
- Paganoni, S. and Ferreira, A.** (2005). Neurite extension in central neurons: a novel role for the receptor tyrosine kinases Ror1 and Ror2. *J Cell Sci* **118**, 433-46.
- Raz, R., Stricker, S., Gazzero, E., Clor, J. L., Witte, F., Nistala, H., Zabski, S., Pereira, R. C., Stadmeier, L., Wang, X. et al.** (2008). The mutation ROR2W749X, linked to human BDB, is a recessive mutation in the mouse, causing brachydactyly, mediating patterning of joints and modeling recessive Robinow syndrome. *Development*.
- Robinow, M., Silverman, F. N. and Smith, H. D.** (1969). A newly recognized dwarfing syndrome. *Am J Dis Child* **117**, 645-51.
- Rodriguez-Niedenfuhr, M., Prols, F. and Christ, B.** (2004). Expression and regulation of ROR-1 during early avian limb development. *Anat Embryol (Berl)* **207**, 495-502.
- Roszmusz, E., Patthy, A., Trexler, M. and Patthy, L.** (2001). Localization of disulfide bonds in the frizzled module of Ror1 receptor tyrosine kinase. *J Biol Chem* **276**, 18485-90.
- Saldanha, J., Singh, J. and Mahadevan, D.** (1998). Identification of a Frizzled-like cysteine rich domain in the extracellular region of developmental receptor tyrosine kinases. *Protein Sci* **7**, 1632-5.
- Sammar, M., Stricker, S., Schwabe, G. C., Sieber, C., Hartung, A., Hanke, M., Oishi, I., Pohl, J., Minami, Y., Sebald, W. et al.** (2004). Modulation of GDF5/BRI-b signalling through interaction with the tyrosine kinase receptor Ror2. *Genes Cells* **9**, 1227-38.
- Schambony, A. and Wedlich, D.** (2007). Wnt-5A/Ror2 regulate expression of XPAPC through an alternative noncanonical signaling pathway. *Dev Cell* **12**, 779-92.
- Schwabe, G. C., Tinschert, S., Buschow, C., Meinecke, P., Wolff, G., Gillessen-Kaesbach, G., Oldridge, M., Wilkie, A. O., Komec, R. and Mundlos, S.** (2000). Distinct mutations in the receptor tyrosine kinase gene ROR2 cause brachydactyly type B. *Am J Hum Genet* **67**, 822-31.
- Schwabe, G. C., Trepczik, B., Suring, K., Brieske, N., Tucker, A. S., Sharpe, P. T., Minami, Y. and Mundlos, S.** (2004). Ror2 knockout mouse as a model for the developmental pathology of autosomal recessive Robinow syndrome. *Dev Dyn* **229**, 400-10.
- Seifert, J. R. and Mlodzik, M.** (2007). Frizzled/PCP signalling: a conserved mechanism regulating cell polarity and directed motility. *Nat Rev Genet* **8**, 126-38.
- Stricker, S., Verhey van Wijk, N., Witte, F., Brieske, N., Seidel, K. and Mundlos, S.** (2006). Cloning and expression pattern of chicken Ror2 and functional characterization of truncating mutations in Brachydactyly type B and Robinow syndrome. *Dev Dyn* **235**, 3456-65.
- Takeuchi, S., Takeda, K., Oishi, I., Nomi, M., Ikeya, M., Itoh, K., Tamura, S., Ueda, T., Hatta, T., Otani, H. et al.** (2000). Mouse Ror2 receptor tyrosine kinase is required for the heart development and limb formation. *Genes Cells* **5**, 71-8.
- van Bokhoven, H., Celli, J., Kayserili, H., van Beusekom, E., Balci, S., Brussel, W., Skovby, F., Kerr, B., Percin, E. F., Akarsu, N. et al.** (2000). Mutation of the gene encoding

the ROR2 tyrosine kinase causes autosomal recessive Robinow syndrome. *Nat Genet* **25**, 423-6.

van de Wetering, M., Cavallo, R., Dooijes, D., van Beest, M., van Es, J., Loureiro, J., Ypma, A., Hursh, D., Jones, T., Bejsovec, A. et al. (1997). Armadillo coactivates transcription driven by the product of the *Drosophila* segment polarity gene dTCF. *Cell* **88**, 789-99.

Veeman, M. T., Axelrod, J. D. and Moon, R. T. (2003). A second canon. Functions and mechanisms of beta-catenin-independent Wnt signaling. *Dev Cell* **5**, 367-77.

Weinberg, R. A. (2006). *The Biology of Cancer*: Garland Science.

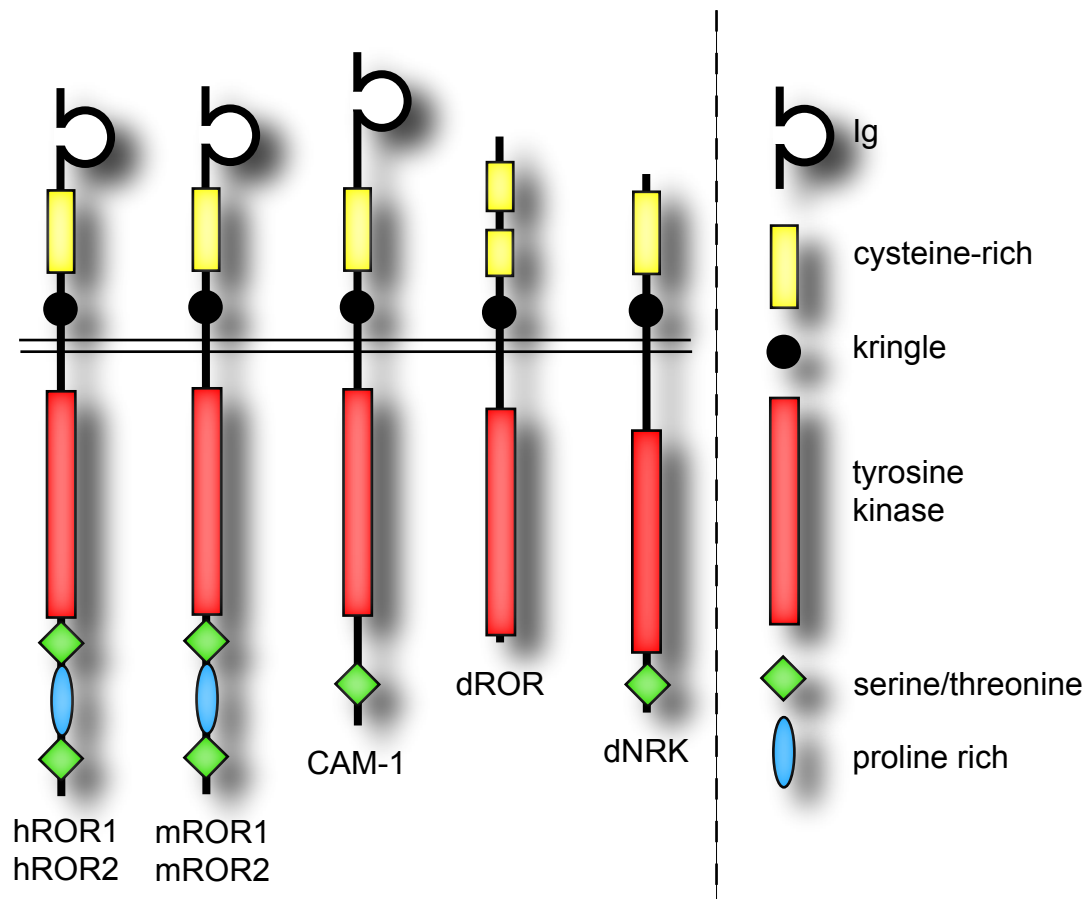
Wilson, C., Goberdhan, D. C. and Steller, H. (1993). Dror, a potential neurotrophic receptor gene, encodes a *Drosophila* homolog of the vertebrate Ror family of Trk-related receptor tyrosine kinases. *Proc Natl Acad Sci U S A* **90**, 7109-13.

Xu, Y. K. and Nusse, R. (1998). The Frizzled CRD domain is conserved in diverse proteins including several receptor tyrosine kinases. *Curr Biol* **8**, R405-6.

Yamaguchi, T. P., Bradley, A., McMahon, A. P. and Jones, S. (1999). A Wnt5a pathway underlies outgrowth of multiple structures in the vertebrate embryo. *Development* **126**, 1211-23.

Yamamoto, H., Yoo, S. K., Nishita, M., Kikuchi, A. and Minami, Y. (2007). Wnt5a modulates glycogen synthase kinase 3 to induce phosphorylation of receptor tyrosine kinase Ror2. *Genes Cells* **12**, 1215-23.

Figure 1. Structure of ROR RTKs in different species



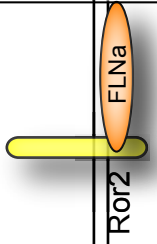
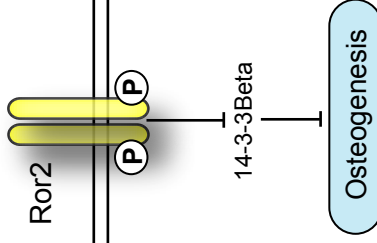
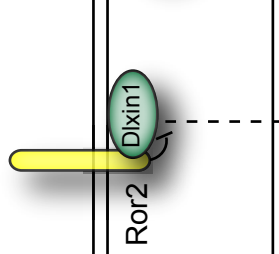
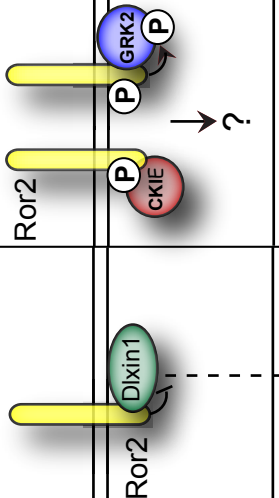
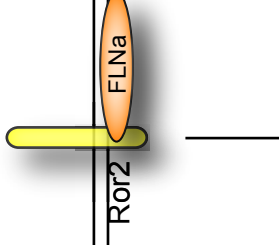
Domain organization (approximately to scale) of ROR proteins in human (hROR1, hROR2), mouse (mROR1, mROR2), *C. elegans* (CAM-1), and *Drosophila* (dROR, dNRK). The N-terminal extracellular domain (ECD) is above and the intracellular domain (ICD) is below (adapted from Forrester, 2002; Hubbard and Till, 2000).

Figure 2. Functions of ROR as a Wnt receptor

A. ROR requesters Wnts	B. ROR2 mediates Wnt5a signal by activating JNK	C. ROR2 mediates Wnt5a antagonism of Wnt3a activity	D. ROR2 potentiates Wnt1 activity (kinase dependent)	E. ROR2 potentiates Wnt3a activity (kinase-independent)	F. ROR2 mediates Wnt5a signal in cell migration	G. ROR and Van Gogh mediate Wnt effects on cell polarity
<i>C. elegans</i> & U2OS cells	<i>Xenopus</i> CE & NIH3T3 cells	293, L, H441, A549, U2OS, HT-29, & T/C28a2 cells	U2OS cells	L & H441 cells	NIH3T3, MEFs, L cells	<i>C. elegans</i>
Required? CRD: intracellular: kinase domain: kinase activity: PRD: S/T:	y y y y ? ?	y y ? ? ? ?	y y y y ? ?	y y ? n n n	y y n n y ?	y y ? ? ?
Kim & Forrester 2003 Billiard et al., 2005 Green et al., 2007	Schambony et al., 2007 Oishi et al., 2003	Mikels et al., 2006 Li et al., 2008 Fukuda et al., 2008 Akbarzadeh et al., 2008	Billiard et al., 2005	Li et al., 2008	Yamamoto et al., 2007 Nishita et al., 2006	Green et al., 2008

Each panel includes a description of ROR function (yellow background), the system in which the function was observed (blue background), a diagram of ROR activity (white background), the domains required (pink background) and the references that describe the function (peach background). Domain abbreviations: CRD (cysteine-rich domain), PRD (proline-rich domain) and S/T (serine/threonine-rich domain). We have taken some liberty in grouping observations from different systems into similar ROR functions and each reference listed may not describe all of the interactions depicted. Within the diagrams, the extracellular space is at the top, cytoplasmic is in the middle and nuclear is at the bottom, separated by double lines. Stars represent transcriptional readouts: STF (SuperTOPFLASH) and XPAPC (paraxial protocadherin). Dotted lines represent inactivity. In (C) and (D), where transcriptional activity has not been described, the phenomenon assay is indicated in a blue box.

Figure 3. Other ROR functions

A. ROR2 regulates filopodia formation 293T, MCF7, B16Bl6, L & T/C28a2 cells	B. ROR2 functions as a homodimer T/C28a2, U2OS, hMSCs, SaOS-2, HOB-01-09 cells & ex vivo bone formation	C. ROR2 recruits Dixin-1 to the membrane 293 cells	D. ROR2 interacts with CKIE and GRK2 293T, NIH3T3 cells	E. ROR2 modulates GDF5/BMPRIb signaling COS7, ATDC5 cells
				
<p>Filopodia formation</p>	<p>Osteogenesis</p>	<p>WIP</p>	<p>SBE</p>	<p>SBE</p>
<p>Required?</p>	<p>?</p>	<p>?</p>	<p>?</p>	<p>?</p>
<p>CRD: intracellular:</p>	<p>?</p>	<p>y</p>	<p>y</p>	<p>y</p>
<p>kinase domain:</p>	<p>?</p>	<p>n</p>	<p>y</p>	<p>y</p>
<p>kinase activity:</p>	<p>y/n</p>	<p>n</p>	<p>y</p>	<p>y</p>
<p>PRD:</p>	<p>?</p>	<p>?</p>	<p>y</p>	<p>?</p>
<p>S/T:</p>	<p>?</p>	<p>?</p>	<p>y</p>	<p>?</p>
<p>Nishita et al., 2006 Schambony et al., 2007 Akbarzadeh et al., 2008</p>	<p>Akbarzadeh et al., 2008 Liu et al., 2007a Liu et al., 2007b</p>	<p>Matsuda et al., 2003</p>	<p>Kani et al., 2004</p>	<p>Sammar et al., 2004</p>

Panels are same as in Figure 2. Transcriptional readouts are: WIP (Msx2 binding site (see Zhang et al., 1997)), SBE (Smad Binding Element).

CHAPTER 2

The *C. elegans* ROR RTK, CAM-1, non-autonomously inhibits the Wnt pathway

This chapter was published as:

The *C. elegans* ROR RTK, CAM-1, non-autonomously inhibits the Wnt pathway.

J. L. Green, T. Inoue, and P. W. Sternberg*

Development. 2007 Nov;143(22):4053-62

Division of Biology, California Institute of Technology, Mail Code 156-29, Pasadena, CA 91125, USA

*Corresponding author 626-395-2181 (phone) 626-568-8012 (fax) pws@caltech.edu

The reverse binding assay was performed in collaboration with Takao Inoue, who also made critical comments on this manuscript. J. Green performed all other experiments and was the primary author of this manuscript.

Abstract

Inhibitors of Wnt signaling promote normal development and prevent cancer by restraining when and where the Wnt pathway is activated. ROR proteins, a class of Wnt-binding receptor tyrosine kinases, inhibit Wnt signaling by an unknown mechanism. To clarify how RORs inhibit the Wnt pathway, we examined the relationship between Wnts and the sole *C. elegans* ROR homolog, *cam-1*, during *C. elegans* vulval development, a Wnt-regulated process. We found that loss and over-expression of *cam-1* causes reciprocal defects in Wnt-mediated cell-fate specification. Our molecular and genetic analysis revealed that the CAM-1 extracellular domain (ECD) is sufficient to non-autonomously antagonize multiple Wnts, suggesting that the CAM-1/ROR ECD sequesters Wnts. A sequestration model is supported by our findings that the CAM-1 ECD binds to several Wnts *in vitro*. These results demonstrate how ROR proteins help to refine the spatial pattern of Wnt activity in a complex multicellular environment.

Introduction

Wnt signaling is necessary for development, but causes cancer when dysregulated. The canonical Wnt pathway is initiated when a secreted Wnt glycoprotein binds to a transmembrane Frizzled (Fz) receptor and ultimately leads to Beta-catenin-mediated regulation of gene transcription (Logan and Nusse, 2004). The Wnt pathway is actively constrained by secreted antagonists and inhibitors of signal transducers (Kawano and Kypta, 2003; Logan and Nusse, 2004). The importance of negative regulators both developmentally and to prevent tumorigenesis prompted us to investigate the mechanistic activity of ROR proteins, a poorly understood class of Wnt inhibitors (Billiard et al., 2005; Forrester et al., 2004; Mikels and Nusse, 2006a; Mikels and Nusse, 2006b).

ROR proteins are conserved receptor tyrosine kinases (RTKs) characterized by an extracellular Frizzled (Fz) domain (also called cysteine-rich-domain (CRD)), an immunoglobulin (Ig) domain, and a kringle domain (Fig. 1A). Mutations in *ROR* genes cause developmental defects including skeletal abnormalities in mice and humans (reviewed by Forrester, 2002). Studies of vertebrate RORs showed that the ROR CRD, like the Fz CRD (Bhanot et al., 1996), can bind to Wnts (Billiard et al., 2005; Hikasa et al., 2002; Kani et al., 2004; Mikels and Nusse, 2006a; Oishi et al., 2003). In cell culture, ROR2 abrogates expression of a canonical Wnt reporter (Billiard et al., 2005; Mikels and Nusse, 2006a); however, whether this antagonistic activity is cell-autonomous is unknown. To study how ROR modulates Wnt signaling in a multicellular environment, we investigated the function of the sole *C. elegans* ROR family member, *cam-1*.

Forrester et al. (Forrester, 2002; Forrester et al., 2004) studied CAM-1, equally similar to ROR1 and to ROR2, for its role in cell migration, where the CRD is required to antagonize EGL-20/Wnt activity. During canal associated neuron (CAN) migration, this CAM-1 function is cell-autonomous (Forrester et al., 1999). Although Forrester and others postulated that CAM-1 sequesters Wnts, reports that ROR2 can bind to Fz receptors (Oishi et al., 2003) raise the question whether CAM-1/ROR inhibits Wnt signaling by interacting with the receptor or the ligand. We addressed these questions using vulva development as a model since this process involves every *C. elegans* Wnt (*lin-44*, *cwn-1*, *egl-20*, *cwn-2* and *mom-2*) and Wnt receptor (*mig-1*, *lin-17*, *mom-5*, *cfz-2* and *lin-18*) (Gleason et al., 2006) and also because the well-characterized cellular phenotypes facilitate identification of signaling defects.

The *C. elegans* vulva comprises 22 cells generated by well-defined signaling events (reviewed by Sternberg, 2005) (Fig. 1B). The vulval cells are descendents of three vulval precursor cells (VPCs) located on the ventral surface of the worm (Sulston and Horvitz, 1977). During larval development, the VPCs are induced to divide by LIN-3 (EGF) secreted by the anchor cell (AC), (Hill and Sternberg, 1992). The VPC most proximal to the AC, P6.p, receives the most LIN-3 inductive signal through the receptor LET-23 (EGFR) (Katz et al., 1995; Yoo et al., 2004) triggering a MAP kinase cascade that induces P6.p to adopt the primary fate (1°) and produce eight vulval progeny. P5.p and P7.p receive lower levels of LIN-3 and a repressive lateral signal from P6.p mediated by LIN-12 (NOTCH) (Simske and Kim, 1995; Sternberg and Horvitz, 1989). These cells adopt the secondary fate (2°) and each produces seven vulval progeny. The remaining VPCs receive sub-threshold LIN-3 signal and adopt either the tertiary fate (3°), dividing once before fusing (P4.p, P8.p and sometimes

P3.p), or the fused fate (F), fusing with the epidermis without dividing (P3.p adopts this fate half the time) (Sulston and Horvitz, 1977). A Wnt pathway involving BAR-1 (Beta-catenin) is required for the VPCs to be induced by LIN-3 and defective Wnt signaling frequently causes P5.p – P7.p to become 3° or F instead of 1° or 2° and also causes P3.p, P4.p and P8.p to become F instead of 3° (Eisenmann et al., 1998).

Because wild-type *C. elegans* development is essentially invariant, even slight deviations from the wild-type induction pattern can be detected and are informative. Worms producing fewer than 22 vulval cells are called Underinduced (UI) and worms producing greater than 22 vulval cells are called Overinduced (OI). The UI phenotype (Fig. 1D) is caused by reduced Wnt signaling or reduced RAS/MAPK signaling. The OI phenotype (Fig. 1E) is caused by increased Ras/MAPK signaling (Ferguson et al., 1987), increased lateral signaling (Greenwald et al., 1983) or increased Wnt activity (Gleason et al., 2002; Korswagen et al., 2002).

Here, we show that CAM-1 inhibits Wnt pathway activity during vulval development by limiting the levels of Wnts that interact with the VPCs. We find that expression of the CAM-1 ECD in non-vulval tissue is sufficient to limit Wnt pathway activity in the VPCs, whereas CAM-1 expression in the VPCs failed to rescue the *cam-1* mutant phenotype, suggesting a non-autonomous mode of inhibition. We also find that the CAM-1 ECD specifically binds to Wnts, supporting the model that CAM-1 sequesters Wnt ligands. Our results demonstrate how CAM-1/ROR contributes to the complex spatial profile of Wnt signaling by modifying the range of Wnt activity.

Results

CAM-1 negatively regulates vulval induction

To study how CAM-1/ROR inhibits Wnt signaling, we investigated the role of CAM-1 in vulval development, a process requiring multiple Wnts. None of the five *cam-1* alleles tested (Fig. 1A) caused induction defects (Table 1). However, since vulval development requires several redundant Wnts and receptors (Gleason et al., 2006), we looked for genetic interactions between *cam-1* and Wnt receptors *lin-17/Frizzled* (Sawa et al., 1996) and *lin-18/Ryk* (Inoue et al., 2004). We found that worms doubly mutant for *cam-1* and loss-of-function (*lf*) mutations in *lin-17* or *lin-18* displayed an OI phenotype (greater than 22 vulval cells). *lin-17(lf)* and *lin-18(lf)* mutants frequently display a polarity defect in the P7.p lineage that is distinct from vulval induction. This polarity defect alters the arrangement, but not the number, of vulval cells. To distinguish between induction defects and polarity defects we counted the vulval nuclei. Both *lin-17(lf)* and *lin-18(lf)* animals have the wild-type pattern of 3-cell induction; P6.p adopts the 1° fate, P5.p and P7.p adopt the 2° fate, and the remaining VPCs are not induced. We found that 17% of *lin-17(lf); cam-1(lf)* double mutants and 12% of *cam-1(lf); lin-18(lf)* double mutants are OI (Table 1) (Fig. 1E) with either 3.5, 4.0 or 4.5 VPCs induced. Since neither *lin-17(lf)* nor *lin-18(lf)* single mutants are OI, these results suggest that CAM-1 negatively regulates vulval induction and that *lin-17(lf)* and *lin-18(lf)* provide a sensitized background in which to observe CAM-1 function. To determine whether the OI phenotype is a common phenotype among *cam-1; Fz* double mutants, we constructed worms doubly mutant for *cam-1(lf)* and two other Fz receptors; *mig-1* and *cfz-2*. 0/21 *mig-1(lf); cam-1(lf)* and 1/22 *cam-1(lf); cfz-2(lf)* double mutant worms were OI indicating that sensitization is specific to *lin-17*.

Analysis of CAM-1 domains and site-of-action

We analyzed the five available *cam-1* alleles (Fig. 1A) in combination with *lin-17(lf)* and *lin-18(lf)* (Table 1). The *cam-1* alleles that caused an OI phenotype are either null (*gm122*) (Forrester et al., 1999), disrupt the CRD (*sa692*) (Ailion and Thomas, 2003; Kim and Forrester, 2003), or disrupt the insertion of the ECD into the membrane (*ak37*) (Francis et al., 2005). In contrast, an allele truncating most of the intracellular domain (*gm105*) (Forrester et al., 1999), and an allele eliminating the kinase domain (*ks52*) (Koga et al., 1999), did not cause increased vulval induction. Analysis of these alleles provides structure-function information about CAM-1. Since the *sa692* allele eliminates a conserved cysteine in the CRD (Wnt-binding) domain, negative regulation of vulval development by CAM-1 requires membrane-insertion of the ECD containing the CRD, but does not require the intracellular domain. RNAi of *cam-1* in *lin-17(lf)* worms recapitulated the OI phenotype and *cam-1* RNAi of *cam-1(lf); lin-17(lf)* worms did not reduce the OI phenotype, confirming that the OI phenotype is due to reduced CAM-1 activity and not to a neomorphic function of mutant *cam-1*.

cam-1 expression has been reported in muscle and neurons (Forrester et al., 1999; Koga et al., 1999). We detected additional expression in the VPCs in a previously characterized *Pcam-1::CAM-1::GFP* strain, WF1863 (Forrester et al., 1999) (see Fig. 3A). To test whether *cam-1* acts in the VPCs, we tried to rescue the *lin-17(lf); cam-1(lf)* OI phenotype with an integrated VPC-specific *CAM-1::GFP* transgene driven by the *lst-1* promoter (Yoo et al., 2004). Although *Plst-1::CAM-1::GFP* was expressed in the relevant VPCs (see Fig. 3G), it failed to rescue the OI phenotype suggesting that CAM-1 is required in other tissues to negatively regulate vulval induction.

cam-1 interacts with genes required for vulval induction

To investigate the signaling involved in CAM-1 inhibition of vulval induction, we first tested whether the synthetic OI phenotype is dependent on the inductive LIN-3 signal. Removing the source of LIN-3 (the AC) by laser ablation of the gonadal primordium eliminates inductive Ras/MAPK signaling. In gonad-ablated wild-type worms, no VPCs are induced (Kimble, 1981; Sulston and White, 1980). Mutations that strongly activate Ras/MAPK signaling can rescue the UI phenotype caused by gonad-ablation (Han and Sternberg, 1990). We ablated the gonad in wild-type and *lin-17(lf); cam-1(lf)* worms and found that vulval induction in *lin-17(lf); cam-1(lf)* worms was gonad-dependent: all 16 ablated animals had no VPCs induced. Because only strong activation of the Ras/MAPK pathway can rescue vulval induction in gonad-ablated worms, we next tested whether *cam-1(lf)* affects induction in worms with mildly reduced LIN-3 activity. *cam-1(lf)* suppressed the UI phenotype of two reduction-of-function (rf) *lin-3* alleles (Table S1), suggesting that *cam-1* acts downstream or parallel to *lin-3*. We then tested for a genetic interaction between *cam-1* and inhibitors of Ras/MAPK signaling, *ark-1*, *sli-1* and *gap-1* (Sternberg, 2005; Sundaram, 2006), which are each silent when mutated singly, but are OI (30-90%) when combined with loss of another negative regulator (Hopper et al., 2000; Yoon et al., 2000). We found no interaction of *cam-1(lf)* with mutations in *ark-1*, *sli-1* or *gap-1*, indicating that CAM-1 is probably not a negative regulator of the Ras/MAPK pathway. *lin-17(lf); gap-1(n1691)* worms are not OI, thus providing further support that loss of CAM-1 does not cause increased Ras/MAPK signaling. Besides Ras/MAPK signaling, Wnt signaling is also required for vulval induction and can cause OI phenotypes when hyperactivated (Gleason et

al., 2002). Mutations in *bar-1/Beta-catenin* cause a UI phenotype (Eisenmann, 2005; Eisenmann et al., 1998). In contrast to the suppression we observed for reduced activity of the Ras/MAPK pathway, *cam-1(lf)* did not suppress the UI phenotype of *bar-1(lf)*, consistent with *cam-1* and *bar-1* functioning in the same pathway.

cam-1 mutants have a withered tail (Wit) phenotype that may position some VPCs closer to the AC and thus increase the local concentration of inductive LIN-3 signal. To investigate whether the OI phenotype is a consequence of increased VPC proximity to the AC, we tested the ability of *cam-1* to affect vulval induction independently of the AC. To do this, we used a gain-of-function (gf) allele of *lin-12/Notch*. When heterozygous, the *lin-12(n952gf)* allele causes gonad-independent specification of 2° lineages in P3.p-P8.p. As *lin-12(gf)/+* also causes loss of the AC, this phenotype is due to increased lateral signaling rather than increased Ras/MAPK signaling. We found that *cam-1(lf)* increased induction in *lin-12(gf)/+* worms (Table S2). Thus, the effect of *cam-1(lf)* on vulval induction cannot be attributed to mispositioning of the VPCs closer to the AC, which is absent in these worms.

Starvation and passage through dauer, an alternate third larval stage usually entered under conditions of starvation or high temperature (Savage-Dunn, 2005), can affect vulval induction (Ferguson and Horvitz, 1985) and *cam-1* mutants are dauer constitutive (Daf-c) (Forrester et al., 1998; Koga et al., 1999). To test whether the OI phenotype we observe is due to passage through dauer, we constructed *lin-17(lf); cam-1(lf); daf-3(lf)* triple mutants. Although *daf-3(lf)* suppresses the Daf-c phenotype of *cam-1(lf)* (Koga et al., 1999), it does not suppress the OI phenotype of *lin-17(lf); cam-1(lf)* double mutants (Table S1) indicating that the OI phenotype is not due to passage through dauer.

CAM-1 antagonizes Wnts

Previous studies of CAN migration demonstrated that CAM-1 inhibits EGL-20 /Wnt function (Forrester et al., 2004). To determine if this is also the role of CAM-1 in vulval induction, we tested whether a strong reduction-of-function (rf) mutation in *egl-20* (Harris et al., 1996) could suppress the OI phenotype of *lin-17(lf); cam-1(lf)* or *cam-1(lf); lin-18(lf)* double mutants (Table 1). *egl-20(rf)* fully suppressed the OI phenotype of *cam-1(lf); lin-18(lf)* worms indicating that the OI phenotype of these worms depends on EGL-20. However, we found that *lin-17(lf); cam-1(lf); egl-20(rf)* triple mutants are still OI (Table 1), indicating that the OI phenotype of these worms is not dependent on EGL-20. The role of CAM-1 in vulval induction is thus only partly attributed to inhibition of EGL-20 activity.

Of the five Wnts, EGL-20, CWN-1, and CWN-2 strongly promote vulval induction (Gleason et al., 2006) (Table 1). To investigate whether *cam-1(lf)* causes increased CWN-1 or CWN-2 activity, we tested the ability of mutations in these Wnt genes to suppress the OI phenotype of *lin-17(lf); cam-1(lf)* or *cam-1(lf); lin-18(lf)* double mutants. We found that *cwn-1(lf)* suppressed the OI phenotype of *cam-1(lf); lin-18(lf)* mutant worms and that *cwn-2(lf)* weakly suppressed the OI phenotype of *lin-17(lf); cam-1(lf)* mutant worms. These results indicate that *cam-1(lf)* increases activity of CWN-1, EGL-20 and possibly CWN-2 (Fig. 1F). The inability of *cwn-1(lf)*, *egl-20(rf)*, or *cwn-2(lf)* to fully suppress the OI phenotype of *lin-17(lf); cam-1(lf)* worms suggests that the OI phenotype in this strain is caused either by one of the remaining Wnts or by multiple Wnts. In some cases, mutation of a Wnt reduced the level of induction in *lin-17(lf); cam-1(lf)* or *cam-1(lf); lin-18(lf)* double mutants to below wild type, consistent with the role of these Wnts in vulval induction.

LIN-17 and LIN-18 function as typical Wnt receptors in P7.p polarity. We speculate that in addition, loss of LIN-17 and LIN-18 increases levels of extracellular Wnt and that loss of CAM-1 further increases these levels, crossing the threshold to induce the VPCs (Fig. 1F). This hypothesis is consistent with observations in the *Drosophila* wing where clones mutant for Frizzleds, *fz* and *fz2*, increase extracellular levels of Wingless (Wnt) (Han et al., 2005). This increase may be caused by reduced endocytosis of ligand-bound receptor. We thus tested whether worms lacking both *lin-17* and *lin-18* display an OI phenotype. Of 51 *lin-17(lf); lin-18(lf)* double mutant worms observed, only one displayed an OI phenotype (Table S2) (Fig. S1). However, it is possible that the class of Wnts elevated by removal of CAM-1 complements those elevated by removal of LIN-17 and LIN-18, but the Wnts elevated by removal of LIN-17 and LIN-18 do not complement each other. Another possibility is that removal of *lin-17* or *lin-18* only mildly increases extracellular Wnt levels and that these levels do not cross the threshold unless *cam-1*, a more important regulator of Wnt levels, is also removed. We next tested whether overexpression of LIN-17 and LIN-18 might reduce extracellular Wnt levels and cause a UI phenotype. *Plin-18::LIN-18::GFP* (Inoue et al., 2004) caused a weak UI phenotype (Table S2) and significantly increased the fraction of *cwn-1(lf)* worms with a more severe UI phenotype (< 2 VPCs induced), consistent with the hypothesis that *lin-18* expression affects extracellular Wnt levels. Although transgenes can sometimes decrease gene expression by titrating out transcriptional activators (Gill and Ptashne, 1988), it is unlikely that the phenotype we see here is caused by reduced *lin-18* expression because *Plin-18::LIN-18::GFP* is an overexpression construct (not a *promoter::GFP* array) and rescues the *lin-18(lf)* phenotype (Inoue et al., 2004). However, we cannot rule out that the phenotype is due to promoter effects on a different gene. In

contrast to *Plin-18::LIN-18::GFP*, *Plin-17::LIN-17::GFP* did not affect vulval induction; however, *Plin-17::LIN-17::GFP* caused a mild, though not statistically significant, increase in the fraction of UI *cwn-1(lf)* worms. Again, it is unlikely that this phenotype is caused by promoter effects on *lin-17* expression because *Plin-17::LIN-17::GFP* rescues the P7.p polarity defect of *lin-17(lf)* worms (data not shown). Also, loss of *lin-17* does not increase the fraction of UI *cwn-1(lf)* worms (see Methods and Table S2). As with *lin-18* overexpression, we cannot rule out that the phenotype is due to promoter effects on a different gene. Because *Plin-17::LIN-17::GFP* displays a more restricted expression pattern than *Plin-18::LIN-18::GFP*, we expressed LIN-17 in body wall muscle using the *myo-3* promoter (Okkema et al., 1993). *Pmyo-3::LIN-17::GFP* did not significantly affect vulval induction, nor did it enhance the UI phenotype of *cwn-1(lf)* worms. Although the mechanism by which *lin-17* and *lin-18* mutations provide a sensitized background for *cam-1* effects on vulval induction is unclear, the role of *cam-1* as an inhibitor of vulval induction is confirmed by other experiments not dependent on *lin-17* or *lin-18* mutants (e.g. *cam-1(lf); lin-3(rf)*, *cam-1(lf); lin-12(gf/+)* see above).

The CAM-1 ECD binds to Wnts CWN-1, EGL-20 and MOM-2.

Our data suggest that non-vulval CAM-1 normally antagonizes Wnt signaling by a mechanism dependent on the CAM-1 ECD, possibly by directly binding to and impeding Wnts. Detecting association of the CAM-1 ECD with Wnts by co-immunoprecipitation experiments was impractical due to the typical insolubility of Wnt proteins and the lack of available recombinant *C. elegans* Wnts. To circumvent these obstacles we employed a reverse binding assay (Rulifson et al., 2000; Wu and Nusse, 2002) where *C. elegans* Wnts

are expressed in stably transfected insect cells and tethered to the membrane by amino-terminal fusion to Neurotactin (Nrt) (Fig. 2A). Binding is determined by measuring the alkaline phosphatase (AP) activity retained by the cells after incubation with secreted CAM-1 CRD-AP fusion proteins. As an internal control we assayed all combinations of *C. elegans* Wnts and Wnt receptors. This set included five Wnts (LIN-44, CWN-1, EGL-20, CWN-2, MOM-2), four Fz receptors (MIG-1, LIN-17, MOM-5, CFZ-2), and two RTKs (CAM-1/ROR, LIN-18/RYK) and confirmed that no Wnt bound indiscriminately to all receptors (Table S3). Consistent with our genetic data, we found that the CAM-1 CRD bound to CWN-1 and EGL-20 significantly more than to control cells (Fig. 2B). The CAM-1 CRD also bound significantly to cells expressing Nrt-MOM-2.

Overexpression of CAM-1 non-autonomously inhibits vulval induction

If CAM-1 negatively regulates Wnt signaling by binding to and impeding Wnts, then overexpression of CAM-1 in non-vulval tissue might cause a UI phenotype. To test this, we made full-length *CAM-1::GFP* translational fusions driven by the tissue-specific promoters *Psnb-1* (pan-neuronal) (Nonet et al., 1998), *Pmyo-3* (muscle) (Okkema et al., 1993), *Pdpy-8* (epidermis), *Plin-31* (VPCs) (Tan et al., 1998), *Psur-2* (VPCs) (Singh and Han, 1995), *Plst-1* (VPCs) (Yoo et al., 2004) and *Pfos-1a* (somatic gonad) (Sherwood and Sternberg, 2003) (Fig. 3). We observed membrane-localized GFP in the expected tissues for all lines except *Plin-31* in which we were unable to detect fluorescence. We found that expression of *CAM-1::GFP* in body wall muscle (*myo-3* promoter) and in neurons (*snb-1* promoter) caused a UI phenotype (Table 2) similar to loss of *bar-1/Beta-catenin* and Wnt genes: specifically, P3.p adopts the F fate at an increased frequency, P4.p is often F instead of 3°, and P5.p

occasionally adopts the F or 3° fate instead of the normal 2° fate. Also similar to mutations in Wnt pathway components, both *Pmyo-3::CAM-1::GFP* and *Psnb-1::CAM-1::GFP* had a greater effect on the anterior VPCs than the posterior VPCs. To test whether this activity of *cam-1* requires the intracellular domain, we expressed a version of *CAM-1::GFP* lacking the intracellular domain (*CAM-1ΔIntra::GFP*) in muscle. *Pmyo-3::CAM-1ΔIntra::GFP* caused a UI phenotype indicating that the intracellular domain is not required. This observation is consistent with our analysis of *cam-1* mutant alleles. Although expressed at levels similar to the other transgenes, based on GFP expression, neither *Psur-2::CAM-1::GFP*, *Plst-1::CAM-1::GFP*, *Pdpy-8::CAM-1::GFP* nor *Pfos-1a::CAM-1::GFP* caused a UI phenotype. These CAM-1 over-expression experiments indicate that CAM-1 can non-autonomously inhibit vulval induction. Because our analysis of *cam-1* mutant alleles suggested that the CAM-1 CRD is necessary to inhibit vulval induction, we tested whether overexpression of the membrane-tethered CAM-1 CRD is sufficient to inhibit vulval induction. The *cwEx164* transgene expresses *CAM-1::GFP* lacking the intracellular domain and the extracellular immunoglobulin and kringle domains (*CAM-1ΔIgKriIntra::GFP*) (Kim and Forrester, 2003). *Pcam-1::CAM-1ΔIgKriIntra::GFP* was sufficient to cause frequent fusion of P3.p and P4.p and to cause occasional F or 3° fates in P5.p. The mild effects on P5.p fate caused by *Pcam-1::CAM-1ΔIgKriIntra::GFP* compared to other transgenes could be due to less robust expression under *Pcam-1* or due to instability of the severely truncated protein.

Loss of any single Wnt causes only minor induction defects (Gleason et al., 2006) (Table 1), therefore *Pmyo-3::CAM-1::GFP* and *Psnb-1::CAM-1::GFP* likely interfere with multiple Wnts. To determine with which Wnts *CAM-1::GFP* interferes, we analyzed *Pmyo-3::CAM-1::GFP* in worms mutant for *cwn-1*, *egl-20* and *cwn-2*, the three Wnts contributing

most to VPC induction (Table 2). Loss of a Wnt that retains inductive activity in a *Pmyo-3::CAM-1::GFP* background should display enhancement of the UI phenotype, whereas loss of a Wnt that is already fully antagonized by *Pmyo-3::CAM-1::GFP* should not enhance the phenotype. Both *egl-20(rf)* and *cwn-2(lf)* significantly enhanced the UI phenotype of *Pmyo-3::CAM-1::GFP* (Table 2), indicating that these Wnts retain some or all of their inductive activity. In contrast, we found that mutation of *cwn-1* did not significantly enhance the UI phenotype, indicating that the inductive activity of CWN-1 is largely abrogated by *Pmyo-3::CAM-1::GFP*.

Discussion

Despite studies in several different organisms, the mechanism of ROR action remains elusive. In this work, we characterized the role of CAM-1/ROR as a regulator of Wnt distribution and determined that one function of ROR proteins is to sequester Wnts (Fig. 4).

Previously, it was hypothesized that CAM-1/ROR can sequester Wnts. Kim et al. (Kim and Forrester, 2003) found that expression of the membrane-anchored CAM-1 ECD was sufficient to rescue the cell migration defects of *cam-1(lf)* worms and that over-expression of the membrane-anchored CAM-1 CRD caused defects in HSN and Q cell migration similar to those caused by mutation of *egl-20/Wnt*, leading these authors to propose that the CAM-1 CRD might sequester EGL-20/Wnt. Indeed, CAM-1 was later shown to inhibit EGL-20 signaling in cell migration independently of the CAM-1 cytoplasmic domain (Forrester et al., 2004). However, the mechanism of this inhibition was not demonstrated. In particular, as the ROR2 CRD is capable of dimerizing with Fz (Oishi et al., 2003), the CAM-1 ECD could potentially function cell-autonomously by inhibiting the WNT receptor.

The genetic data presented here indicate that CAM-1 antagonizes Wnt signaling during vulval development. We found that in *lin-17* and *lin-18* mutant backgrounds, *cam-1* mutations cause an OI phenotype due to elevated levels of Wnt activity. Loss of *lin-17* or *lin-18* might provide a sensitized background if LIN-17 and LIN-18, like CAM-1, also affect the extracellular distribution of Wnts. According to this hypothesis, mutation of *lin-17* or *lin-18* would similarly result in elevated extracellular Wnt levels; however, our data do not conclusively support this hypothesis.

Using vulval development as a model, we showed conclusively that CAM-1/ROR can act non-autonomously. The source of the Wnts required for vulval induction is unknown and a sequestration model would require that *Pmyo-3::CAM-1::GFP* (muscle expression) and *Psnb-1::CAM-1::GFP* (neuronal expression) are expressed in positions that enable them to restrict diffusion or transport of the Wnts to the VPCs (Fig. 3H). EGL-20/Wnt forms a gradient of decreasing concentration from its site of expression in the tail extending anteriorly past the VPCs (Coudreuse et al., 2006). The distance between the source of EGL-20 and the VPCs provides ample opportunity for CAM-1 expressed in nervous or muscle tissue to prevent EGL-20 from reaching the VPCs. CWN-1/Wnt is expressed in ventral cord neurons (VCNs) and posterior body wall muscle (Gleason et al., 2006; Hilliard and Bargmann, 2006). Endogenous CAM-1 expression in body wall muscle and VCNs, which are in close proximity to the VPCs (Fig. 3H), could place CAM-1 between the source of *cwn-1* expression and the VPCs allowing CAM-1 to act as a barrier and limit the amount of Wnt signal received by the VPCs (Fig. 4). CAM-1 could also function at the Wnt source to limit secretion. Consistent with inhibition by sequestration, CAM-1 over-expression antagonizes

Wnt signaling independently of the cytoplasmic domain. Also, phenotypes of *cam-1* mutants indicate that the membrane-anchored ECD is sufficient to inhibit Wnt signaling.

A sequestration model also predicts that CAM-1 specifically binds the Wnts that it antagonizes. In agreement with our genetic data, we found that the CAM-1 CRD can bind to Wnts CWN-1, EGL-20 and MOM-2 *in vitro*. Our initial experimental design included measuring binding at various concentrations of CRD-AP that would allow us to calculate the binding affinity of each receptor-ligand pair. However, our preliminary results showed high background binding to untransfected S2 cells. We thus chose the concentration of CRD-AP where we saw the greatest difference between binding to Nrt-Wnt-expressing and to untransfected cells and tested all of the combinations at this concentration in triplicate. Wu and Nusse (Wu and Nusse, 2002) report that DFz2CRD-AP bound to Nrt-Wg expressing cells 10-fold higher than to untransfected cells. In our experiments, we never observed a difference greater than two-fold. Weaker binding could be caused by a species barrier whereby the *Drosophila* cells do not express a necessary cofactor or do not process Wnts in a manner conducive to high-affinity binding to *C. elegans* receptors. Although the binding we detected is not as robust as that observed for *Drosophila* Wnts and Fzs we feel that it may still be informative and have included these values in a supplemental table (Table S3).

While sequestration through Wnt-CRD binding can account for many functions of CAM-1/ROR, there are examples where CAM-1 may function by a different mechanism. The membrane-anchored ECD, but not the membrane-anchored CRD alone, was sufficient to rescue all cell migration defects of *cam-1(lf)* worms (Kim and Forrester, 2003). In cases where the CRD was not sufficient, ligand binding may require additional CAM-1 ECD(s) – e.g. the Kringle or Ig domain - or may be cases where CAM-1 functions by a non-

sequestration mechanism. Other examples of CAM-1 function that are probably not due to sequestration include cell-autonomous roles in CAN migration (Forrester et al., 1999) and development of the ASI sensory neuron (Koga et al., 1999). Also, CAM-1 function in Pn.aap division orientation in males requires CAM-1 kinase activity (Forrester et al., 1999; Kim and Forrester, 2003). While our study has furthered our understanding of ROR function, the role of the cytoplasmic domains remains elusive. CAM-1 shares 44% identity in the kinase domain to hROR1 and hROR2 and none of the 21 invariant amino acids is altered (Forrester, 2002). Although ROR proteins have demonstrated kinase activity (Masiakowski and Carroll, 1992; Oishi et al., 1999), the precise function of this activity has not been identified.

Our genetic and biochemical observations that CAM-1 interacts not only with EGL-20, but also with other Wnts, suggest that CAM-1 is an important general regulator of Wnt activity rather than a specific EGL-20 antagonist. As a system where neighboring cells reproducibly adopt distinct fates, vulva induction has enabled us to study how CAM-1 affects the precision of Wnt distribution. The subtle effects we observed upon *cam-1* manipulation suggest that CAM-1 serves to buffer Wnt levels rather than to dramatically affect Wnt localization. Such buffering mechanisms may provide robustness to the Wnt morphogen gradient. The high degree of similarity between CAM-1 and vertebrate ROR proteins (Forrester, 2002), in addition to the ability of ROR proteins to inhibit Wnt signaling in a kinase-independent manner, suggest a conserved function of ROR proteins to fine-tune the spatial profile of Wnt activity and to help create regions of distinct cell fate in complex multicellular organisms.

Acknowledgements

We thank Gladys Medina and Barbara Perry for technical assistance and members of the Sternberg lab for helpful discussions. For useful reagents and worms we thank W. Forrester, C. Wu, A. Fire, A.V. Maricq, M. Francis, D. Sherwood, I. Greenwald and H. Sawa. Some Nematode strains were from the *Caenorhabditis* Genetics Center, funded by the NIH National Center for Research Resources. We thank Cheryl Van Buskirk, Ryan Baugh, Jagan Srinivasan and Mihoko Kato for critically reading the manuscript. We are grateful to the Benzer lab (especially Gil Carvallo) for use of their microplate spectrophotometer, the Hay lab for use of their tissue culture hood, Jost Vielmetter and Inderjit Nangiana of Caltech Protein Expression Facility for production of CRD-AP conditioned media, and Julie Gleason for kindly exchanging *lin-17* and *mom-5* mutant alleles. PWS is an investigator with HHMI and JLG was supported by the Thomas Hunt Morgan Fellowship for graduate study toward the Doctor of Philosophy degree in Biology at the California Institute of Technology.

Materials and Methods

Strains and Genetics

C. elegans was handled as described previously (Brenner, 1974). All strains used are derivatives of *C. elegans* N2 Bristol strain. LGI: *lin-17(n671)*, *lin-17(n677)*, *lin-44(n1792)*, *mom-5(or57)*, *mom-5(zu193)*. LGII: *cwn-1(ok546)*, *cam-1(gm122)*, *cam-1(ks52)*, *cam-1(gm105)*, *cam-1(sa692)*, *cam-1(ak37)*, *rol-6(e187)*. LGIII: *lin-12(n952)*, *unc-119(ed4)*. LGIV: *lin-3(e1417)*, *lin-3(n378)*, *ark-1(sy247)*, *dpy-20(e1282)*, *egl-20(n585)*, *egl-20(hu120)*, *cwn-2(ok895)*. LGV: *him-5(e1490)*. LGX: *lin-18(e620)*, *bar-1(ga80)*, *gap-1(n1691)*, *unc-2(e55)*, *sli-1(sy143)*, *daf-3(mgDf90)*. For RNAi experiments, gravid hermaphrodites were fed RNAi-expressing bacteria and L4 progeny were scored.

Vulval phenotypes

Vulval induction was scored in mid-L4 stage hermaphrodites by counting vulval cell nuclei using Nomarski DIC optics. If both VPC daughters divided, that VPC was counted as induced (1.0). If only one VPC daughter divided, that VPC was counted as half-induced (0.5). *Pmyo-3::CAM-1::GFP* displayed increased penetrance of the UI phenotype at 25C. Thereafter, all *CAM-1::GFP* transgenic worms (except *cwEx164*) were grown at 25C. All other strains were grown at 20C.

Contributions of LIN-17 and MOM-5 to vulval induction

Our results are inconsistent with the positive role for LIN-17 in vulva induction reported by Gleason et al. (2006). While Gleason et al. (2006) report that 12% of *lin-17(n671)* worms

are UI, we did not observe any UI *lin-17(n671)* worms. To address this discrepancy we obtained *lin-17(n671)* worms used by Gleason et al. (2006) from the Eisenmann lab (-*DE*) and did not detect any UI worms (Table S2). By contrast, we observed one *lin-17(n671)-DE* worm that was OI and had 5 VPCs induced (Figure S1). Our examination of *mig-1(e1787); lin-17(n671)* and *lin-17(n671); cfz-2(ok1201)* double mutants did not reveal a UI phenotype. Also, *lin-17(lf)* did not enhance the UI phenotype of *cwn-1(lf)* mutant worms. *lin-17(n671)-DE; cam-1(lf)* double mutants worms recapitulated the synthetic OI phenotype, as did double mutants containing another *lin-17* allele, *n677*. The elevated Wnt signaling observed in the *lin-17(lf); cam-1(lf)* background, which cannot be explained by signaling through LIN-17, is likely due to increased signaling through another Frizzled receptor such as MOM-5. Thus, we examined vulval induction in *mom-5* mutants (Table S2). In contrast to *lin-17*, we found that mutation of *mom-5* caused a dramatic UI phenotype, suggesting that *mom-5*, but not *lin-17*, is required for vulval induction.

Transgenics

Extrachromosomal arrays were generated by co-injecting *CAM-1b::GFP* driven by various promoters with *unc-119 (+)* [60ng/μl] into *unc-119(ed4)* hermaphrodites as described (Mello et al., 1991). Of the three *cam-1* splice variants, the ‘b’ isoform was selected because it appears to have a weak signal sequence, whereas the ‘a’ and ‘c’ variants have no detectable signal sequence. *cam-1* tissue-specific constructs were made by shuttling various promoters upstream of *CAM-1b::GFP* using 5’ BamHI and 3’ NotI restriction sites. All constructs were injected at [50ng/μL] except *syEx863*, *syEx864*, and *syIs198*, which were injected at [75ng/μl]. To facilitate examination of *Pcam-1::CAM-1::GFP* and *Pcam-1::CAM-*

lΔIgKriIntra::GFP, *dpy-20(e1282)* was crossed into strains WF1863 and WF1729, respectively (Forrester et al., 1999; Kim and Forrester, 2003), to suppress the roller phenotype. *syIs75(Plin-18::LIN-18::GFP)* is an integrated line of *syEx363[pTI00.43(60ng/μl) + unc-119(+)(30ng/μl)]* (Inoue et al., 2004). *syEx1022[LIN-17::GFP(40ng/μl) + unc-119(+)(90ng/μl) + myo-2::DsRed(15ng/μl)]* was made with plasmid PSH22 (gift from H. Sawa). *syEx1020[Pmyo-3::LIN-17::GFP(50ng/μl) + unc-119(+)(90ng/μl) + Pmyo-2::DsRed(15ng/μl)]* contains a *Pmyo-3::LIN-17::GFP* plasmid that was made by amplifying the N-terminal portion of *lin-17* from PSH22 (forward primer: TCCATCTAGAGGCTCCTTCTCCAAAATGATGCATTCTTTGGGC, reverse primer: GCACAATGCGACTTGGGATCGTGTGG). The *lin-17* C-terminal portion was amplified from cDNA (forward primer: CCAAGCCAACCGGGTGCCCCAG, reverse primer: TCTTCCGGAACGACCTTACTGGGTCTCCATGAATTCTG). The C-terminal portion was cleaved by BamHI and BspEI and transferred into Fire vector L4817 (*Pmyo-3*) that had been cleaved by AgeI and BamHI. The N-terminal portion was then cleaved by XbaI (cuts twice) and BamHI. The XbaI-BamHI fragment was transferred in first, followed by the XbaI-XbaI fragment.

Generating CAM-1b::GFP backbone

To make the *CAM-1b::GFP* backbone, C01G6.8a cDNA was first inserted into Fire vector pPD49.83 using the NheI site. To create *hs::CAM-1::GFP*, BspEI and ApaI sites were used to switch the 3' end of *cam-1* with the 3' end of *CAM-1::GFP* from plasmid pMini3 (gift from Wayne Forrester) which also includes the last two small introns of *cam-1*. Next, the 5' end of C01G6.8b was amplified from cDNA using forward primer

ATAAGATGCGGCCGCATGGAGGGTACATCAACTGGTCAACG to add a NotI site to the 5' end (reverse primer TTCCAATGCATTGGCATCTAGCCATCGTTCTGATACAGC). C01G6.8b 5' end was then cloned into pBluescript via NotI and BstXI and transferred into *hs::CAM-1::GFP* using BamHI and BstEII creating *CAM-1b::GFP* with a NotI site 5' of the ATG.

Tissue-specific constructs

syEx778, *syEx781* and *syEx814* contain 2.4kb of *Pmyo-3* (*myo-3* 5' regulatory region) amplified from Fire vector L4817 with forward primer

CGCGGATCCGGTCGGCTATAATAAGTTCTTGAATA and reverse primer

ATAGTTTAGCGGCCTCTAGATGGATCTAGTGGTCGTG. *syEx798* and *syEx799*

contain 3.4 kb of *Pdpy-8* amplified from genomic DNA using forward primer

CGCGGATCCGAACTGAGAATGCTGACGGATG and reverse primer

ATAGTTTAGCGGCCGATGGGAAAATAAGAAAAGGAAATGTGG. *syEx863* and

syEx864 contain 5.5kb of *Psur-2* amplified from cosmid F39B2 using forward primer

CGCGGATCCCGAAATTCGGTAGATTTGGGC and reverse primer

ATAGTTTAGCGGCCGCTTGTTCCTGAAAATGTAATAATTTTC. *syEx780* and

syEx777 contain 4.9kb of *Pfos-1a* amplified from plasmid pDRS46 (Sherwood and

Sternberg, 2003) using forward primer

CGCGGATCCTGGGCAGCTGTAAAACGTCTTTAC and reverse primer

ATAGTTTAGCGGCCTCCACTCTCTTATATAGCAGAGGTG. *syEx775* and *syEx776*

contain 3kb of *Psnb-1* amplified from plasmid *Psnb-1::slo-1* (Davies et al., 2003) using

forward primer CGCGGATCCAAGCTTTTTGCTGAAATCTAGGATTAC and reverse

primer ATAGTTTAGCGGCCGCTGTTCCCTGAAATGAAGCGA. *syIs198* contains 1.6kb of *Plst-1* amplified from plasmid *lst-1p-gfp-lacz* (gift from Iva Greenwald c/o Andrew Yoo) using forward primer CGCGGATCCCAATTGTTACTACTGACGGCATTCC and reverse primer

ATAGTTTAGCGGCCGCGTCAAATAATTCTTTTGAATGAGAAAGAACTTGGC. To make *Pmyo-3::CAM-1ΔIntra::GFP*, blunt HpaI and MscI sites were used to switch the C-terminus of *Pmyo-3::CAM-1b::GFP* with an HpaI-HpaI fragment (10.8kb) from pDM108 (Francis et al., 2005) that contains *cam-1* minus the kinase domain (removal of C-terminal 346 codons), fused to GFP.

Immunoblotting

Lysates of transfected and untransfected *Drosophila* S2 cells were run on a 4–12% NuPAGE Bis-Tris gel (Invitrogen) and probed with anti-HA monoclonal antibody G036 (Abm) or polyclonal anti-GAPDH (Sullivan et al., 2003).

Reverse binding assay

The CRD-AP fusion proteins were made in 293T cells as previously described for *Drosophila* CRD-AP fusions (Wu and Nusse, 2002). The CRD of the sFRP3-AP fusion was replaced with the CRD (or WIF) of *C. elegans* receptors. Each construct contains sFRP3 signal sequence, *C. elegans* CRD (or WIF), C-terminal domain of sFRP3 and AP. Sequences across the signal sequence fusion junction are (CRD/WIF in bold): CAM-1, PGAQAAGSNYAPVA, LIN-18, PGAQANVNM**FISK**, LIN-17, PGAQASIFDQAVKG, MOM-5, PGAQADQRLS**S**TSI, CFZ-2, PGAQALFG**KRQ**KCE, MIG-1,

PGAQA**QRCQKVDHE**. Downstream fusion junctions are (CRD/WIF domains in bold):

CAM-1, **STSNCIHALAIVTAD**, LIN-18, **TDSIDKTRALAIVTAD**, LIN-17,

PPELCMNALAIVTAD, MOM-5, **VTDLCVDALAIVTAD**, CFZ-2,

TGNICADALAIVTAD, MIG-1, **NREKMCMNALAIVTAD**. To determine the

concentration of CRD-AP fusion protein in the conditioned medium we immunoprecipitated

the CRD-AP fusion proteins with anti-AP antibody (Sigma A-2951), resolved the

immunocomplexes by SDS-PAGE and estimated the protein concentration after staining with

Coomassie Blue. Activities of the CRD-AP fusion proteins were assayed colorimetrically

after incubation with the AP substrate. Each of the CRD-AP fusion proteins was determined

to have similar specific activity of 3 pmol/unit activity. The protein was concentrated by

ammonium sulfate precipitation (3.2 M) followed by dialysis against Hank's Balanced Salt

Solution without calcium and magnesium (HBSS) and the samples were then normalized by

AP activity. The Neurotactin (Nrt) -HA-Wnt fusion proteins were made as previously

described for *Drosophila* Nrt-HA-Wnt fusions (Wu and Nusse, 2002), with the exception that

we used the pCoBlast selection vector (Invitrogen) and 25 µg/ml Blasticidin for selection.

The sequences around the regions linking HA and the Wnts are (Wnt sequences are bold):

Nrt-CWN-1, WEDEEAS**LAANRFD**, Nrt-CWN-2 WEDEEAS**LVQSL**L, Nrt-EL-20

WEDEEAS**PSATYST** WEDEEAS**GHNVKP**, Nrt-MOM-2 WEDEEAS**KSADAWW**, and

Nrt-LIN-44 WEDEEAS**APAGKIV**. For complete binding assay protocol and raw data see

Table S3.

- Ailion, M. and Thomas, J. H.** (2003). Isolation and characterization of high-temperature-induced Dauer formation mutants in *Caenorhabditis elegans*. *Genetics* **165**, 127-44.
- Bhanot, P., Brink, M., Samos, C. H., Hsieh, J. C., Wang, Y., Macke, J. P., Andrew, D., Nathans, J. and Nusse, R.** (1996). A new member of the frizzled family from *Drosophila* functions as a Wingless receptor. *Nature* **382**, 225-30.
- Billiard, J., Way, D. S., Seestaller-Wehr, L. M., Moran, R. A., Mangine, A. and Bodine, P. V.** (2005). The orphan receptor tyrosine kinase Ror2 modulates canonical Wnt signaling in osteoblastic cells. *Mol Endocrinol* **19**, 90-101.
- Brenner, S.** (1974). The genetics of *Caenorhabditis elegans*. *Genetics* **77**, 71-94.
- Coudreuse, D. Y., Roel, G., Betist, M. C., Destree, O. and Korswagen, H. C.** (2006). Wnt Gradient Formation Requires Retromer Function in Wnt-Producing Cells. *Science*.
- Davies, A. G., Pierce-Shimomura, J. T., Kim, H., VanHoven, M. K., Thiele, T. R., Bonci, A., Bargmann, C. I. and McIntire, S. L.** (2003). A central role of the BK potassium channel in behavioral responses to ethanol in *C. elegans*. *Cell* **115**, 655-66.
- Eisenmann, D. M.** (2005). Wnt Signaling. In *Wormbook*, (ed. I. Greenwald): The *C. elegans* Research Community, WormBook.
- Eisenmann, D. M., Maloof, J. N., Simske, J. S., Kenyon, C. and Kim, S. K.** (1998). The beta-catenin homolog BAR-1 and LET-60 Ras coordinately regulate the Hox gene *lin-39* during *Caenorhabditis elegans* vulval development. *Development* **125**, 3667-80.
- Ferguson, E. L. and Horvitz, H. R.** (1985). Identification and characterization of 22 genes that affect the vulval cell lineages of the nematode *Caenorhabditis elegans*. *Genetics* **110**, 17-72.
- Ferguson, E. L., Sternberg, P. W. and Horvitz, H. R.** (1987). A genetic pathway for the specification of the vulval cell lineages of *Caenorhabditis elegans*. *Nature* **326**, 259-67.
- Forrester, W. C.** (2002). The Ror receptor tyrosine kinase family. *Cell Mol Life Sci* **59**, 83-96.
- Forrester, W. C., Dell, M., Perens, E. and Garriga, G.** (1999). A *C. elegans* Ror receptor tyrosine kinase regulates cell motility and asymmetric cell division. *Nature* **400**, 881-5.
- Forrester, W. C., Kim, C. and Garriga, G.** (2004). The *Caenorhabditis elegans* Ror RTK CAM-1 inhibits EGL-20/Wnt signaling in cell migration. *Genetics* **168**, 1951-62.
- Forrester, W. C., Perens, E., Zallen, J. A. and Garriga, G.** (1998). Identification of *Caenorhabditis elegans* genes required for neuronal differentiation and migration. *Genetics* **148**, 151-65.
- Francis, M. M., Evans, S. P., Jensen, M., Madsen, D. M., Mancuso, J., Norman, K. R. and Maricq, A. V.** (2005). The Ror receptor tyrosine kinase CAM-1 is required for ACR-16-mediated synaptic transmission at the *C. elegans* neuromuscular junction. *Neuron* **46**, 581-94.
- Gill, G. and Ptashne, M.** (1988). Negative effect of the transcriptional activator GAL4. *Nature* **334**, 721-4.
- Gleason, J. E., Korswagen, H. C. and Eisenmann, D. M.** (2002). Activation of Wnt signaling bypasses the requirement for RTK/Ras signaling during *C. elegans* vulval induction. *Genes Dev* **16**, 1281-90.
- Gleason, J. E., Szyleyko, E. A. and Eisenmann, D. M.** (2006). Multiple redundant Wnt signaling components function in two processes during *C. elegans* vulval development. *Dev Biol*.
- Greenwald, I. S., Sternberg, P. W. and Horvitz, H. R.** (1983). The *lin-12* locus specifies cell fates in *Caenorhabditis elegans*. *Cell* **34**, 435-44.

- Han, C., Yan, D., Belenkaya, T. Y. and Lin, X.** (2005). *Drosophila* glypicans Dally and Dally-like shape the extracellular Wingless morphogen gradient in the wing disc. *Development* **132**, 667-79.
- Han, M. and Sternberg, P. W.** (1990). *let-60*, a gene that specifies cell fates during *C. elegans* vulval induction, encodes a ras protein. *Cell* **63**, 921-31.
- Harris, J., Honigberg, L., Robinson, N. and Kenyon, C.** (1996). Neuronal cell migration in *C. elegans*: regulation of Hox gene expression and cell position. *Development* **122**, 3117-31.
- Hikasa, H., Shibata, M., Hiratani, I. and Taira, M.** (2002). The *Xenopus* receptor tyrosine kinase *Xror2* modulates morphogenetic movements of the axial mesoderm and neuroectoderm via Wnt signaling. *Development* **129**, 5227-39.
- Hill, R. J. and Sternberg, P. W.** (1992). The gene *lin-3* encodes an inductive signal for vulval development in *C. elegans*. *Nature* **358**, 470-6.
- Hilliard, M. A. and Bargmann, C. I.** (2006). Wnt signals and frizzled activity orient anterior-posterior axon outgrowth in *C. elegans*. *Dev Cell* **10**, 379-90.
- Hopper, N. A., Lee, J. and Sternberg, P. W.** (2000). ARK-1 inhibits EGFR signaling in *C. elegans*. *Mol Cell* **6**, 65-75.
- Inoue, T., Oz, H. S., Wiland, D., Gharib, S., Deshpande, R., Hill, R. J., Katz, W. S. and Sternberg, P. W.** (2004). *C. elegans* LIN-18 is a Ryk ortholog and functions in parallel to LIN-17/Frizzled in Wnt signaling. *Cell* **118**, 795-806.
- Kani, S., Oishi, I., Yamamoto, H., Yoda, A., Suzuki, H., Nomachi, A., Iozumi, K., Nishita, M., Kikuchi, A., Takumi, T. et al.** (2004). The receptor tyrosine kinase Ror2 associates with and is activated by casein kinase Iepsilon. *J Biol Chem* **279**, 50102-9.
- Katz, W. S., Hill, R. J., Clandinin, T. R. and Sternberg, P. W.** (1995). Different levels of the *C. elegans* growth factor LIN-3 promote distinct vulval precursor fates. *Cell* **82**, 297-307.
- Kawano, Y. and Kypta, R.** (2003). Secreted antagonists of the Wnt signalling pathway. *J Cell Sci* **116**, 2627-34.
- Kim, C. and Forrester, W. C.** (2003). Functional analysis of the domains of the *C. elegans* Ror receptor tyrosine kinase CAM-1. *Dev Biol* **264**, 376-90.
- Kimble, J.** (1981). Alterations in cell lineage following laser ablation of cells in the somatic gonad of *Caenorhabditis elegans*. *Dev Biol* **87**, 286-300.
- Koga, M., Take-uchi, M., Tameishi, T. and Ohshima, Y.** (1999). Control of DAF-7 TGF- α expression and neuronal process development by a receptor tyrosine kinase KIN-8 in *Caenorhabditis elegans*. *Development* **126**, 5387-98.
- Korswagen, H. C., Coudreuse, D. Y., Betist, M. C., van de Water, S., Zivkovic, D. and Clevers, H. C.** (2002). The Axin-like protein PRY-1 is a negative regulator of a canonical Wnt pathway in *C. elegans*. *Genes Dev* **16**, 1291-302.
- Logan, C. Y. and Nusse, R.** (2004). The Wnt signaling pathway in development and disease. *Annu Rev Cell Dev Biol* **20**, 781-810.
- Masiakowski, P. and Carroll, R. D.** (1992). A novel family of cell surface receptors with tyrosine kinase-like domain. *J Biol Chem* **267**, 26181-90.
- Mello, C. C., Kramer, J. M., Stinchcomb, D. and Ambros, V.** (1991). Efficient gene transfer in *C. elegans*: extrachromosomal maintenance and integration of transforming sequences. *Embo J* **10**, 3959-70.
- Mikels, A. J. and Nusse, R.** (2006a). Purified Wnt5a Protein Activates or Inhibits beta-Catenin-TCF Signaling Depending on Receptor Context. *PLoS Biol* **4**, e115.

- Mikels, A. J. and Nusse, R.** (2006b). Wnts as ligands: processing, secretion and reception. *Oncogene* **25**, 7461-8.
- Nonet, M. L., Saifee, O., Zhao, H., Rand, J. B. and Wei, L.** (1998). Synaptic transmission deficits in *Caenorhabditis elegans* synaptobrevin mutants. *J Neurosci* **18**, 70-80.
- Oishi, I., Suzuki, H., Onishi, N., Takada, R., Kani, S., Ohkawara, B., Koshida, I., Suzuki, K., Yamada, G., Schwabe, G. C. et al.** (2003). The receptor tyrosine kinase Ror2 is involved in non-canonical Wnt5a/JNK signalling pathway. *Genes Cells* **8**, 645-54.
- Oishi, I., Takeuchi, S., Hashimoto, R., Nagabukuro, A., Ueda, T., Liu, Z. J., Hatta, T., Akira, S., Matsuda, Y., Yamamura, H. et al.** (1999). Spatio-temporally regulated expression of receptor tyrosine kinases, mRor1, mRor2, during mouse development: implications in development and function of the nervous system. *Genes Cells* **4**, 41-56.
- Okkema, P. G., Harrison, S. W., Plunger, V., Aryana, A. and Fire, A.** (1993). Sequence requirements for myosin gene expression and regulation in *Caenorhabditis elegans*. *Genetics* **135**, 385-404.
- Rulifson, E. J., Wu, C. H. and Nusse, R.** (2000). Pathway specificity by the bifunctional receptor frizzled is determined by affinity for wingless. *Mol Cell* **6**, 117-26.
- Savage-Dunn, C.** (2005). TGF- β signaling. In *WormBook*, ed., (ed. I. Greenwald): The C. elegans Research Community, WormBook.
- Sawa, H., Lobel, L. and Horvitz, H. R.** (1996). The *Caenorhabditis elegans* gene lin-17, which is required for certain asymmetric cell divisions, encodes a putative seven-transmembrane protein similar to the *Drosophila* frizzled protein. *Genes Dev* **10**, 2189-97.
- Sherwood, D. R. and Sternberg, P. W.** (2003). Anchor cell invasion into the vulval epithelium in *C. elegans*. *Dev Cell* **5**, 21-31.
- Simske, J. S. and Kim, S. K.** (1995). Sequential signalling during *Caenorhabditis elegans* vulval induction. *Nature* **375**, 142-6.
- Singh, N. and Han, M.** (1995). sur-2, a novel gene, functions late in the let-60 ras-mediated signaling pathway during *Caenorhabditis elegans* vulval induction. *Genes Dev* **9**, 2251-65.
- Sternberg, P. W.** (2005). Vulval development. In *WormBook*, (ed. B. J. Meyer): The C. elegans Research Community, WormBook.
- Sternberg, P. W. and Horvitz, H. R.** (1989). The combined action of two intercellular signaling pathways specifies three cell fates during vulval induction in *C. elegans*. *Cell* **58**, 679-93.
- Sullivan, D. T., MacIntyre, R., Fuda, N., Fiori, J., Barrilla, J. and Ramizel, L.** (2003). Analysis of glycolytic enzyme co-localization in *Drosophila* flight muscle. *J Exp Biol* **206**, 2031-8.
- Sulston, J. E. and Horvitz, H. R.** (1977). Post-embryonic cell lineages of the nematode, *Caenorhabditis elegans*. *Dev Biol* **56**, 110-56.
- Sulston, J. E. and White, J. G.** (1980). Regulation and cell autonomy during postembryonic development of *Caenorhabditis elegans*. *Dev Biol* **78**, 577-97.
- Sundaram, M. V.** (2006). RTK/Ras/MAPK signaling. In *WormBook*, ed., (ed. I. Greenwald): The C. elegans Research Community, WormBook,.
- Tan, P. B., Lackner, M. R. and Kim, S. K.** (1998). MAP kinase signaling specificity mediated by the LIN-1 Ets/LIN-31 WH transcription factor complex during *C. elegans* vulval induction. *Cell* **93**, 569-80.
- Wu, C. H. and Nusse, R.** (2002). Ligand receptor interactions in the Wnt signaling pathway in *Drosophila*. *J Biol Chem* **277**, 41762-9.

Yoo, A. S., Bais, C. and Greenwald, I. (2004). Crosstalk between the EGFR and LIN-12/Notch pathways in *C. elegans* vulval development. *Science* **303**, 663-6.

Yoon, C. H., Chang, C., Hopper, N. A., Lesa, G. M. and Sternberg, P. W. (2000). Requirements of multiple domains of SLI-1, a *Caenorhabditis elegans* homologue of c-Cbl, and an inhibitory tyrosine in LET-23 in regulating vulval differentiation. *Mol Biol Cell* **11**, 4019-31.

Table 1. CAM-1 inhibits vulval development

Genotype	% OI*	% UI**	Average no. of VPCs induced	n	P value†
+	0	0	3.00	many	
<i>cam-1(gm122)</i>	2	0	3.01 ± 0.01	55	
<i>cam-1(sa692)</i>	2	0	3.02 ± 0.02	51	
<i>cam-1(ak37)</i>	0	0	3.00 ± 0.00	53	
<i>cam-1(gm105)</i>	0	0	3.00 ± 0.00	54	
<i>cam-1(ks52)</i>	0	0	3.00 ± 0.00	53	
<i>lin-17(n671)</i>	0	0	3.00 ± 0.00	113	
<i>lin-17(n671); cam-1(gm122)</i>	17	0	3.13 ± 0.04	52	<.0001^a
<i>lin-17(n671); cam-1(sa692)</i>	14	0	3.09 ± 0.04	51	0.0007^a
<i>lin-17(n671); cam-1(ak37)</i>	14	0	3.12 ± 0.04	56	0.0003^a
<i>lin-17(n671); cam-1(gm105)</i>	8	0	3.02 ± 0.02	52	not sig. ^a
<i>lin-17(n671); cam-1(ks52)</i>	0	2	2.98 ± 0.02	53	not sig. ^a
<i>lin-17(n671); cam-1(gm122); cam-1 RNAi</i>	15	0	3.11 ± 0.06	27	
<i>lin-17(n671); cam-1 RNAi</i>	8	0	3.08 ± 0.06	25	0.03^a
<i>lin-18(e620)</i>	0	0	3.00 ± 0.00	113	
<i>cam-1(gm122); lin-18(e620)</i>	12	0	3.09 ± 0.04	52	0.0008^b
<i>cam-1(sa692); lin-18(e620)</i>	10	4	3.03 ± 0.04	54	0.0101^b
<i>cam-1(ak37); lin-18(e620)</i>	4	0	3.03 ± 0.02	51	not sig. ^b
<i>cam-1(gm105); lin-18(e620)</i>	0	0	3.00 ± 0.00	53	not sig. ^b
<i>cam-1(ks52); lin-18(e620)</i>	0	0	3.00 ± 0.00	53	not sig. ^b
<i>cwn-1(ok546)</i>	0	13	2.87 ± 0.04	62	
<i>cwn-2(ok895)</i>	0	0	3.00 ± 0.00	58	
<i>egl-20(n585)</i>	0	0	3.00 ± 0.00	51	
<i>egl-20(hu120)</i>	0	8	2.92 ± 0.04	50	
<i>cwn-1(ok546); cwn-2(ok895)</i>	0	27	2.68 ± 0.09	44	
<i>cwn-1(ok546); egl-20(n585)</i>	0	84	1.52 ± 0.13	61	
<i>lin-17(n671); cwn-1(ok546); cam-1(gm122)</i>	8	12	2.92 ± 0.07	50	not sig. ^c
<i>lin-17(n671); cam-1(gm122); cwn-2(ok895)</i>	4	0	3.04 ± 0.03	50	0.052 ^c
<i>lin-17(n671); cam-1(gm122); egl-20(n585)</i>	18	4	3.12 ± 0.06	51	not sig. ^c
<i>cwn-1(ok546); cam-1(gm122); lin-18(e620)</i>	0	13	2.83 ± 0.07	53	0.013^d
<i>cam-1(gm122); cwn-2(ok895); lin-18(e620)</i>	6	0	3.06 ± 0.03	53	not sig. ^d
<i>cam-1(gm122); egl-20(n585); lin-18(e620)</i>	0	10	2.91 ± 0.04	50	0.027^d
<i>lin-17(n671); cam-1(gm122); syls198[Plst-1::CAM-1::GFP]</i>	8	3	2.99 ± 0.09 [#]	38	not sig. ^c

Worms were grown and scored 20C. Induced values are Mean ± Std Error of Mean

* OI animals are those with greater than three VPCs induced. ** UI animals have fewer than three VPCs induced.

† P values were calculated using Fisher's Exact Test comparing the fraction of worms that are Muv vs. not Muv.

P < 0.05 considered significant and represented by bold type. ^a compared to *lin-17(n671)*, ^b compared to *lin-18(e620)*,

^c compared to *cam-1(gm122); lin-17(n671)*, ^d compared to *cam-1(gm122); lin-18(e620)*.

[#]1/38 worms was UI. This worm had 0 VPCs induced and appeared to be missing the anchor cell.

Table 2. Overexpression of CAM-1 in muscle or neurons inhibits vulval development in a Wnt-dependent manner

Relevant Genotype*	% F fates: 3° fates: Induced fates observed										n	
	P3.p	P4.p	P5.p	P6.p	P7.p	P8.p	% UI†					
+	58:42:0	0:100:0	0:0:100	0:0:100	0:0:100	0:0:100	0:100:0	0				62
<i>bar-1(ga80)</i>	100:0:0	91:7:2	39:7:54	10:0:90	12:8:80	36:62:2	64				59	
<i>cam-1(gm122)</i>	23:77:0	0:100:0	0:0:100	0:0:100	0:0:100	0:100:0	0				34	
<i>cwn-1(ok546); egl-20(n585)</i>	100:0:0	87:13:0	69:10:21	13:10:77	21:10:69	46:54:0	85				39	
<i>cwn-1(ok546); cwn-2(ok895)</i>	91:9:0	75:25:0	23:2:75	2:0:98	2:0:98	2:98:0	27				44	
<i>syEx778[Pmyo-3::CAM-1::GFP]</i>	95:5:0	67:33:0	29:5:66	5:0:95	0:0:100	0:100:0	29				21	
<i>syEx781[Pmyo-3::CAM-1::GFP]</i>	76:24:0	40:60:0	16:8:76	0:0:100	0:0:100	4:96:0	28				25	
<i>syEx798[Pdpy-8::CAM-1::GFP]</i>	65:35:0	5:95:0	0:0:100	0:0:100	0:0:100	0:100:0	0				20	
<i>syEx799[Pdpy-8::CAM-1::GFP]</i>	65:35:0	0:100:0	0:0:100	0:0:100	0:0:100	0:100:0	0				20	
<i>syEx780[Pfos-1a::CAM-1::GFP]</i>	38:62:0	0:100:0	0:0:100	0:0:100	0:0:100	0:100:0	0				21	
<i>syEx777[Pfos-1a::CAM-1::GFP]</i>	76:24:0	5:95:0	0:0:100	0:0:100	0:0:100	0:100:0	0				21	
<i>syEx775[Psnb-1::CAM-1::GFP]</i>	82:18:0	45:55:0	18:0:82	5:0:95	5:0:95	9:91:0	27				22	
<i>syEx776[Psnb-1::CAM-1::GFP]</i>	55:45:0	14:86:0	5:0:95	0:0:100	0:0:100	5:95:0	5				22	
<i>syEx863[Psur-2::CAM-1::GFP]</i>	23:77:0	0:95:5 [#]	0:0:100	0:0:100	0:5:95	0:100:0	0				20	
<i>syEx864[Psur-2::CAM-1::GFP]</i>	15:85:0	0:100:0	0:0:100	0:0:100	0:0:100	0:100:0	0				22	
<i>syIs198[P1st-1::CAM-1::GFP]</i>	23:77:0	0:100:0	0:0:100	0:0:100	0:0:100	0:100:0	0				22	
<i>syEx814[Pmyo-3::CAM-1ΔIntra::GFP]</i>	100:0:0	75:25:0	20:0:80	0:10:90	5:0:95	0:100:0	20				20	
<i>cwEx164[Pcam-1::CAM-1ΔIgKriIntra::GFP]</i>	91:9:0	59:41:0	5:5:91	0:0:100	0:0:100	5:95:0	9				22	
<i>cwn-2(ok895); syEx778[Pmyo-3::CAM-1::GFP]</i>	100:0:0	84:12:4	40:36:24	4:8:88	12:4:84	36:64:0	88^a				25	
<i>cwn-1(ok546); syEx778[Pmyo-3::CAM-1::GFP]</i>	100:0:0	70:25:5	40:0:60	0:0:100	5:15:80	30:70:0	40^b				20	
<i>egl-20(n585); syEx778[Pmyo-3::CAM-1::GFP]</i>	95:5:0	95:5:0	50:0:50	15:0:85	10:10:80	70:30:0	60^c				20	

Strains containing *syEx* transgenes were grown at 25C, all other strains were grown at 20C.

* *syEx* transgenic lines carry *unc-119(ed4)*; *him-5(e1490)* and an *unc-119(+)* rescuing plasmid. *dpy-20(e1282)* was used to suppress the roller phenotype of *cwEx164*, which was co-injected with pRF4.

† % Underinduced. Percentage of animals that have fewer than three VPCs induced. Bold indicates occurrence of Underinduced.

The occurrence of an induced fate here represents an animal where the vulval was shifted anteriorly, but was not Overinduced.

^a $P < 0.0001$, ^b $P > 0.05$, ^c $P = 0.026$ compared to *syEx778* using Fisher's Exact Test.

Table S1. *cam-1* genetically interacts with known regulators of vulval induction

Relevant Genotype*	Average no. of VPCs induced	n	<i>P</i> value [†]
<i>bar-1(ga80)</i>	1.50 ± 0.29	50	
<i>cam-1(gm122); bar-1(ga80)</i>	1.45 ± 0.13	52	not sig. ^a
<i>lin-3(e1417)</i>	0.28 ± 0.16	20	
<i>cam-1(gm122); lin-3(e1417)</i>	0.76 ± 0.20	21	0.04 ^b
<i>lin-3(n378)</i>	0.78 ± 0.19	32	
<i>cam-1(gm122); lin-3(n378)</i>	1.68 ± 0.23	20	0.007 ^b
<i>cam-1(gm122)</i>	3.01 ± 0.01	55	
<i>cam-1(gm122); ark-1(sy247)</i>	3.00 ± 0.00	21	not sig. ^c
<i>cam-1(gm122); sli-1(syl43)</i>	3.05 ± 0.03	22	not sig. ^c
<i>cam-1(gm122); gap-1(n1691)</i>	3.05 ± 0.05	22	not sig. ^c
<i>lin-17(n671); gap-1(n1691)</i>	3.00 ± 0.00	22	not sig. ^d
<i>lin-12(n952/+)</i>	0.87 ± 0.14	63	
<i>cam-1(gm122); lin-12(n952/+)</i>	1.85 ± 0.24	34	0.001 ^e
<i>lin-17(n671); cam-1(gm122); daf-3(mgDf90)</i>	3.14 ± 0.08	21	not sig. ^f

Worms were grown and scored 20C. Induced values are Mean ± Std Error of Mean

* *gap-1(n1691)* linked to *unc-2(e55)*, *ark-1(sy247)* linked to *dpy-20(e1282)*. *cam-1(gm122); lin-12(n952)* male worms were crossed into *cam-1(gm122); rol-6(e187)* and non-roller F1s were scored.

[†]*P* values were calculated using Mann-Whitney two-tailed test. *P* < 0.05 considered significant

^a compared to *bar-1(ga80)* alone, ^b compared to *lin-3(rf)* alone, ^c compared to *cam-1(gm122)* alone, ^d compared to *lin-17(n671)* alone, ^e compared to *lin-12(n952/+)*, ^f compared to *cam-1(gm122); lin-17(n671)*.

Table S2. Contribution of Wnt receptors MOM-5, LIN-17 and LIN-18 to vulval induction

Genotype	% OI*	% UI**	Average no. of VPCs induced	n
+	0	0	3	many
<i>lin-17(n671)</i>	0	0	3 ± 0.00	113
<i>lin-18(e620)</i>	0	0	3 ± 0.00	113
<i>lin-17(n671); lin-18(e620)</i>	2	0	3.02 ± 0.02 ^a	51
<i>syIs75[LIN-18::GFP]</i>	0	13	2.97 ± 0.02	53
<i>cwn-1(ok546)</i>	0	13	2.87 ± 0.04	62
<i>cwn-1(ok546); syIs75[LIN-18::GFP]</i>	0	21	2.68 ± 0.11 ^b	53
<i>syEx1022[LIN-17::GFP]</i>	0	0	3.00 ± 0.00	53
<i>cwn-1(ok546); syEx1022[LIN-17::GFP]</i>	0	28	2.72 ± 0.09	25
<i>syEx1020[Pmyo-3::LIN-17::GFP]</i>	0	3	2.99 ± 0.01	39
<i>cwn-1(ok546); syEx1020[Pmyo-3::LIN-17::GFP]</i>	0	15	2.85 ± 0.08	20
<i>lin-17(n671)-DE[†]</i>	2	0	3.04 ± 0.04 ^c	51
<i>lin-17(n671)-DE[†]; cam-1(gm122)</i>	10	2	3.07 ± 0.05	50
<i>mom-5(zu193)</i>	0	49	2.52 ± 0.07 ^d	51
<i>mom-5(zu193)-DE[†]</i>	2	39	2.63 ± 0.07 ^d	56
<i>mom-5(or57)</i>	0	67	2.26 ± 0.08 ^d	52
<i>lin-17(n677)</i>	5	0	3.05 ± 0.05	22
<i>lin-17(n677); cam-1(gm122)</i>	18	0	3.11 ± 0.06	22
<i>mig-1(e1787); lin-17(n671)</i>	5	0	3.02 ± 0.02	23
<i>lin-17(n671); cfz-2(ok1201)</i>	5	0	3.02 ± 0.03	22
<i>lin-17(n671); cwn-1(ok546)</i>	0	7	2.93 ± 0.03	58

Worms were grown and scored at 20C. Induced values are Mean ± Std Error of Mean.

*Overinduced animals are those with greater than three VPCs induced. **Underinduced animals are those with less than 3 VPCs induced.

^a1/51 *lin-17(n671); lin-18(e620)* double mutant worms had 4 VPCs induced (Figure S1).

^b*syIs75* increased the fraction of *cwn-1(lf)* worms that had a more severe UI phenotype (less than 2 VPCs induced) *P*=0.04.

^c1/51 *lin-17(n671)-DE* worms had 5 VPCs induced (Figure S1).

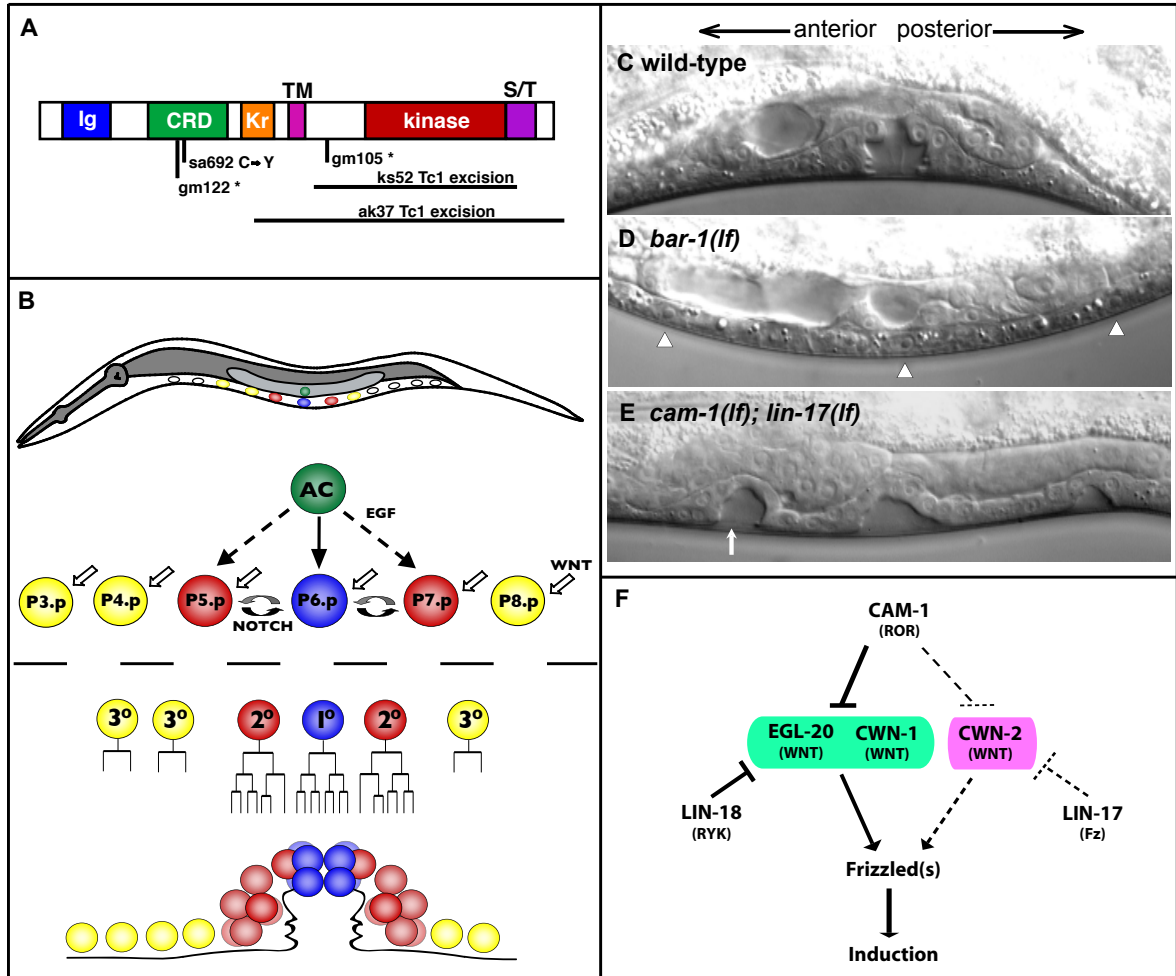
^d*mom-5* mutant worms frequently had only 2 VPCs induced (Figure S1).

[†]These strains were obtained from the Eisenmann laboratory and were compared to strains from the Sternberg laboratory.

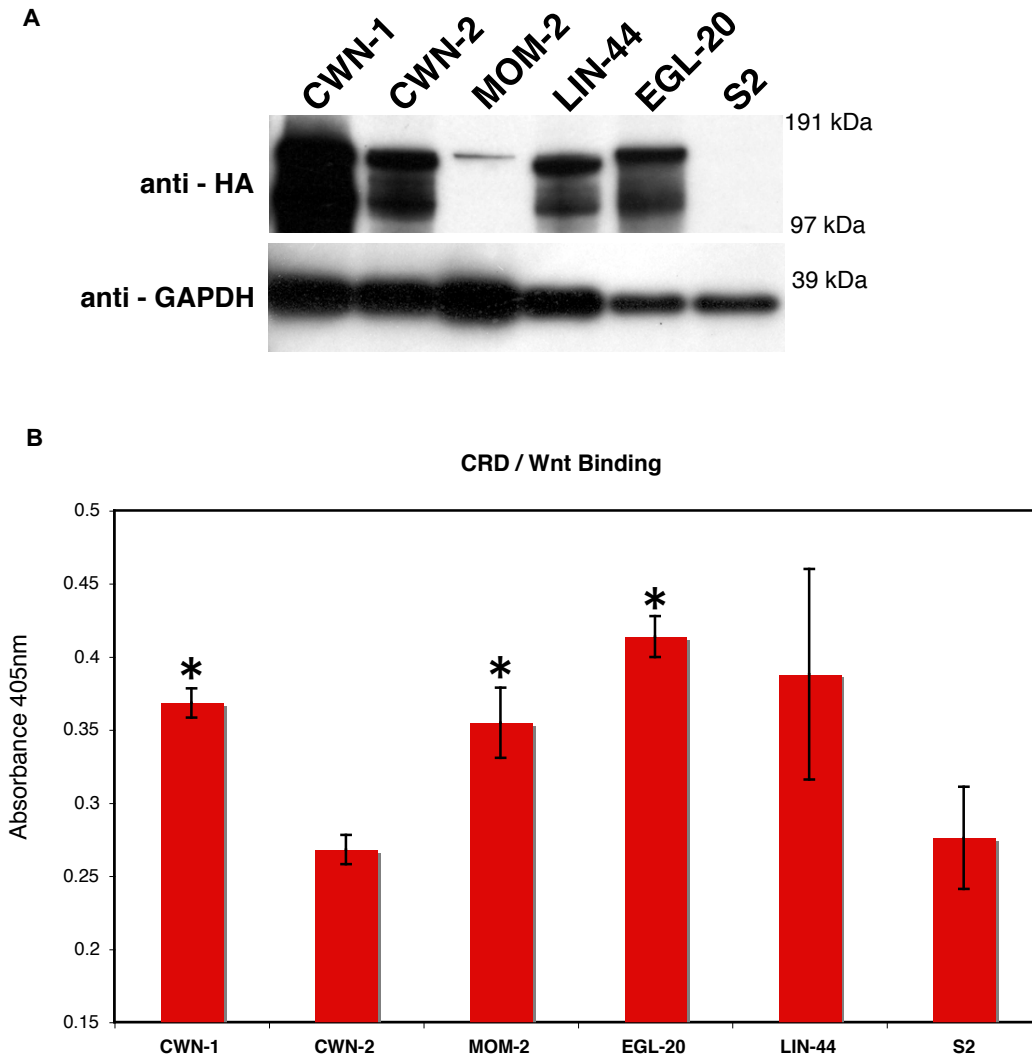
Table S3. Binding assay raw data

CRD-AP	LIN-44	CWN-1	EGL-20	CWN-2	MOM-2	S2
MIG-1	0.177	0.163	0.236	0.158	0.205	0.169
	0.208	0.211	0.259	0.224	0.236	0.214
	0.233	0.181	0.199	0.210	0.260	
mean	0.206	0.185	0.231	0.197	0.234	0.192
LIN-17	0.166	0.158	0.193	0.218	0.151	0.172
	0.193	0.141	0.197	0.196	0.182	0.167
	0.257	0.210	0.236	0.211	0.143	0.141
mean	0.205	0.170	0.209	0.208	0.159	0.160
MOM-5	0.159	0.177	0.167	0.203	0.167	0.145
	0.148	0.287	0.174	0.151	0.185	0.179
	0.153	0.195	0.177	0.152	0.159	
mean	0.153	0.220	0.173	0.169	0.170	0.162
CAM-1	0.255	0.385	0.387	0.254	0.375	0.301
	0.276	0.370	0.421	0.263	0.382	0.206
	0.482	0.350	0.433	0.287	0.307	0.321
mean	0.338	0.368	0.414	0.268	0.355	0.276
CFZ-2	0.139	0.196	0.232	0.201	0.209	0.195
	0.166	0.192	0.200	0.187	0.198	0.129
	0.202	0.180	0.187	0.167	0.164	
mean	0.169	0.189	0.206	0.185	0.190	0.162
LIN-18	0.089	0.091	0.098	0.088	0.095	0.102
	0.093	0.092	0.097	0.109	0.099	0.089
		0.125	0.090	0.087	0.093	0.101
mean	0.091	0.103	0.095	0.095	0.096	0.097

Table lists 405nm absorbance values after incubation of CRD-AP supernatant with the chromogenic substrate p-nitrophenyl phosphate. The binding assay protocol was adapted from those previously published (Cheng and Flanagan, 1994; Flanagan and Leder, 1990; Wu and Nusse, 2002). We observed that Nrt-HA-Wnt expression decreased with time as cells were passaged. Because of this observation and the non-clonality of the stable lines, we performed the binding assays as soon as sufficient cell numbers recovered from antibiotic selection and used equal cell numbers for the assay rather than normalizing to levels of Wnt expression. S2 cells stably transfected with the Nrt-HA-Wnt fusion constructs were counted with a hemacytometer, heat-shocked for 45 minutes at 37C, and incubated at 25C for 2hrs. At this point, aliquots of 500,000 cells were frozen for Western analysis. The remaining cells were then resuspended in HBSS plus 10% BSA and incubated with CRD-AP [7×10^{-8} M] in eppendorf tubes for 90 minutes at 25C. Three binding reactions of 30,000 cells each were done for 26 of 30 combinations. For the remaining four combinations (MIG-1, MOM-5 and CFZ-2 CRDs with untransfected S2 cells and LIN-18 CRD with Nrt-HA-LIN-44 expressing cells), only two reactions of 30,000 cells each were done. After washing cells three times with HBSS, cells were lysed by adding HBSS plus 1% Triton with brief vortexing and then heated at 70C for 10 min to kill background phosphatase activity. Supernatant was transferred to a 96 well untreated microplate and incubated with the chromogenic substrate p-nitrophenyl phosphate (Sigma N-7653). After 24 hours absorbance was read at 405nm using a microplate spectrophotometer (BioRAD).

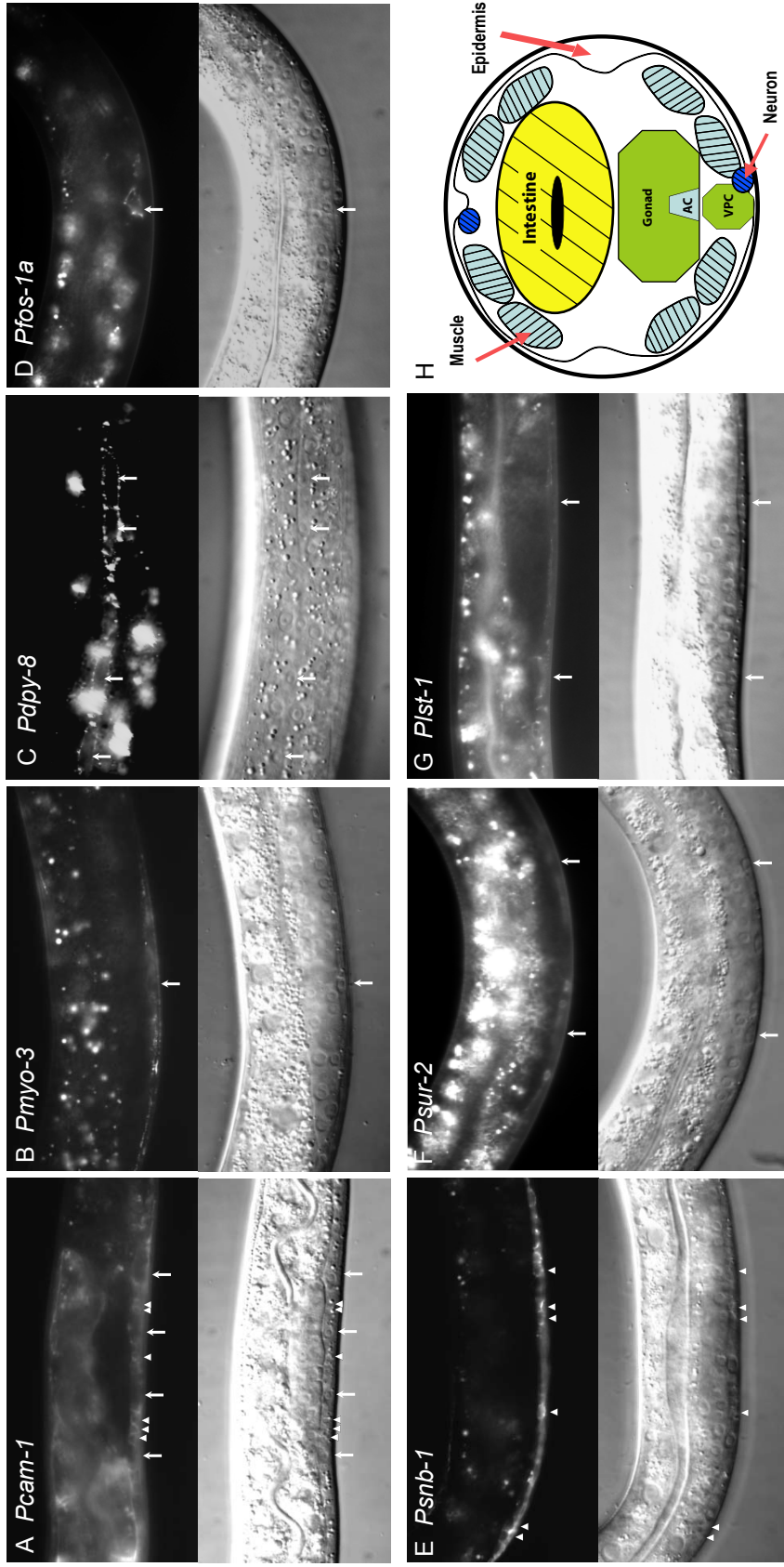
Figure 1. CAM-1 structure, vulval development and vulval phenotypes, model.

A) CAM-1 protein structure depicting Ig (Immunoglobulin) domain, CRD (cysteine-rich domain), Kr (kringle domain), TM (transmembrane) domain, kinase domain and S/T (serine/threonine-rich) domain. Amino terminus is to the left. Molecular lesions of *cam-1* mutant alleles is given below. B) Schematic of vulval induction process. C-E) Nomarski images of hermaphrodite vulvae. Anterior is to the left, posterior is to the right, dorsal is up and ventral is down. C) wild-type vulva formed from 22 progeny of 3 VPCs: P5.p, P6.p, and P7.p. D) a UI *bar-1(ga80)* mutant with no VPCs induced. Arrowheads point to nuclei of P5.p, P6.p, and P7.p that have adopted the F fate. E) *lin-17(n671); cam-1(gm122)* double mutant displaying an OI phenotype. Arrow points to ectopic invagination caused by induction of P4.p. F) Proposed model of CAM-1 interaction with Wnts. Arrows represent positive interaction, bars represent negative interaction, dashed lines indicate a possible interaction.

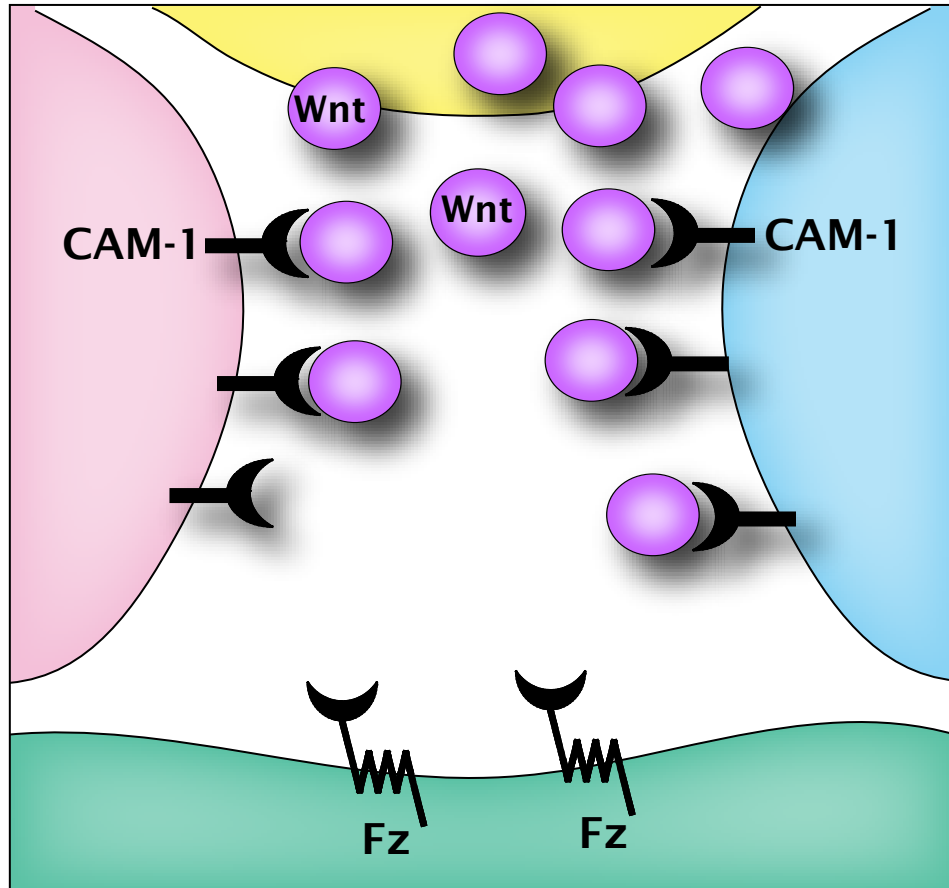
Figure 2. CAM-1 CRD binds Wnts CWN-1, EGL-20 and MOM-2

Drosophila S2 cells expressing Neurotactin-HA tagged *C. elegans* Wnts were incubated with secreted CRDs of *C. elegans* Wnt receptors fused to alkaline phosphatase (CRD-AP). A) Levels of Neurotactin (Nrt) -HA-Wnt fusion proteins (~130kD) expressed by S2 cells were measured by anti-HA immunoblot. Wnts are post-translationally modified and this may account for the detection of multiple bands. Anti-GAPDH is a loading control. B) Amount of CAM-1 CRD-AP retained by Neurotactin-HA-Wnt-expressing S2 cells. The assay was performed in triplicate. As the untransfected sample appeared to contain slightly fewer cells, we used cells expressing Nrt-CWN-2 (which expressed Wnt, but did not bind CAM-1 CRD-AP) as a negative control for statistical analysis. Values in the bar graph are the absorbance at 405nm. Asterisks represent a *P* value of less than 0.05 calculated using Fisher's Exact Test. Error bars reflect standard error of the mean.

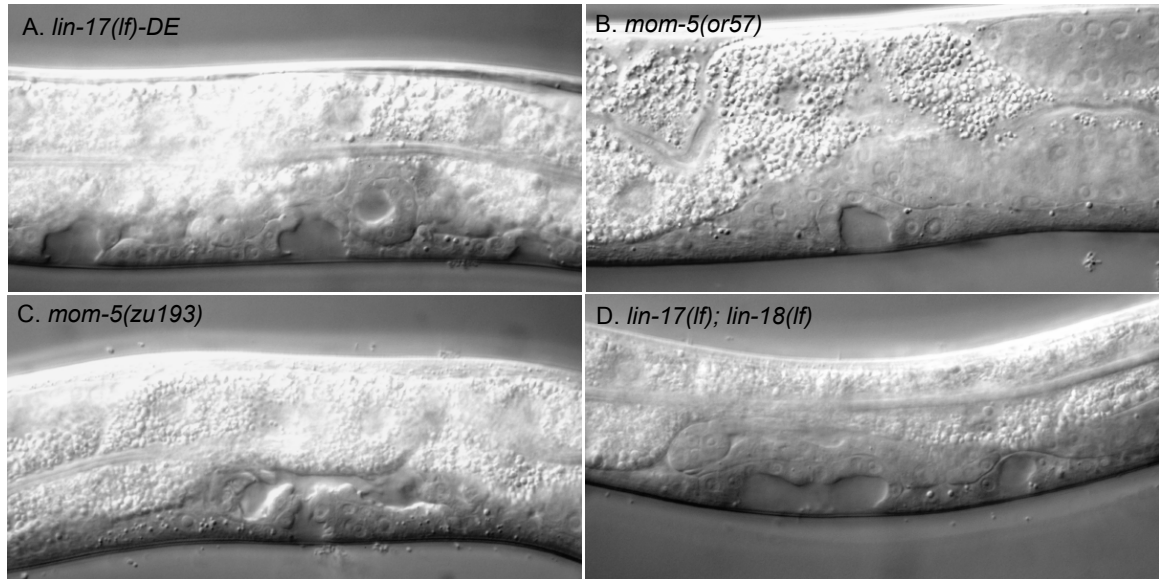
Figure 3. Transgene expression and worm cross-section



Fluorescent (top) and Nomarski (bottom) images of animals carrying *CAM-1::GFP* translational fusions. Anterior is to the left and posterior is to the right. A) *CAM-1::GFP* driven by the *cam-1* promoter. Membrane-localized expression is seen here in the ventral cord neurons (arrowheads) and VPCs (arrows). B) *Pmyo-3::CAM-1::GFP* is expressed in body wall muscle (arrow). C) *Pdp-8::CAM-1::GFP* is expressed in the hypodermis. Arrows point to hypodermal seam cell nuclei. D) *Pfos-1a::CAM-1::GFP* is expressed in the AC (arrow). E) *Psnb-1::CAM-1::GFP* is expressed in nervous tissue. Expression shown here is in VCNs (arrowheads). F) *Psur-2::CAM-1::GFP* is expressed in the VPCs (arrows) and few VCNs. G) *Plst-1::CAM-1::GFP* is expressed in the VPCs (arrows). H) Schematic cross section of *C. elegans* hermaphrodite at the vulva. Major tissues are labeled, hatched areas represent sites of *cwn-1* and *cwn-2* expression.

Figure 4. Model: CAM-1 sequesters Wnts

CAM-1 expressed in tissues between the source of Wnt expression and the recipient tissue can sequester Wnt by direct binding to the CRD and thus limit the amount of Wnt reaching the recipient tissue.

Figure S1. Vulval phenotypes of Wnt receptor mutants

A-D) Nomarski images of hermaphrodite vulvae. Anterior is to the left, posterior is to the right. A) an OI *lin-17(n671)* worm. B) a UI *mom-5(or57)* worm. C) a UI *mom-5(zu193)* worm. D) an OI *lin-17(n671); lin-18(e620)* double mutant worm.

CHAPTER 3

Opposing Wnt signals orient cell polarity during organogenesis

Takao Inoue initially observed that *egl-20(lf)* suppressed the *lin-17(lf)* P-Rv1 phenotype and made critical comments on this manuscript. J. Green performed all other experiments and was the primary author of this manuscript.

Abstract

The orientation of asymmetric cell division contributes to the organization of cells within a tissue or organ. For example, mirror-image symmetry of the *C. elegans* vulva is achieved by the opposite division orientation of the vulval precursor cells (VPCs) flanking the axis of symmetry. We characterized the molecular mechanisms contributing to this division pattern. Wnts MOM-2 and LIN-44 are expressed at the axis of symmetry and orient the VPCs towards the center. These Wnts act via Fz/LIN-17 and Ryk/LIN-18 to control β -catenin localization and activate gene transcription. In addition, VPCs on both sides of the axis of symmetry possess a uniform underlying “ground” polarity, established by the instructive activity of *Wnt/egl-20*. EGL-20 establishes ground polarity via a novel type of signaling involving the Ror receptor tyrosine kinase CAM-1 and the Planar Cell Polarity component Van Gogh/VANG-1.

Introduction

In organized epithelial tissues, the polarity of component cells is precisely controlled and its loss is a major factor in tumor formation and progression (reviewed by Wodarz and Nathke, 2007). During development, coordinating cell polarity is requisite for normal tissue architecture. For example, the orientation of an asymmetrically dividing cell will determine the arrangement of the daughter cells within the tissue. This is particularly important during organogenesis, where oriented divisions contribute greatly to organ size and shape (Baena-Lopez et al., 2005; Strutt, 2005), and cells often adopt a novel coordinate system to suit the architectural needs of the developing organ. In such cases, cells in an organ primordium must interpret complex and sometimes conflicting polarizing information. A simple model for the study of this phenomenon is *C. elegans* vulval development, in which certain cells within the same epithelium invariantly divide in opposite orientations. Here, we investigate how multiple Wnt signals interact to orient the vulval precursor cells (VPCs).

Wnts are a class of secreted glycoproteins that are conserved among all metazoa. Work from several systems reveals a variety of mechanisms by which Wnt signals are transduced (reviewed by Gordon and Nusse, 2006). In one well-conserved pathway, Wnt binding to Frizzled receptors leads to activation of target genes through the TCF/ β -catenin transcription factor complex. However, β -catenin-independent Wnt pathways also exist. For example, Planar Cell Polarity (PCP) is mediated by Frizzled, but involves components different from the pathway leading to TCF/ β -catenin regulation. More recently, receptor-tyrosine-kinases Ryk and Ror have emerged as alternative Wnt-binding receptors, although function of these RTK Wnt receptors is not yet well understood.

The *C. elegans* vulva is formed from the reproducible divisions of three VPCs — P5.p, P6.p and P7.p— arranged along the anterior-posterior (AP) axis in the ventral epithelium (Figure 1) (reviewed by Sternberg, 2005; Sulston and Horvitz, 1977). The Wnt, EGF, and Notch signaling pathways instruct the VPCs to adopt fates that correspond to particular lineage patterns. P6.p, the central VPC, divides symmetrically three times to produce eight cells that detach from the epidermis and form the vulval lumen (the 1° lineage pattern). P5.p and P7.p, after three rounds of asymmetric cell division (the 2° lineage pattern), produce the anterior and posterior sides of the vulva. The outermost progeny of both 2° VPCs adhere to the epidermis while the inner 2° progeny detach from the epidermis and join the 1° progeny cells to form the lumen. The 2° progeny are arranged so that P5.p descendants display mirror-image symmetry to P7.p descendants. Thus, the vulva is organized along a proximal-distal (PD) axis with the axis of symmetry at the center. While vulva development is one of the simplest and best understood models of organogenesis, why P5.p and P7.p divide in opposite orientations is poorly understood.

There are five Wnts in *C. elegans*: LIN-44, CWN-1, CWN-2, EGL-20, and MOM-2. LIN-44, CWN-1, CWN-2, and MOM-2 are known to regulate P7.p orientation. LIN-44 and MOM-2 play a major role and function in parallel, undefined pathways with their respective receptors, Frizzled (Fz)/LIN-17 and Ryk/LIN-18 (Ferguson et al., 1987; Gleason et al., 2006; Inoue et al., 2004; Sawa et al., 1996; Sternberg and Horvitz, 1988). In the absence of this signaling, the P7.p lineage displays the reverse, P5.p-like, orientation such that the invaginating cells are posterior to the adherent cells (hereby called “facing posteriorly”). This reversal in the P7.p lineage results in a second invagination posterior to the main vulva, a phenotype called P-Rvl for “posterior-reversed vulval lineage,” also known as Bivulva

(Figure 2B) (Ferguson and Horvitz, 1985; Ferguson et al., 1987). A similar phenotype in P5.p, A-Rvl (anterior-reversed vulval lineage), has not been described (Figure 2C). To explain why *lin-17* and *lin-18* mutations do not affect P5.p, Deshpande et al. (2005) proposed that both P5.p and P7.p face posteriorly by default, and *lin-17* and *lin-18* re-orient P7.p toward the center. However, they did not determine why the default orientation of P7.p is to face posteriorly, nor were they able to examine the role of Fz/LIN-17 and Ryk/LIN-18 in P5.p orientation.

Here, we present evidence that the Wnt signaling-independent orientation of both P5.p and P7.p is random. Wnt/EGL-20 acts as a directional cue to confer an underlying AP polarity causing both P5.p and P7.p to face the posterior. A novel pathway involving the Ror receptor tyrosine kinase CAM-1 and the Planar Cell Polarity component Van Gogh/VANG-1 mediates the EGL-20 signal. In response to MOM-2 and LIN-44, the central-orienting Wnts, Fz/LIN-17 and Ryk/LIN-18 instruct P5.p and P7.p to face the center, thus reversing P7.p orientation and reinforcing P5.p orientation. These results demonstrate that multiple Wnt pathways operating in different directions contribute to organized polarity in a developing organ.

Results

Wnt/egl-20 antagonizes *Fz/lin-17* and *Ryk/lin-18* in P7.p

We wished to understand the apparent default posterior-facing orientation of P5.p and P7.p. and reasoned that mutations disrupting this default polarity should suppress the P-Rv1 phenotype of *lin-17* and *lin-18* mutants. As reported by Gleason et al. (2006), we found that a loss-of-function (lf) mutation in *Wnt/cwn-1* mildly suppressed the *Fz/lin-17(lf)* P-Rv1 phenotype, but did not significantly suppress the *Ryk/lin-18(lf)* P-Rv1 phenotype (Table 1). In addition, we tested the involvement of *Wnt/egl-20*, whose role in VPC orientation was unknown, and found that strong reduction-of-function (rf) and lf alleles of *Wnt/egl-20* strongly suppressed the P-Rv1 phenotype of both *lin-17(lf)* and *lin-18(lf)* mutants. Thus, like *cwn-1*, *egl-20* antagonizes the function of *lin-17*, but additionally antagonizes the function of *lin-18*. We constructed triple mutants defective in both receptors and each of these Wnts and found that mutations in *egl-20* suppressed the phenotype of *lin-17(lf); lin-18(lf)* double mutants from 100% P-Rv1 to 50% P-Rv1, whereas only weak suppression was seen with *cwn-1(lf)*. Since Fz/LIN-17 and Ryk/LIN-18 function in parallel pathways to orient P7.p (Inoue et al., 2004), the ability of *egl-20* mutations to suppress the receptor double loss-of-function mutants suggests that Wnt/EGL-20 functions via a different receptor in a third parallel pathway. Moreover, EGL-20 has an opposing effect on P7.p orientation and instructs P7.p to face posteriorly. Because the effects of *cwn-1(lf)* and *cwn-2(lf)* are mild (Gleason et al., 2006), we investigated the mechanisms by which *egl-20*, *lin-44*, and *mom-2* influence VPC orientation.

Wnt/EGL-20 is required for the posterior-facing (ground) orientation of P5.p and P7.p

The above analysis suggested that Wnt/EGL-20 promotes P7.p orientation to face posteriorly. We next investigated whether EGL-20 is also involved in orienting P5.p posteriorly. We found that a small percentage of *lin-17(lf); egl-20(rf or lf); lin-18(lf)* triple mutants are A-Rv1 (Figure 2C), a novel phenotype observed in neither *lin-17(lf); lin-18(lf)* nor *egl-20(lf or rf)* mutants (Table 1). In addition, some of these triple mutants displayed simultaneous reversals in both P5.p and P7.p (the AP-Rv1 phenotype, Figure 2D). These results suggest that Fz/LIN-17, Ryk/LIN-18, and Wnt/EGL-20 function redundantly to orient P5.p posteriorly. The low penetrance of the A-Rv1 phenotype might be due to Wnt/CWN-1 activity, which weakly promotes the posterior-facing orientation in P7.p. Based on these results, we propose that Wnt/EGL-20 acts as a global cue to establish a uniform underlying polarity, which we call ground polarity, in which both P5.p and P7.p face posteriorly (Figure 2E, see Figure 5C).

Default orientation in the absence of Wnts

That 50% of *Fz/lin-17(lf); Wnt/egl-20(lf); Ryk/lin-18(lf)* triple mutants are P-Rv1 suggested a model that P5.p and P7.p orient randomly along the AP axis in the absence of all Wnt signaling (true default). However, lethality of *Wnt/mom-2(lf)* mutant worms and lack of a vulva in *cwn-1(lf); egl-20(rf or lf)* double mutants (Gleason et al., 2006) prevented us from analyzing P7.p orientation in quintuple Wnt (*lin-44, cwn-1, egl-20, cwn-2, mom-2*) mutants. We therefore used heat-shock-controlled over-expression of Ror/CAM-1 (*hs::CAM-1*) (Figure S1), which sequesters Wnts (Green et al., 2007), as an inducible method of

eliminating Wnt activity (see Supplemental Material for controls). Inducing CAM-1 over-expression after vulval induction and before polarity specification caused all four polarity outcomes predicted to occur in the absence of Wnt signaling: A-Rv1, P-Rv1, AP-Rv1, and wild type (Table 1). Consistent with the result that the CAM-1 CRD binds to CWN-1, EGL-20, and MOM-2 *in vitro*, but not to LIN-44 (Green et al., 2007), these phenotypes became more penetrant in a *Wnt/lin-44(lf)* mutant background. The most severe phenotype, AP-Rv1, is underrepresented, possibly due to residual Wnt activity. Analysis of cell-type-specific markers *ceh-2::YFP* and *cdh-3::CFP* (Deshpande et al., 2005; Inoue et al., 2002) confirmed that the phenotype is indeed due to a patterning defect and not a migration defect (data not shown). These results support the model in which VPCs orient randomly in the absence of Wnt signaling.

The anchor cell is an important Wnt source during VPC orientation

While Wnt/LIN-44 and Wnt/MOM-2 are redundantly required to re-orient P7.p (Gleason et al., 2006; Inoue et al., 2004), their relevant site of expression is not clear. In addition to other tissues, *mom-2* and *lin-44* are expressed in the anchor cell (AC) at the axis of symmetry (Figure S2B) (Inoue et al., 2004), suggesting that Wnts might function as centrally-orienting cues. To test this, we interfered with Wnt activity from the AC by expressing CAM-1::GFP specifically in the AC membrane (*Pfos-1a::CAM-1::GFP*) using the AC-specific promoter *Pfos-1a* (Sherwood et al., 2005) (Figure S2C). Because Ror/CAM-1 can sequester Wnts and appears to bind MOM-2, but not LIN-44, *in vitro* (Green et al., 2007), we reasoned that expression of this construct would antagonize MOM-2 expressed from the AC and therefore confer a P-Rv1 phenotype to *lin-44(lf)* mutants. Consistently, we

observed a 46% P-Rv1 phenotype in *lin-44(lf); Pfos-1a::CAM-1::GFP* animals (Table 1). Supported by control experiments (see Supplemental Material), these results indicate that MOM-2 (and possibly Wnt/LIN-44) expressed from the AC acts as a local cue to orient P5.p and P7.p towards the center, which we call “refined” polarity (Figure 2F, see Figure 5D).

EGL-20 acts instructively

egl-20 is expressed in the tail (Whangbo and Kenyon, 1999) and forms a posterior-to-anterior concentration gradient (Coudreuse et al., 2006), suggesting that EGL-20 functions instructively (imparts directional information) rather than permissively (does not provide directional information but is required for polarization). However, there is precedent for EGL-20 having both types of activity (Pan et al., 2006; Whangbo and Kenyon, 1999). To discriminate between these possibilities, we tested if changing the direction of the *egl-20* gradient affects VPC orientation. We first expressed *egl-20* broadly using the heat-shock promoter (*Phs::EGL-20*). If EGL-20 acts permissively, *Phs::EGL-20* expression should restore the P-Rv1 phenotype of *lin-17(lf); egl-20(lf)* double mutants (i.e. restores the *lin-17(lf)* phenotype). On the other hand, if EGL-20 is an instructive cue, then *Phs::EGL-20* expression in *lin-17(lf); egl-20(lf)* double mutants should result in all four VPC phenotypes: P-Rv1, A-Rv1, AP-Rv1, WT. We observed all four phenotypes upon heat shock, consistent with instructive EGL-20 function (Table 1).

To further assess whether EGL-20 acts instructively or permissively, we moved the source of *egl-20* expression from the posterior to the anterior side of P7.p. While we were unable to reverse the *egl-20* gradient over the entire length of the worm (see Supplemental Material), we used *Pfos-1a* to express *egl-20* from the AC, anterior to P7.p. We expressed

Pfos-1a::EGL-20::GFP in *Fz/lin-17*; *Wnt/egl-20*; *Ryk/lin-18* triple mutants, which are 50% P-Rvl. If EGL-20 is a permissive cue, *Pfos-1a::EGL-20::GFP* should restore the P-Rvl phenotype of these worms to 100%, as in *Fz/lin-17*; *Ryk/lin-18* double mutants. In contrast, instructive EGL-20 activity from the AC is expected to orient P5.p and P7.p towards the source of *egl-20* expression and thus rescue the 50% P-Rvl phenotype to wild-type.

Expression of *Pfos-1a::EGL-20::GFP* rescued the P-Rvl phenotype (Table 1), consistent with an instructive function. We next tested whether *Pfos-1a::EGL-20::GFP* could compete with endogenous *egl-20* when expressed in *lin-17(lf)* single mutants. *Pfos-1a::EGL-20::GFP* rescued the *lin-17(lf)* phenotype; therefore, P7.p orients towards higher levels of EGL-20. Together, these results indicate that reversing the EGL-20 gradient can reverse the ground polarity of the VPCs.

Wnt/ β -catenin asymmetry pathway components

To begin to distinguish the molecular mechanisms by which spatially resolved Wnts exert opposing effects on cell polarity; we investigated the involvement of potential downstream components. Wnt signals are often transduced by β -catenin, and three *C. elegans* β -catenin-related proteins, SYS-1, WRM-1, and BAR-1, function in two distinct pathways. BAR-1 functions as a classic β -catenin and will be discussed later. SYS-1 and WRM-1 are components of the Wnt/ β -catenin asymmetry pathway, which also includes TCF/POP-1 and Nemo-like-kinase/LIT-1. The Wnt/ β -catenin asymmetry pathway ensures different ratios of SYS-1 to POP-1, and thus differential transcription of Wnt target genes, between daughters of an asymmetric cell division (reviewed by Mizumoto and Sawa, 2007). In many tissues, POP-1 asymmetry is generated by WRM-1 and LIT-1, which together

promote nuclear export of POP-1 (Lo et al., 2004; Maduro et al., 2002). POP-1 is asymmetrically localized between P7.p daughter nuclei in a low (P7.pa)–high (P7.pp) pattern (Deshpande et al., 2005). GFP::LIT-1 (Rocheleau et al., 1999) and WRM-1::GFP (Takeshita and Sawa, 2005) are localized in a reciprocal pattern to POP-1 in P7.p daughter nuclei (Figure S3), indicating that the relationship between POP-1, WRM-1, and LIT-1 in the VPCs is similar to other tissues. A rescuing fluorescent SYS-1 fusion protein, (VNS::SYS-1), is also asymmetrically localized in a high (P7.pa)–low (P7.pp) pattern reciprocal to POP-1 (Figure 3A) (Phillips et al., 2007). By monitoring VNS::SYS-1 localization during division, we confirmed that this asymmetry reflects the orientation of the parent cell rather than signaling to P7.p daughters immediately following division (Figure 3B) (see Supplemental Material).

As reported for the somatic gonadal precursors (SGPs) in *Fz* mutants (Phillips et al., 2007), VNS::SYS-1 asymmetry in P7.p daughters was sometimes lost in *lin-17(lf)* mutants (Figure 3A, 3B). We additionally observed a loss of VNS::SYS-1 asymmetry in *lin-18(lf)* mutants, indicating that Ryk/LIN-18 also controls VNS::SYS-1 asymmetry. Unlike in the SGPs, in the VPCs, *lin-17(lf)* and *lin-18(lf)* mutants also frequently displayed a reversed VNS::SYS-1 localization pattern in which VNS::SYS-1 was enriched in P7.pp instead of P7.pa, suggesting the presence of an additional factor that controls SYS-1 asymmetry and promotes the opposite pattern, i.e., low (P7.pa)–high (P7.pp). Our analysis of the P-Rv1 phenotype suggested that EGL-20 promotes the posterior orientation of P7.p. Consistently, *egl-20(lf)* drastically suppressed the VNS::SYS-1 localization defects caused by *lin-17(lf)*, confirming that EGL-20 promotes reversed VNS::SYS-1 localization in P7.p daughters. In *lin-17(lf); lin-18(lf)* double mutants, VNS::SYS-1 localization defects consisted only of

reversals with no case of symmetric distribution observed. *egl-20(lf)* suppressed the reversed VNS::SYS-1 phenotype of *lin-17(lf); lin-18(lf)* double mutants such that the majority of triply mutant worms now displayed symmetric localization of VNS::SYS-1 between P7.p daughter nuclei. These results show that EGL-20 promotes the reversed localization of VNS::SYS-1 in the absence of the LIN-17 and LIN-18 branches of Wnt signaling, and that in the absence of all three branches of Wnt signaling, VNS::SYS-1 asymmetry is lost. VNS::SYS-1 asymmetry, however, is not the only determinant of VPC orientation. While 75% of *lin-17(lf); egl-20(lf); lin-18(lf)* triple mutants displayed symmetric VNS::SYS-1 localization, only 50% displayed the P-Rv1 phenotype, and no cases were observed in which anterior and posterior halves of the P7.p-derived tissue are symmetric. Thus one explanation for these results is that symmetric VNS::SYS-1 localization is an intermediate phenotype in which P7.p randomly adopts either orientation.

Curiously, *pop-1*, *sys-1*, *wrm-1*, and *lit-1* mutants do not display a P-Rv1 phenotype (Table 1). This could indicate that they are not involved in VPC orientation, or that like *egl-20*, their involvement is masked in single mutant worms. Consistent with the latter scenario, *lit-1(lf)* suppressed the P-Rv1 phenotype of *lin-17(lf)* and *lin-18(lf)* mutants.

β-catenin function during VPC orientation

Although they function in different pathways, both SYS-1 and BAR-1, a classic β-catenin, can function as transcriptional co-activators with TCF/POP-1, raising the possibility of redundancy (Kidd et al., 2005; Korswagen et al., 2000). Although *bar-1(lf)* mutants also did not display VPC polarity defects (Table 1), 15% of *sys-1(rf); bar-1(lf)* double mutants were P-Rv1, indicating that *sys-1* and *bar-1* play a minor redundant role in P7.p re-

orientation. We attempted to test whether β -catenin/WRM-1 was also functionally redundant with SYS-1 and BAR-1; however, all *wrm-1(rf); bar-1(lf)* double mutants examined (n=28) were Vulvaless due to an earlier requirement for β -catenin in vulval induction, and therefore could not be scored. Because BAR-1 appeared to play a minor role in VPC orientation, we examined BAR-1 localization in the VPC progeny. In wild-type animals, BAR-1::GFP (Eisenmann et al., 1998) is localized asymmetrically with higher nuclear levels in the proximal daughters of P5.p and P7.p (Figure 3C). Asymmetric distribution of BAR-1 during division had not previously been described; therefore, we tested whether BAR-1 asymmetry is generated by regulation of BAR-1 protein or by unequal transcription, by making a *bar-1* transcriptional reporter (*Pbar-1::4XNLS::GFP*) that has the same 5.1kb promoter sequence as the BAR-1::GFP fusion protein. Unlike BAR-1::GFP, *Pbar-1::4XNLS::GFP* was expressed at equivalent levels in both daughters of P5.p and P7.p suggesting that BAR-1 asymmetry is regulated at the protein level (Figure 3D). We next tested whether *Fz/lin-17(lf)* or *Ryk/lin-18(lf)* are required for BAR-1 asymmetry. In *Fz/lin-17(lf)* and *Ryk/lin-18(lf)* mutants, BAR-1::GFP was no longer enriched in either daughter nucleus. Thus, BAR-1 asymmetry is different than SYS-1 asymmetry, which is reversed in *lin-17(lf)* and *lin-18(lf)* mutants. We conclude that Fz/LIN-17 and Ryk/LIN-18 regulate the localization of BAR-1 protein by increasing its level in the proximal daughter nuclei and that unlike SYS-1, BAR-1 localization in the VPC daughters is not regulated by EGL-20. Because nuclear enrichment of β -catenin is expected to regulate the transcription of Wnt target genes, we next investigated whether Wnt pathway targets are expressed during P7.p re-orientation.

Fz/LIN-17 and Ryk/LIN-18 regulate POPTOP expression in the VPC progeny

Wnt signaling activity is commonly measured *in vitro* using the TOPFLASH reporter, consisting of multiple TCF binding sites driving expression of luciferase (Molenaar et al., 1996; van de Wetering et al., 1997). To measure TCF/POP-1 activity *in vivo*, we made an analogous *C. elegans* reporter, POPTOP; POP-1 and TCF Optimal Promoter, that contains seven copies of the TCF/POP-1 binding site and a minimal promoter driving expression of the fluorescent protein *mCherry* (McNally et al., 2006). Control experiments showed that POPTOP expression reflects POP-1 induced gene expression (see Supplemental Material). In wild-type worms, POPTOP is expressed at low levels in the proximal, but not distal, daughters of P5.p and P7.p, and at moderate and equal levels in the proximal granddaughters of P5.p and P7.p (Figure 4, Table S2, S3). POPTOP expression is reciprocal to POP-1 localization after the first division, (Deshpande et al., 2005), which is consistent with reports that TCF/POP-1, while functioning as an activator at low levels, functions as a repressor when present in the nucleus at high levels (Shetty et al., 2005).

POPTOP expression in the VPC progeny was elevated upon removal of *Axin/pry-1* (a negative regulator of Wnt signaling) and was eliminated in *pop-1* mutants, confirming that POPTOP is regulated by Wnt signaling (Figure 4, Table S3). Both β -catenins *sys-1* and *bar-1* are expressed in a pattern that would allow them to serve as a transcriptional co-activator with TCF/POP-1 (Figure 3A,C); therefore, we examined POPTOP expression in *bar-1(lf)* and *sys-1(rf)* mutant worms. POPTOP expression in P7.p granddaughters was reduced, though not significantly, in *sys-1(rf)* and *bar-1(lf)* mutants (Table S3) demonstrating that

SYS-1 and BAR-1 probably function redundantly to activate Wnt target genes in these cells. In *lin-17(lf)* and *lin-18(lf)* mutants, POPTOP expression in the VPC progeny was eliminated, indicating that Fz/LIN-17 and Ryk/LIN-18 activate Wnt target genes in the proximal daughters of P5.p and P7.p. *egl-20(lf)*, which rescues the *lin-17(lf)* P-Rv1 phenotype, does not restore POPTOP expression in *lin-17(lf); egl-20(lf)* double mutants (Table S3), suggesting that refined polarity is largely independent of differential transcription of Wnt target genes. That POPTOP expression was eliminated in *lin-17(lf)* and *lin-18(lf)* mutants, instead of being reversed, indicates that POPTOP is not influenced by ground polarity signaling.

Van Gogh/VANG-1 functions in ground polarity

Besides appearing independent of transcription, ground polarity presented an enigma because the receptor for EGL-20 was unknown. Loss of the receptor for EGL-20 should mimic loss of *egl-20* and also suppress the P-Rv1 phenotype of *lin-17(lf)* worms. However, the three remaining Fz receptors promote anterior P7.p orientation and removing them (by mutation or RNAi) does not suppress *lin-17(lf)* (Gleason et al., 2006). This suggests that EGL-20 acts via an alternative mechanism. We therefore considered Planar Cell Polarity (PCP), another mechanism of cellular orientation in which Fz can act positively or negatively.

VPC orientation bears the hallmark of PCP: the polarization of an epithelial tissue along the plane of the cell layer, perpendicular to the apical-basal axis of the cells comprising the epithelium. In *Drosophila* and vertebrates, PCP is regulated by a core set of PCP pathway components, including Frizzled, Van Gogh, Prickle, and Flamingo (recently reviewed by Jones and Chen, 2007; Seifert and Mlodzik, 2007; Wang and Nathans, 2007; Zallen, 2007).

Also like PCP, VPC orientation does not appear to depend on gene transcription. While the PCP pathway has not been clearly demonstrated in *C. elegans*, the resemblance of VPC orientation to PCP raised the possibility that PCP components might be involved. Thus, we tested for involvement of *Van Gogh/vang-1*, a PCP pathway-specific four-pass transmembrane protein that is conserved in *C. elegans* (Park et al., 2004). We first generated a *vang-1::YFP* reporter and observed expression in the VPC progeny (Figure 3E). While *vang-1(lf)* worms did not display VPC polarity defects, we found that *vang-1(lf)* significantly suppressed the P-Rvl phenotype of *Fz/lin-17(lf)* worms (Table 1). *vang-1(lf)* also significantly suppressed the reversed VNS::SYS-1 localization pattern of *lin-17(lf)* worms such that fewer animals displayed the reversed localization and an increased number had symmetric localization.

To test whether *vang-1* acts downstream of *egl-20* during the establishment of ground polarity, we ectopically expressed EGL-20 in the anchor cell (AC) using *Pfos-1a::EGL-20::GFP*, which reduces the P-Rvl phenotype of *lin-17(lf)* worms. Upon removal of *vang-1*, *Pfos-1a::EGL-20::GFP* no longer reoriented P7.p towards the center (Table 1), indicating that *Van Gogh/vang-1* acts downstream of *egl-20* during VPC orientation (Figure 5A). *vang-1(lf)* suppression of *lin-17(lf)* is much weaker (50% P-Rvl) than the suppression seen with *egl-20(lf)* (6% P-Rvl). Additionally, the *lin-17(lf); egl-20(lf); vang-1(lf)* triple mutants (2% P-Rvl) were not significantly different than the *lin-17(lf); egl-20(lf)* double mutants, demonstrating that *egl-20* acts partly via *vang-1*, and partly via another mechanism.

ROR/CAM-1 functions in ground polarity

Van Gogh is a transmembrane protein without an obvious Wnt-binding domain. We therefore investigated how EGL-20 might activate VANG-1. Since none of the Fz and Ryk receptors were apparently required for ground polarity, we tested the only other known Wnt receptor in *C. elegans*, *Ror/cam-1*. ROR proteins are receptor tyrosine kinases (RTKs) containing an extracellular Wnt-binding Frizzled (Fz) domain (also called cysteine-rich-domain or CRD), an immunoglobulin (Ig) domain, and a Kringle domain (Figure S4). We previously showed that *cam-1*, the sole *C. elegans* Ror family member, is expressed in the VPCs and physically interacts with EGL-20 *in vitro* (Green et al., 2007). To investigate if *cam-1* is involved in ground polarity, we tested whether the *cam-1(lf)* mutation, *gm122*, suppressed the *lin-17(lf)* P-Rvl phenotype. *cam-1(lf)* suppressed *lin-17(lf)* P-Rvl to 46%, similar to the suppression seen with *vang-1(lf)* (Table 1). *cam-1(lf)* also suppressed the VNS::SYS-1 localization defects of *lin-17(lf)* worms in a way similar to *vang-1(lf)*: fewer animals displayed the reversed localization and an increased number had symmetric localization (Figure 3A). To test whether *cam-1* functions in the same pathway as *egl-20* and *vang-1*, we constructed *lin-17(lf); cam-1(lf or rf); vang-1(lf)* triple mutants using either of two different *cam-1* alleles. In both strains, the P-Rvl phenotype was not different from the *lin-17(lf); cam-1(rf or lf)* double mutants indicating that *cam-1* and *vang-1* function in the same pathway. To confirm that *cam-1* acts in the *egl-20/vang-1* pathway, we introduced *Pfos-1a::EGL-20:GFP* into *lin-17(lf); cam-1(lf)* worms. Like *vang-1(lf)*, removal of *cam-1* prevented *Pfos-1a::EGL-20:GFP* from re-orienting P7.p. Together, these results indicate that *cam-1* functions in the same pathway as *egl-20* and *vang-1* (Figure 5A) and raise the interesting possibility that CAM-1 and VANG-1 may function as co-receptors for EGL-20.

CAM-1 can act non-autonomously by sequestering Wnts (Green et al., 2007) and we showed earlier that overexpression of CAM-1 can abolish ground polarity. To test whether the function of CAM-1 in ground polarity (*lin-17(lf)* suppression) is distinct from the Wnt-sequestration function, we used the five available *cam-1* mutant alleles to perform structure-function analysis (Figure S4). All five *cam-1* alleles examined suppressed the *lin-17(lf)* P-Rvl phenotype, including a missense mutation in the Wnt binding domain (*sa692*) and a deletion of the intracellular kinase domain (*ks52*). Therefore, membrane insertion of a functional CRD, which is sufficient for sequestration (Supplemental Material) (Green et al., 2007), is not sufficient for CAM-1 function in ground polarity, suggesting a requirement for the CAM-1 intracellular domain, and thus a cell-autonomous site-of-action. Expression of CAM-1 in muscles (*myo-3* promoter) or neurons (*snb-1* promoter) (Green et al., 2007) did not restore the P-Rvl phenotype, further supporting a cell-autonomous role.

Since vertebrate Ror proteins activate c-Jun N-terminal kinase (JNK) in response to Wnt5a (Oishi et al., 2003; Schambony and Wedlich, 2007), we tested whether *jnk-1*, the JNK ortholog, acts in the same pathway as *cam-1* during VPC orientation. *jnk-1(lf)* did not suppress the *lin-17(lf)* P-Rvl phenotype (Table 1), indicating that *jnk-1* is not required for *cam-1* to establish ground polarity.

Discussion

Our results describe the contributions of multiple Wnt pathways to the orientation of cell polarity in the *C. elegans* vulval epithelium (Figure 5A). As no factor required for the posterior orientation of P5.p or P7.p had previously been identified, this orientation was thought to be signaling-independent or “default.” However, by using a new approach to reduce Wnt levels in a spatio-temporally controlled manner (over-expression of Ror/CAM-1, a Wnt-sink), we show that the true default orientation of P5.p and P7.p is random (Figure 5B). The posterior orientation seen in the absence of *Fz/lin-17* and *Ryk/lin-18* depends on the instructive activity of Wnt/EGL-20. We refer to this polarity as “ground” polarity (Figure 2E, 5C). In response to centrally located Wnt/MOM-2 (and possibly Wnt/LIN-44), the receptors Fz/LIN-17 and Ryk/LIN-18 orient P5.p and P7.p towards the center. This re-orientation of P7.p, “refined” polarity, provides the mirror-image symmetry required for a functional organ (Figure 2F, 5D).

That P7.p is oriented toward the center in wild-type worms suggests that Wnts LIN-44 and MOM-2 have a greater ability to affect P7.p orientation than does EGL-20. Although the posterior-anterior EGL-20 gradient reaches the VPCs, EGL-20 levels may be much lower here than the levels of Wnts secreted from the nearby AC (Coudreuse et al., 2006). Indeed, we found that local expression of *egl-20* in the AC can overcome the effects of distally expressed *egl-20*. *lin-44* is expressed in the tail (Herman et al., 1995) in addition to the AC, but has not been shown to have long-range activity. It is thus possible that this posterior source of *lin-44* does not affect P7.p orientation, and that LIN-44, in addition to MOM-2, acts as a central cue.

LIN-17 and LIN-18 were previously reported to re-orient P7.p and to reverse the AP pattern of nuclear TCF/POP-1 levels in P7.p daughters (Deshpande et al., 2005; Inoue et al., 2004). We extended our knowledge of the signaling downstream of Fz/LIN-17 and Ryk/LIN-18 by showing that these receptors control the asymmetric localization of two β -catenins, SYS-1 and BAR-1, the first evidence that Ryk proteins regulate β -catenin. Disruption of several Wnt/ β -catenin pathway components (*pop-1(RNAi)*, *sys-1(rf)*, and *wrm-1(rf)*) causes a weakly penetrant P-Rvl phenotype, suggesting that the Wnt/ β -catenin asymmetry pathway plays a minor role in refined polarity. We also showed that LIN-17 and LIN-18 activate Wnt target genes in the proximal VPC daughters. However, this transcription is not required for P7.p re-orientation, since transcriptional states observed by POPTOP, a reporter of Wnt target genes, do not always correspond with the morphological phenotype. The situation may be analogous to the spindle re-orientation of the EMS cell during *C. elegans* embryogenesis, in which Wnt signaling affects the cytoskeleton independent of Wnt's effect on gene expression (Schlesinger et al., 1999).

What then, is the purpose of the Wnt/ β -catenin asymmetry pathway in the VPCs? The weakly penetrant A-Rvl phenotype seen in *wrm-1(rf)* and *lin-17(lf); lit-1(lf)* worms, combined with our observation that EGL-20 regulates SYS-1 asymmetry, suggests that the Wnt/ β -catenin asymmetry pathway functions in ground polarity. Therefore, it is likely that both ground and refined polarity converge on regulation of these components, although they are not absolutely required for refined polarity. Because the localization of Wnt/ β -catenin asymmetry pathway components in ground polarity matches the reiterative pattern seen in most other asymmetric cell divisions in *C. elegans* (Huang et al., 2007), we hypothesize that localization of these components is initially established as part of a global anterior-posterior

polarity. It is likely that LIN-17 and LIN-18 overcome ground polarity by inhibiting the Wnt/ β -catenin asymmetry pathway, a scenario consistent with the ability of *lit-1(rf)* to suppress *lin-17(lf)* and *lin-18(lf)* mutations.

Remarkably, it is only by peeling back the layer of refined polarity that ground polarity can be observed and manipulated. By doing so, we found that Wnt/EGL-20, expressed from a distant posterior source, imparts uniform AP polarity to the field of VPCs via a new pathway involving *Van Gogh/vang-1*, a core Planar Cell Polarity (PCP) pathway component. It is noteworthy that Fz is also a core PCP pathway component, yet it does not seem to be involved in EGL-20–VANG-1 signaling. This is not incompatible with other descriptions of PCP. For example, in the *Drosophila* wing, Vang Gogh and Fz antagonize each other and cause wing hairs to orient in opposite directions (reviewed by Seifert and Mlodzik, 2007). The molecular mechanism by which VANG-1 functions in ground polarity is unknown; however, regulation of SYS-1 by VANG-1 provides evidence that EGL-20 – VANG-1 signaling is associated with the Wnt/ β -catenin asymmetry pathway.

A major difference between VPC orientation in *C. elegans* and PCP in *Drosophila* is that no Wnt has been directly implicated in *Drosophila* PCP. Therefore, VPC orientation may be more similar to PCP in vertebrates, where Wnts act as permissive polarizing factors. VPC orientation is strikingly similar to hair cell orientation in the utricular epithelia of the mammalian inner ear, wherein hair cells flanking the axis of symmetry are oriented in opposite directions (Figure 6). In this system, both medial and lateral hair cells possess a uniform underlying polarity as evidenced by asymmetric localization of Prickle, a core PCP pathway component (Deans et al., 2007). Prickle is localized to the medial side of cells in both populations despite their opposite morphological orientation, which is apparent from the

location of the stereociliary bundle. Van Gogh is required for proper Prickle asymmetry, perhaps similarly to the role of *vang-1* in ground polarity of the VPCs. It is not understood how the position of the utricular axis of symmetry is determined, but the similarities between these two systems suggest that it may represent a local source of Wnt.

By moving the source of EGL-20 from the posterior to the anterior side of P7.p and thereby reversing P7.p orientation, we showed that EGL-20 acts as a directional cue. While it is not presently clear if the EGL-20–VANG-1 pathway is mechanistically similar to the PCP pathway described in *Drosophila* and vertebrates, our result nonetheless provides a long-sought example of a Wnt that acts instructively via a PCP pathway component. Detailed description of the subcellular localization of Van Gogh/VANG-1 and other PCP pathway components in the VPCs will be required to make meaningful comparisons between VPC orientation and established models of PCP.

In addition to *vang-1*, we also identified a role of *Ror/cam-1* in ground polarity. Our results provide the first evidence that Ror proteins interpret directional Wnt signals, as well as the first evidence that they interact with Van Gogh. Although a *Xenopus* Ror homolog, Xror2, was previously described to function in PCP during convergent extension (Hikasa et al., 2002), a recent report indicates that the involvement of Xror2 in convergent extension (CE) is actually via a different pathway (Schambony and Wedlich, 2007). In response to Wnt5a, Xror2 activates JNK by a mechanism requiring Xror2 kinase activity. In contrast to Wnt5a/Xror2 signaling, Ror/CAM-1 function in ground polarity does not require JNK. Therefore, the ground polarity pathway involving Wnt/EGL-20–Ror/CAM-1–Van Gogh/VANG-1 may be a new type of Wnt signaling.

Using *C. elegans* vulva development as a model, we showed that multiple coexisting Wnt pathways with distinct ligand specificities and signaling mechanisms act in concert to regulate the polarity of individual cells during their assembly into complex structures.

Acknowledgements

We thank Gladys Medina, Barbara Perry, and Shahla Gharib for technical assistance, members of our lab for helpful discussions, Andrea Choe for artistic input, and Marianne Bronner-Fraser, Scott Fraser, Cheryl Van Buskirk, Mihoko Kato, Elissa Hallem, and Adeline Seah for critically reading the manuscript. Many strains used in this study were provided by the *Caenorhabditis* Genetics Center, funded by NIH, National Center for Research Resources. We are grateful to the late Peter Snow for his valuable assistance in making our CAM-1 antibody. PWS is an investigator with the HHMI, who supported this work, and JLG was supported by the Moore Foundation Fellowship for graduate study toward the Doctor of Philosophy degree in Biology at the California Institute of Technology.

Material and Methods

Genetics

C. elegans was handled as described (Brenner, 1974). Strains used were derivatives of *C. elegans* N2 Bristol strain, which was the wild type in this study. Mutations used: LGI: *lin-17(n671)*, *pop-1(q645)*, *lin-44(n1792)*, *sys-1(q544)*. LGII: *cam-1(gm122, gm105, sa692, ks52, ak37)*, *cwn-1(ok546)*. LGIII: *wrm-1(ne1982)*, *lit-1(or131ts)*. LGIV: *jnk-1(gk7)*, *egl-20(n585, hu120)*, *cwn-2(ok895)*. LGV: *mom-2(or42)*. LGX: *vang-1(ok1142)*, *lin-18(e620)*, *bar-1(ga80)*. The *wrm-1(ne1982); bar-1(ga80)* double mutants were a kind gift from Craig Mello. P-Rvl and A-Rvl phenotypes were scored at the mid-L4 stage. Animals were classified as P-Rvl or A-Rvl if the primary and secondary VPCs were induced but separated by adherent cells. We consider the previously used description “Bivulva” misleading as it implies the presence of extra vulval tissue and thus decided to call the phenotype Rvl for “reversed vulval lineage.”

Transgenics (see Supplemental Material)

Heat-shock Ror/CAM-1

Worms carrying the *syEx710[Pheat-shock::CAM-1]* transgene were kept for 45 min at 33°C. Total lysates from heat-shocked, wild-type, and *cam-1(lf)* worms were separated by SDS-PAGE and probed with an anti-CAM-1 rabbit polyclonal antibody (B9851) that we raised (using BioSource International) against the C-terminus (aa 858-928) of CAM-1 (C01G6.8a).

POPTOP (POP-1 and TCF Optimal Promoter)

Seven copies of the TCF binding site, AGATCAAAGG, were transferred from Super8XTOPflash (plasmid M50) (Veeman et al., 2003) into Fire lab vector L3135 (<http://www.addgene.org>) to place them upstream of the *pes-10* minimal promoter. The product was cloned into mCherry plasmid (PJIM20) with *let-858* 3' UTR (kind gift from Jon Audhya) using sites SpeI and AvrII. The POPTOP plasmid was sequenced to confirm the integrity of the insert. POPFOP (POP-1 Far from Optimal Promoter) was made by a similar strategy using mutated TCF binding sites from plasmid Super8xFOPflash (plasmid M51). For details on POPTOP construction, characterization and validation, see Supplemental Materials.

Supplemental Material

VNS::SYS-1 localization during P7.p division

Previously, divisions of P5.p and P7.p were considered asymmetric in that their daughters produce cells with different fates. However, the formal possibility that the division is symmetric and the different fates are a result of signaling immediately following the division had not been ruled out. To distinguish between these possibilities, we monitored the localization of VNS::SYS-1 during P7.p division (Figure 4B). During metaphase, VNS::SYS-1 became concentrated in spots at the anterior and posterior poles of the nuclear membrane, probably corresponding to centrosomes (Phillips et al., 2007). Five minutes after metaphase, the VNS::SYS-1 associated with the anterior daughter nucleus appeared to spread throughout the nucleus, while the VNS::SYS-1 associated with the posterior daughter nucleus disappeared. Since VNS::SYS-1 asymmetry is observed during the division, we conclude that P7.p is polarized before or during cell division. In contrast to wild-type worms, VNS::SYS-1 in *lin-17(lf)* mutants remained associated with the posterior daughter nucleus and either disappeared from the anterior daughter nucleus or persisted in both cells. Thus *lin-17(lf)* affects the polarity of the P7.p cell prior to or during division.

Heat-shock cam-1

To confirm that the phenotypes we observed upon heat-shock were not due to intracellular signaling by Ror/CAM-1, we generated a kinase-inactive version of Ror/CAM-1 by changing two conserved lysines in the kinase domain to arginine (Forrester et al., 1999). Heat-shock of transgenic worms carrying a *hs::CAM-1(kinase-dead)* transgene caused both

P-Rvl and A-Rvl phenotypes (Table S1), indicating that these phenotypes are independent of Ror/CAM-1 kinase activity. As it remained possible that Ror/CAM-1 signals intracellularly despite lacking kinase activity, we also generated transgenic worms carrying heat-shock inducible Ror/CAM-1 in which most of the intracellular domain is removed (*hs::CAM-1del-intra::GFP*). While heat-shock of worms carrying this transgene did not cause a Rvl phenotype, we did observe P-Rvl worms when combined with a *Wnt/lin-44(lf)* mutation. The reduced activity of this transgene compared to the full-length *hs::CAM-1* or *hs::CAM-1(kinase-dead)* transgenes may be due to a requirement of the intracellular domain for efficient membrane localization. We also note that P5.p polarity may be less sensitive to perturbation than P7.p because the posterior-facing orientation is reinforced by multiple signaling events. Finally, overexpression of full-length *CAM-1* in the VPCs using the *sur-2* (Singh and Han, 1995), and *lst-1* (Yoo et al., 2004) 5' regulatory sequences did not cause VPC polarity defects, confirming that the *CAM-1* overexpression phenotype is not due to *CAM-1* signaling in the VPCs. In addition to VPC polarity defects, *hs::CAM-1* also caused VPC induction defects (when younger worms were heat-shocked) and severe gonad migration defects, both phenotypes consistent with general loss of Wnt signaling.

The anchor cell is the relevant source of MOM-2

The following experiments demonstrate that *Pfos-1a::CAM-1::GFP* interferes specifically with *mom-2* in the AC to produce a P7.p orientation defect. Like *mom-2(rf)*, *Pfos-1a::CAM-1::GFP* enhanced the *lin-17(lf)* P-Rvl phenotype to nearly 100% (Table S1). Because *mom-2(rf)* is the only Wnt mutant that enhances the P-Rvl phenotype of *lin-17(lf)*, this suggests that *Pfos-1a::CAM-1::GFP* interferes with *mom-2* in the AC. Furthermore,

expression of *mom-2* in the AC (*Pfos1a::MOM-2::YFP*) rescued the P-Rvl phenotype of *lin-44(lf); mom-2(rf)* double mutants (Table S1).

EGL-20 gradient

We attempted to completely reverse the EGL-20 gradient such that the EGL-20 source would also be anterior to P5.p. Although we observed GFP expression from our transgenes, EGL-20 expressed in the head using *Pmyo-2* (pharyngeal muscle) or *Plim-4* (few head neurons) promoters in *lin-17; egl-20* double mutant worms neither rescued the P-Rvl phenotype nor caused any A-Rvl phenotype (not shown), suggesting that sufficient EGL-20 failed to reach the VPCs. The *Pmyo-2::EGL-20::GFP* construct we used was previously shown to rescue Q cell migration, a process that occurs in the first larval stage, in a dose-dependent manner (Whangbo and Kenyon, 1999). However, VPC division occurs in the third larval stage when the worms are much larger and the Wnts have both a greater distance to travel and a greater volume to diffuse into. It is possible that the cells expressing EGL-20 using *Pmyo-2* are less efficient than the endogenous EGL-20 source and that the amount of functional EGL-20 reaching the VPCs is not sufficient to orient their polarity. The *Plim-4::EGL-20::GFP* construct we used (Pan et al., 2006) was previously shown to partially rescue the HSN overmigration phenotype of *vab-8* and *ceh-10* mutants and to repel growth cones of the AVM and PVM neurons. However, these experiments have not been demonstrated to convey long-range *egl-20* activity because: 1) HSN migration occurs during embryogenesis and 2) AVM and PVM growth cones did not turn away until they were extremely close to the *egl-20* source. Therefore, our results are inconclusive as it is unknown whether we generated an EGL-20 gradient that reached the VPCs.

POPTOP

Seven copies of the TCF binding site, AGATCAAAGG, were transferred from Super8XTOPflash (plasmid M50) (Veeman et al., 2003) into Fire lab vector L3135 to place them downstream of the *pes-10* minimal promoter. The seven TCF sites and the *pes-10* minimal promoter were amplified using forward primer AAGCTTGGTACCGAGCTCGG and reverse primer ATGCCTAGGCAATCAATGCCTGAAAGTTAAAAATTAC. The product was then cloned into mCherry plasmid (PJIM20) with *let-858* 3' UTR (kind gift from Jon Audhya) using sites SpeI and AvrII. We also generated a control reporter, POPFOP; POP-1 Far from Optimal Promoter, that contains mutated Tcf/POP-1 binding sites. POPFOP was made by a similar strategy as POPTOP using mutated TCF binding sites from plasmid Super8xFOPflash (plasmid M51).

Worms carrying an integrated POPTOP transgene display a dynamic expression pattern in many cells affected by Wnt signaling as well as cells in which Wnt has not been shown to function (Table S2). It is likely that POPTOP exhibits some background expression due to activity of the minimal promoter, the sequence linking or flanking the Tcf/POP-1 sites, or the 3' UTR.

To determine in which cases POPTOP represents a true readout of canonical Wnt pathway activity, we compared the POPTOP expression pattern to the that of POPFOP and to worms carrying *pop-1(q645)*, a mutation that disrupts the transactivation (β -catenin-binding) domain of Tcf/POP-1 (Siegfried and Kimble, 2002). In some cases, we also compared the POPTOP expression pattern to that in worms carrying a null mutation in *Axin/pry-1*, a negative regulator of Wnt signaling (Korswagen et al., 2002). We considered expression present in wild type worms carrying POPTOP and absent both in worms carrying POPFOP

and in worms mutant for *Tcf/pop-1* to be a valid occurrence of Wnt activity. Elevated POPTOP expression in *Axin/pry-1* mutant worms further validated this conclusion and identified potential sites, such as body wall muscle, where Wnt activity is suppressed. A review by M. Herman (Herman, 2002), delineates the known examples of Wnt signaling in *C. elegans*. Canonical Wnt signaling influences QL.d migration, P12 and VPC fate specification. Non-canonical Wnt signaling controls cell polarity and has been reported to regulate the T and B cells, Z1/Z4 somatic gonadal precursors (SGPs), V5 and the EMS blastomere. We observed POPTOP expression in many of these cells including the Q cells and their descendants, the T cell, the B cell, V5 and the SGPs. We also observed POPTOP expression in the male hook precursor cells, whose division is regulated by *Fz/lin-17* (Sternberg and Horvitz, 1988). We did not detect POPTOP expression in the embryo until the gastrulation stage. This could be because POPTOP expression is too weak to be detected earlier, or it could be due to the common phenomenon of germline silencing of transgenes (Kelly et al., 1997). POPTOP is expressed in the P cells and the Pn.p cells, however, this expression was also present in *Tcf/pop-1* mutant worms and in POPFOP negative control worms and was thus considered to be background expression. This background expression prevented any analysis of P12 specification or VPC induction. Background Pn.p expression vanished at the L3 stage allowing us to analyze POPTOP expression in the VPC daughters and granddaughters. Besides the known sites of Wnt activity, we also observed non-background expression in the distal tip cells (DTCs) and uterine cells (Table S2). Between strains, POPTOP expression often differed in intensity rather than “on” or “off.” Thus, to compare expression between strains, we selected conditions (Texas Red filter, one-second exposure, contrast set to zero, Openlab by Improvion version 5.0.2 software) where

we regularly observed expression in wild type worms, but not in *pop-1(q645)* mutants, and held these conditions constant during our analysis of different strains. At these conditions, POPTOP expression in the VPC progeny was scored as detectable or not detectable (Table S3).

Transgenics

Extrachromosomal arrays were generated by co-injecting a transgene with *unc-119(+)* [60ng/ μ L] into *unc-119(ed4)* hermaphrodites or with *pha-1(+)* [90 ng/ μ L] into *pha-1(e2123ts)* hermaphrodites as described (Mello et al., 1991) except for *vang-1::YFP*, which was generated using bombardment (Praitis et al., 2001). Construction of transgenes *syEx710*, *syEx777*, *syEx780*, *syEx864* and *syIs198* was described previously (Green et al., 2007). *syIs202 [vang-1::YFP]* contains *vang-1* genomic DNA amplified with forward primer TTCTACCGGTGTGGAATAGGAAACCTGAAATTATGAATTATG and reverse primer CCAATCGTATGGCCGTTAATTAAGATACGCTTAAAGCTGG and includes coding sequence up to the beginning of the 5th exon and 3kb of sequence 5' of ATG. *Pfos-1a::EGL-20::GFP* was made by replacing the *myo-2* promoter of pJW33 (Whangbo and Kenyon, 1999) with the *fos-1a* promoter amplified using primer CGCGGATCCTGGGCAGCTGTAAAACGTCTTTAC (Bam HI site engineered 5') and reverse primer GCAGCTAGCTCCACTCTCTTATATAGCAGAGGTG (Nhe I site engineered 3'). To make *Pfos-1a::MOM-2::YFP*, the above *fos-1a* promoter was transferred into Fire vector L4817 using BglIII and NheI. *mom-2* cDNA, amplified by forward primer AGCATGCTAGCCATGCACATCAACACGCCAGTTC and reverse primer CTACCGGTACCAAACAGTAGTTTCTTTCTACTAACTTCTT, was then introduced

using sites *NheI* and *AgeI*. *syEx1005[Pheat-shock::CAM-1(del-intra)]* was made by switching the DNA encoding the carboxy-terminus of *syEx710[Pheat-shock::CAM-1]* with *syEx814[Pmyo-3::CAM-1(del-intra)]* (Green et al., 2007) using *NotI* and *SbfI*. To make *Pheat-shock::CAM-1(kinase-dead)*, we started with *syEx710* and changed codons 624 and 625 from encoding lysines to encoding arginines, as previously done to inactivate the CAM-1 kinase domain (Forrester et al., 1999). Because worms carrying *Pmyo-3::CAM-1::GFP* and *Psnb-1::CAM-1::GFP* as extrachromosomal arrays (Green et al., 2007) did not perform well in crosses, these plasmid were injected into *lin-17(n671); cam-1(gm122)* double mutants and progeny that carried the arrays were scored. We did not obtain stable lines for either of these transgenes. *BAR-1::GFP (gals45)* (Eisenmann et al., 1998), *GFP::POP-1 (qIs74)* (Siegfried et al., 2004), *VNS::SYS-1 (qIs95)* (Phillips et al., 2007), *WRM-1::GFP (osEx158)* (Takeshita and Sawa, 2005), *GFP::LIT-1* (Rocheleau et al., 1999) and *Pheat-shock::EGL-20* (pJW30) (Whangbo and Kenyon, 1999) were previously described. Our attempts to reverse the EGL-20 gradient utilized plasmids pJW33 [*Pmyo-2::EGL-20::GFP*] (Whangbo and Kenyon, 1999) injected at 15ng/ μ l, 20ng/ μ L and 80ng/ μ L and [*Plim-4::EGL-20::GFP*] (Pan et al., 2006) injected at 20ng/ μ l.

- Baena-Lopez, L. A., Baonza, A. and Garcia-Bellido, A.** (2005). The orientation of cell divisions determines the shape of *Drosophila* organs. *Curr Biol* **15**, 1640-4.
- Brenner, S.** (1974). The genetics of *Caenorhabditis elegans*. *Genetics* **77**, 71-94.
- Coudreuse, D. Y., Roel, G., Betist, M. C., Destree, O. and Korswagen, H. C.** (2006). Wnt gradient formation requires retromer function in Wnt-producing cells. *Science* **312**, 921-4.
- Deans, M. R., Antic, D., Suyama, K., Scott, M. P., Axelrod, J. D. and Goodrich, L. V.** (2007). Asymmetric distribution of prickle-like 2 reveals an early underlying polarization of vestibular sensory epithelia in the inner ear. *J Neurosci* **27**, 3139-47.
- Deshpande, R., Inoue, T., Priess, J. R. and Hill, R. J.** (2005). *lin-17*/Frizzled and *lin-18* regulate POP-1/TCF-1 localization and cell type specification during *C. elegans* vulval development. *Dev Biol* **278**, 118-29.
- Eisenmann, D. M., Maloof, J. N., Simske, J. S., Kenyon, C. and Kim, S. K.** (1998). The beta-catenin homolog BAR-1 and LET-60 Ras coordinately regulate the Hox gene *lin-39* during *Caenorhabditis elegans* vulval development. *Development* **125**, 3667-80.
- Ferguson, E. L. and Horvitz, H. R.** (1985). Identification and characterization of 22 genes that affect the vulval cell lineages of the nematode *Caenorhabditis elegans*. *Genetics* **110**, 17-72.
- Ferguson, E. L., Sternberg, P. W. and Horvitz, H. R.** (1987). A genetic pathway for the specification of the vulval cell lineages of *Caenorhabditis elegans*. *Nature* **326**, 259-67.
- Forrester, W. C., Dell, M., Perens, E. and Garriga, G.** (1999). A *C. elegans* Ror receptor tyrosine kinase regulates cell motility and asymmetric cell division. *Nature* **400**, 881-5.
- Gleason, J. E., Szyleyko, E. A. and Eisenmann, D. M.** (2006). Multiple redundant Wnt signaling components function in two processes during *C. elegans* vulval development. *Dev Biol*.
- Gordon, M. D. and Nusse, R.** (2006). Wnt signaling: multiple pathways, multiple receptors, and multiple transcription factors. *J Biol Chem* **281**, 22429-33.
- Green, J. L., Inoue, T. and Sternberg, P. W.** (2007). The *C. elegans* ROR receptor tyrosine kinase, CAM-1, non-autonomously inhibits the Wnt pathway. *Development* **134**, 4053-62.
- Herman, M. A.** (2002). Control of cell polarity by noncanonical Wnt signaling in *C. elegans*. *Semin Cell Dev Biol* **13**, 233-41.
- Herman, M. A., Vassilieva, L. L., Horvitz, H. R., Shaw, J. E. and Herman, R. K.** (1995). The *C. elegans* gene *lin-44*, which controls the polarity of certain asymmetric cell divisions, encodes a Wnt protein and acts cell nonautonomously. *Cell* **83**, 101-10.
- Hikasa, H., Shibata, M., Hiratani, I. and Taira, M.** (2002). The *Xenopus* receptor tyrosine kinase *Xror2* modulates morphogenetic movements of the axial mesoderm and neuroectoderm via Wnt signaling. *Development* **129**, 5227-39.
- Huang, S., Shetty, P., Robertson, S. M. and Lin, R.** (2007). Binary cell fate specification during *C. elegans* embryogenesis driven by reiterated reciprocal asymmetry of TCF POP-1 and its coactivator beta-catenin SYS-1. *Development* **134**, 2685-95.
- Inoue, T., Oz, H. S., Wiland, D., Gharib, S., Deshpande, R., Hill, R. J., Katz, W. S. and Sternberg, P. W.** (2004). *C. elegans* LIN-18 is a Ryk ortholog and functions in parallel to LIN-17/Frizzled in Wnt signaling. *Cell* **118**, 795-806.
- Inoue, T., Sherwood, D. R., Aspöck, G., Butler, J. A., Gupta, B. P., Kirouac, M., Wang, M., Lee, P. Y., Kramer, J. M., Hope, I. et al.** (2002). Gene expression markers for *Caenorhabditis elegans* vulval cells. *Mech Dev* **119 Suppl 1**, S203-9.

- Jones, C. and Chen, P.** (2007). Planar cell polarity signaling in vertebrates. *Bioessays* **29**, 120-32.
- Kelly, W. G., Xu, S., Montgomery, M. K. and Fire, A.** (1997). Distinct requirements for somatic and germline expression of a generally expressed *Caenorhabditis elegans* gene. *Genetics* **146**, 227-38.
- Kidd, A. R., 3rd, Miskowski, J. A., Siegfried, K. R., Sawa, H. and Kimble, J.** (2005). A beta-catenin identified by functional rather than sequence criteria and its role in Wnt/MAPK signaling. *Cell* **121**, 761-72.
- Korswagen, H. C., Coudreuse, D. Y., Betist, M. C., van de Water, S., Zivkovic, D. and Clevers, H. C.** (2002). The Axin-like protein PRY-1 is a negative regulator of a canonical Wnt pathway in *C. elegans*. *Genes Dev* **16**, 1291-302.
- Korswagen, H. C., Herman, M. A. and Clevers, H. C.** (2000). Distinct beta-catenins mediate adhesion and signalling functions in *C. elegans*. *Nature* **406**, 527-32.
- Lo, M. C., Gay, F., Odom, R., Shi, Y. and Lin, R.** (2004). Phosphorylation by the beta-catenin/MAPK complex promotes 14-3-3-mediated nuclear export of TCF/POP-1 in signal-responsive cells in *C. elegans*. *Cell* **117**, 95-106.
- Maduro, M. F., Lin, R. and Rothman, J. H.** (2002). Dynamics of a developmental switch: recursive intracellular and intranuclear redistribution of *Caenorhabditis elegans* POP-1 parallels Wnt-inhibited transcriptional repression. *Dev Biol* **248**, 128-42.
- McNally, K., Audhya, A., Oegema, K. and McNally, F. J.** (2006). Katanin controls mitotic and meiotic spindle length. *J Cell Biol* **175**, 881-91.
- Mello, C. C., Kramer, J. M., Stinchcomb, D. and Ambros, V.** (1991). Efficient gene transfer in *C. elegans*: extrachromosomal maintenance and integration of transforming sequences. *Embo J* **10**, 3959-70.
- Mizumoto, K. and Sawa, H.** (2007). Two betas or not two betas: regulation of asymmetric division by beta-catenin. *Trends Cell Biol* **17**, 465-73.
- Molenaar, M., van de Wetering, M., Oosterwegel, M., Peterson-Maduro, J., Godsave, S., Korinek, V., Roose, J., Destree, O. and Clevers, H.** (1996). XTcf-3 transcription factor mediates beta-catenin-induced axis formation in *Xenopus* embryos. *Cell* **86**, 391-9.
- Oishi, I., Suzuki, H., Onishi, N., Takada, R., Kani, S., Ohkawara, B., Koshida, I., Suzuki, K., Yamada, G., Schwabe, G. C. et al.** (2003). The receptor tyrosine kinase Ror2 is involved in non-canonical Wnt5a/JNK signalling pathway. *Genes Cells* **8**, 645-54.
- Pan, C. L., Howell, J. E., Clark, S. G., Hilliard, M., Cordes, S., Bargmann, C. I. and Garriga, G.** (2006). Multiple Wnts and frizzled receptors regulate anteriorly directed cell and growth cone migrations in *Caenorhabditis elegans*. *Dev Cell* **10**, 367-77.
- Park, F. D., Tenlen, J. R. and Priess, J. R.** (2004). *C. elegans* MOM-5/frizzled functions in MOM-2/Wnt-independent cell polarity and is localized asymmetrically prior to cell division. *Curr Biol* **14**, 2252-8.
- Phillips, B. T., Kidd, A. R., 3rd, King, R., Hardin, J. and Kimble, J.** (2007). Reciprocal asymmetry of SYS-1/beta-catenin and POP-1/TCF controls asymmetric divisions in *Caenorhabditis elegans*. *Proc Natl Acad Sci U S A* **104**, 3231-6.
- Praitis, V., Casey, E., Collar, D. and Austin, J.** (2001). Creation of low-copy integrated transgenic lines in *Caenorhabditis elegans*. *Genetics* **157**, 1217-26.
- Rocheleau, C. E., Yasuda, J., Shin, T. H., Lin, R., Sawa, H., Okano, H., Priess, J. R., Davis, R. J. and Mello, C. C.** (1999). WRM-1 activates the LIT-1 protein kinase to transduce anterior/posterior polarity signals in *C. elegans*. *Cell* **97**, 717-26.

- Sawa, H., Lobel, L. and Horvitz, H. R.** (1996). The *Caenorhabditis elegans* gene *lin-17*, which is required for certain asymmetric cell divisions, encodes a putative seven-transmembrane protein similar to the *Drosophila* frizzled protein. *Genes Dev* **10**, 2189-97.
- Schambony, A. and Wedlich, D.** (2007). Wnt-5A/Ror2 regulate expression of XPAPC through an alternative noncanonical signaling pathway. *Dev Cell* **12**, 779-92.
- Schlesinger, A., Shelton, C. A., Maloof, J. N., Meneghini, M. and Bowerman, B.** (1999). Wnt pathway components orient a mitotic spindle in the early *Caenorhabditis elegans* embryo without requiring gene transcription in the responding cell. *Genes Dev* **13**, 2028-38.
- Seifert, J. R. and Mlodzik, M.** (2007). Frizzled/PCP signalling: a conserved mechanism regulating cell polarity and directed motility. *Nat Rev Genet* **8**, 126-38.
- Sherwood, D. R., Butler, J. A., Kramer, J. M. and Sternberg, P. W.** (2005). FOS-1 promotes basement-membrane removal during anchor-cell invasion in *C. elegans*. *Cell* **121**, 951-62.
- Shetty, P., Lo, M. C., Robertson, S. M. and Lin, R.** (2005). *C. elegans* TCF protein, POP-1, converts from repressor to activator as a result of Wnt-induced lowering of nuclear levels. *Dev Biol* **285**, 584-92.
- Siegfried, K. R., Kidd, A. R., 3rd, Chesney, M. A. and Kimble, J.** (2004). The *sys-1* and *sys-3* genes cooperate with Wnt signaling to establish the proximal-distal axis of the *Caenorhabditis elegans* gonad. *Genetics* **166**, 171-86.
- Siegfried, K. R. and Kimble, J.** (2002). POP-1 controls axis formation during early gonadogenesis in *C. elegans*. *Development* **129**, 443-53.
- Singh, N. and Han, M.** (1995). *sur-2*, a novel gene, functions late in the *let-60* ras-mediated signaling pathway during *Caenorhabditis elegans* vulval induction. *Genes Dev* **9**, 2251-65.
- Sternberg, P. W.** (2005). Vulval development. In *WormBook*, (ed. B. J. Meyer): The *C. elegans* Research Community, WormBook.
- Sternberg, P. W. and Horvitz, H. R.** (1988). *lin-17* mutations of *Caenorhabditis elegans* disrupt certain asymmetric cell divisions. *Dev Biol* **130**, 67-73.
- Strutt, D.** (2005). Organ shape: controlling oriented cell division. *Curr Biol* **15**, R758-9.
- Sulston, J. E. and Horvitz, H. R.** (1977). Post-embryonic cell lineages of the nematode, *Caenorhabditis elegans*. *Dev Biol* **56**, 110-56.
- Takehita, H. and Sawa, H.** (2005). Asymmetric cortical and nuclear localizations of WRM-1/beta-catenin during asymmetric cell division in *C. elegans*. *Genes Dev* **19**, 1743-8.
- van de Wetering, M., Cavallo, R., Dooijes, D., van Beest, M., van Es, J., Loureiro, J., Ypma, A., Hursh, D., Jones, T., Bejsovec, A. et al.** (1997). Armadillo coactivates transcription driven by the product of the *Drosophila* segment polarity gene *dTCF*. *Cell* **88**, 789-99.
- Veeman, M. T., Slusarski, D. C., Kaykas, A., Louie, S. H. and Moon, R. T.** (2003). Zebrafish *prickle*, a modulator of noncanonical Wnt/Fz signaling, regulates gastrulation movements. *Curr Biol* **13**, 680-5.
- Wang, Y. and Nathans, J.** (2007). Tissue/planar cell polarity in vertebrates: new insights and new questions. *Development* **134**, 647-58.
- Whangbo, J. and Kenyon, C.** (1999). A Wnt signaling system that specifies two patterns of cell migration in *C. elegans*. *Mol Cell* **4**, 851-8.
- Wodarz, A. and Nathke, I.** (2007). Cell polarity in development and cancer. *Nat Cell Biol* **9**, 1016-24.

- Yoo, A. S., Bais, C. and Greenwald, I.** (2004). Crosstalk between the EGFR and LIN-12/Notch pathways in *C. elegans* vulval development. *Science* **303**, 663-6.
- Zallen, J. A.** (2007). Planar polarity and tissue morphogenesis. *Cell* **129**, 1051-63.

Table 1. Reversed vulval lineage phenotype

Relevant Genotype	% P-Rvl	% A-Rvl	% AP-Rvl [†]	n	P value
<i>lin-17(n671)</i>	74	0	0	113	
<i>lin-18(e620)</i>	36	0	0	113	
<i>lin-17(n671); lin-18(e620)*</i>	100	0	0	63	
<i>egl-20(n585)</i>	0	0	0	22	
<i>lin-17(n671); egl-20(n585)</i>	8	0	0	64	<0.001 ^a
<i>egl-20(n585); lin-18(e620)</i>	7	0	0	70	<0.001 ^b
<i>egl-20(hu120)</i>	0	0	0	66	
<i>lin-17(n671); egl-20(hu120)</i>	6	0	0	52	<0.001 ^a
<i>egl-20(hu120); lin-18(e620)</i>	8	0	0	51	<0.001 ^b
<i>lin-17(n671); egl-20(n585); lin-18(e620)</i>	48	6	2	66	<0.001 ^c
<i>lin-17(n671); egl-20(hu120); lin-18(e620)</i>	50	2	0	52	<0.001 ^c
<i>cwn-1(ok546)</i>	0	0	0	38	
<i>lin-17(n671); cwn-1(ok546)</i>	52	0	0	54	0.005 ^a
<i>cwn-1(ok546); lin-18(e620)</i>	26	0	0	53	0.222 ^b
<i>lin-17(n671); cwn-1(ok546); lin-18(e620)</i>	92	0	0	47	0.075 ^c
parent strain [#]	0	0	0	40	
<i>syEx710[Pheat-shock::CAM-1][‡]</i>	12	14	2	59	<0.001 ^d
<i>lin-44(n1792); syEx710[Pheat-shock::CAM-1][‡]</i>	43	35	8	84	<0.001 ^e
<i>mom-2(or42)*</i>	1	0	0	83	
<i>lin-44(n1792)*</i>	0	0	0	120	
<i>lin-44(n1792); mom-2(or42)*</i>	59	0	0	127	<0.001 ^e
<i>syEx780[Pfos-1a::CAM-1::GFP]</i>	0	0	0	21	
<i>syEx777[Pfos-1a::CAM-1::GFP]</i>	0	0	0	21	
<i>lin-44(n1792); syEx780[Pfos-1a::CAM-1::GFP]</i>	46	2	2	54	<0.001 ^e
<i>lin-17(n671); egl-20(hu120)[‡]</i>	0	0	0	51	
<i>lin-17(n671); egl-20(hu120); syEx1024[Pheat-shock::EGL-20][‡]</i>	75	54	46	28	
<i>lin-17(n671); egl-20(hu120); syEx1025[Pheat-shock::EGL-20][‡]</i>	76	48	33	21	
<i>lin-17(n671); egl-20(hu120); lin-18(e620); syEx1031[Pfos-1a::EGL-20::GFP]</i>	13	0	0	23	0.002 ^f
<i>lin-17(n671); syEx1031[Pfos-1a::EGL-20::GFP]</i>	25	0	0	44	<0.001 ^a
<i>pop-1(q645)</i>	0	0	0	18	
<i>pop-1(RNAi)</i>	3	0	0	39	
<i>sys-1(q544)</i>	2	0	0	44	
<i>wrm-1(ne1982)</i>	4	4	0	23	
<i>lit-1(or131)</i>	0	0	0	22	
<i>lin-17(n671); lit-1(or131)</i>	11	6	0	36	<0.001 ^a
<i>lit-1(or131); lin-18(e620)</i>	17	0	0	64	0.010 ^b
<i>bar-1(ga80)</i>	0	0	0	20	
<i>sys-1(q544); bar-1(ga80)</i>	15	3	0	40	
<i>vang-1(ok1142)</i>	0	0	0	58	
<i>lin-17(n671); vang-1(ok1142)</i>	48	3	3	60	0.005 ^a
<i>lin-17(n671); egl-20(hu120); vang-1(ok1142)</i>	2	0	0	50	
<i>lin-17(n671); vang-1(ok1142); syEx1031[Pfos-1a::EGL-20::GFP]</i>	46	0	0	71	0.030 ^g
<i>cam-1(gm122)</i>	0	0	0	54	
<i>lin-17(n671); cam-1(gm122)</i>	46	2	0	54	0.005 ^a
<i>cam-1(sa692)</i>	0	0	0	50	
<i>lin-17(n671); cam-1(sa692)</i>	51	0	0	45	0.008 ^a
<i>cam-1(ak37)</i>	0	0	0	53	
<i>lin-17(n671); cam-1(ak37)</i>	38	0	0	48	<0.001 ^a
<i>cam-1(gm105)</i>	0	0	0	54	
<i>lin-17(n671); cam-1(gm105)</i>	55	0	0	53	0.013 ^a
<i>cam-1(ks52)</i>	0	0	0	53	
<i>lin-17(n671); cam-1(ks52)</i>	23	0	0	52	<0.001 ^a
<i>lin-17(n671); cam-1(gm122); syEx1031[Pfos-1a::EGL-20::GFP]</i>	52	4	0	23	0.033 ^g
<i>lin-17(n671); cam-1(gm122); vang-1(ok1142)</i>	38	8	5	61	0.449 ^h
<i>lin-17(n671); cam-1(ks52); vang-1(ok1142)</i>	28	2	2	53	0.656 ⁱ
<i>lin-17(n671); cam-1(gm122); egl-20(n585)</i>	15	3	0	40	
<i>lin-17(n671); cam-1(gm122); Ex[Psnb-1::CAM-1::GFP]</i>	49	3	0	39	0.863 ^h
<i>lin-17(n671); cam-1(gm122); Ex[Pmyo-3::CAM-1::GFP]</i>	55	0	0	20	0.604 ^h
<i>lin-17(n671); jnk-1(gk7)</i>	74	2	0	43	1.0 ^a

For each genotype, only worms with wild-type vulval induction, i.e. 3.0, were scored.

pop-1(q645), *sys-1(q544)* and *mom-2(or42)* are homozygous progeny from heterozygous mothers. *lit-1(or131)* and *wrm-1(ne1982)* are temperature-sensitive alleles; L1 worms were raised at 25°C.

*values originally reported in Inoue et al., 2004. [†]AP-Rvl worms are also included in A-Rvl and P-Rvl categories.

[#] Mixed stage worms were heat-shocked 45 min. (CAM-1) or 20 min. (EGL-20) at 33°, mid-L4 animals were scored 16 hours later.

^a compared to *lin-17(n671)*, ^b compared to *lin-18(e620)*, ^c compared to *lin-17(n671); lin-18(e620)*,

^d compared to *pha-1(e2123); him-5(e1490)*, ^e compared to *lin-44(n1792)*, ^f compared to *lin-17(n671); egl-20(hu120); lin-18(e620)*, ^g compared to *lin-17(n671); syEx1031[Pfos-1a::EGL-20::GFP]*, ^h compared to *lin-17(n671); cam-1(gm122)*, and ⁱ compared to *lin-17(n671); cam-1(ks52)* using Fisher's Exact Test.

Table S1. CAM-1 over-expression to inhibit Wnts

Relevant Genotype	% P-Rvl	% A-Rvl	% AP-Rvl [^]	n	P value
parent strain [#]	0	0	0	40	
<i>Ex[Pheat-shock::CAM-1(kinase-dead)][#]</i>	5	8	0	39	0.026 ^a
<i>syEx1005[Pheat-shock::CAM-1(del-intra)::GFP][#]</i>	0	0	0	20	
<i>lin-44(n1792); syEx1005[Pheat-shock::CAM-1(del-intra)::GFP][#]</i>	16	0	0	69	<.0001 ^b
<i>syIs198[P1st-1::CAM-1::GFP]</i>	0	5	0	22	
<i>syEx864[Psur-2::CAM-1::GFP]</i>	0	0	0	38	
<i>lin-17(n671)</i>	74	0	0	113	
<i>lin-17(n671); lin-44(n1792)*</i>	58	0	0	186	
<i>lin-17(n671); cwn-1(ok546)</i>	52	0	0	54	
<i>lin-17(n671); cwn-2(ok895)</i>	75	0	0	40	
<i>lin-17(n671); mom-2(or42)*</i>	100	0	0	103	<.0001 ^c
<i>lin-17(n671); syEx780[Pfos-1a::CAM-1::GFP]</i>	98	0	0	41	.0009 ^c
<i>lin-44(n1792); mom-2(or42)*</i>	59	0	0	127	
<i>lin-44(n1792); mom-2(or42); syEx[Pfos-1a::MOM-2::GFP]</i>	33	0	0	24	.0254 ^d

For each genotype, only worms with wild-type vulval induction, i.e. 3.0, were scored.

mom-2(or42) are homozygous progeny from heterozygous mothers.

*values originally reported in Inoue et al., 2004. [^]AP-Rvl worms are also included in A-Rvl and P-Rvl categories.

[#] Mixed stage worms were heat-shocked 45 min. (CAM-1) or 20 min. (EGL-20) at 33°, mid-L4 animals were scored 16 hours later.

^a compared to *pha-1(e2123);him-5(e1490)*, ^b compared to *lin-44(n1792)*, ^c compared to *lin-17(n671)*, ^d compared to *lin-44(n1792); mom-2(or42)* using Fisher's Exact Test.

Table S2. Partial expression pattern and validation of POPTOP

cells (stage)	<i>Wild type</i> POPTOP	<i>Wild type</i> POPFOP	<i>pop-1(q645)</i> POPTOP	<i>pry-1(mu38)</i> POPTOP
P cells (L1)	+ ^a	+	+ ^b	ND
QL and QR cells (L1-L2)	+ ^c	-	- ^d	ND
SGPs (L1)	+	-	-	ND
V cells (L1)	+	-	ND	ND
B cell (L1)	+	ND	ND	ND
T cell (L1)	+	-	-	ND
VCNs (L1-L4)	+	+	+	+
Pn.ps (L1-late L2)	+	+	+	+
Pn.p (early L3)	-	-	-	ND
Pn.px (mid L3)	-	-	-	+++
Pn.pxx (mid L3)	+	-	-	+++
male hook precursors (L1-L4)	+	ND	ND	+
DTCs (L2-L3)	+	-	NA	++
vulval cells (L3-L4)	+	-	-	+++
uterine cells (L4)	+	-	-	+++
body wall muscle (L1-L4)	-	-	-	+++
vulval muscle (adult)	+	-	-	ND
many unidentified cells in head (all)	+	+	+	ND
many unidentified cells in tail (all)	+	+	+	ND

QL, QR: left and right Q neuroblasts. SGP: somatic goandal precursor. VCN: ventral cord neuron. DTC: distal tip cell. ^aP cell expression in 100% of worms n=34. ^bP cell expression in 100% of worms n=37. ^cQL expression in 91% of worms n=34. ^dQL expression in 27% of worms n=37. *P*<0001 using Fisher's Exact Test. ND= not determined

Table S3. POPTOP expression in VPC granddaughters

genotype:	#% reporter expression in both daughters of (<i>P</i> value):						n
	P5.pa	P5.pp	P6.pa	P6.pp	P7.pa	P7.pp	
<i>POPTOP syIs186</i>	5	24	10	10	33	5	21
<i>POPTOP syIs187</i>	0	38	5	5	29	0	21
<i>POPTOP syIs188</i>	0	43	4	11	36	0	28
<i>pop-1(q645)*; syIs187</i>	0	0(.001)	0	0	0(.009)	0	22
<i>pry-1(mu38); syIs188</i>	30	95(<.001)	100	100	80(.003)	40	20
<i>lin-17(n671); syIs187</i>	0	0(.003)	0	0	0(.021)	0	20
<i>lin-18(e620); syIs186</i>	0	13(.457)	0	0	0(.003)	13	24
<i>sys-1(q544)*; syIs187</i>	0	0(.003)	0	0	10(.238)	10	20
<i>bar-1(ga80); syIs188</i>	0	15(.060)	0	0	20(.338)	10	20
<i>egl-20(hu120); syIs186</i>	0	48(.197)	0	5	48(.530)	5	21
<i>lin-17(n671); egl-20(hu120); syIs188</i>	0	5(.003)	0	0	5(.014)	0	21

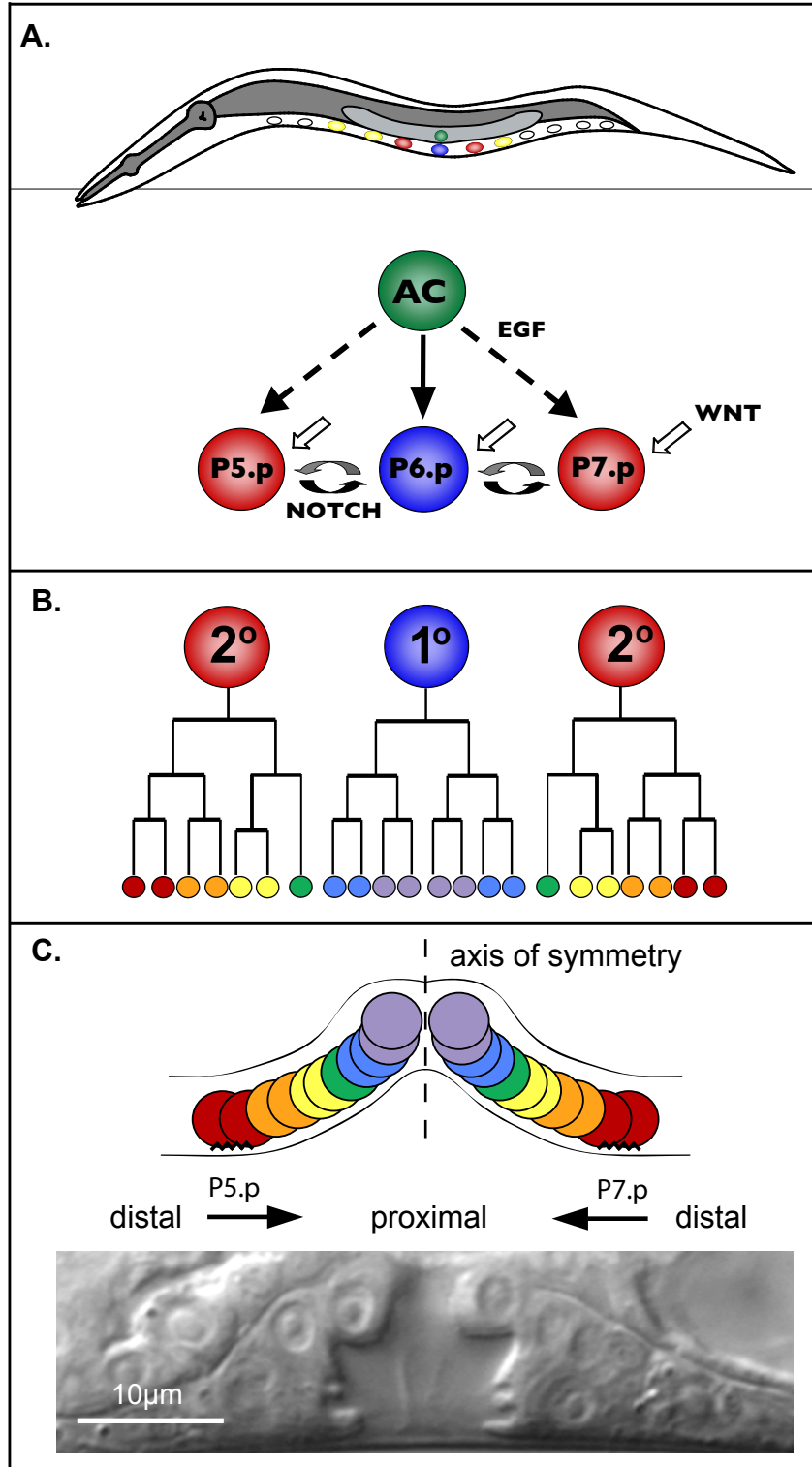
POPTOP expression was scored as positive if it was detectable in a one-second exposure.

#Percentages are of worms with wild-type vulval induction (3.0). *P* values represent a comparison to the corresponding transgenic strains in wild-type background and were calculated using Fisher's Exact Test.

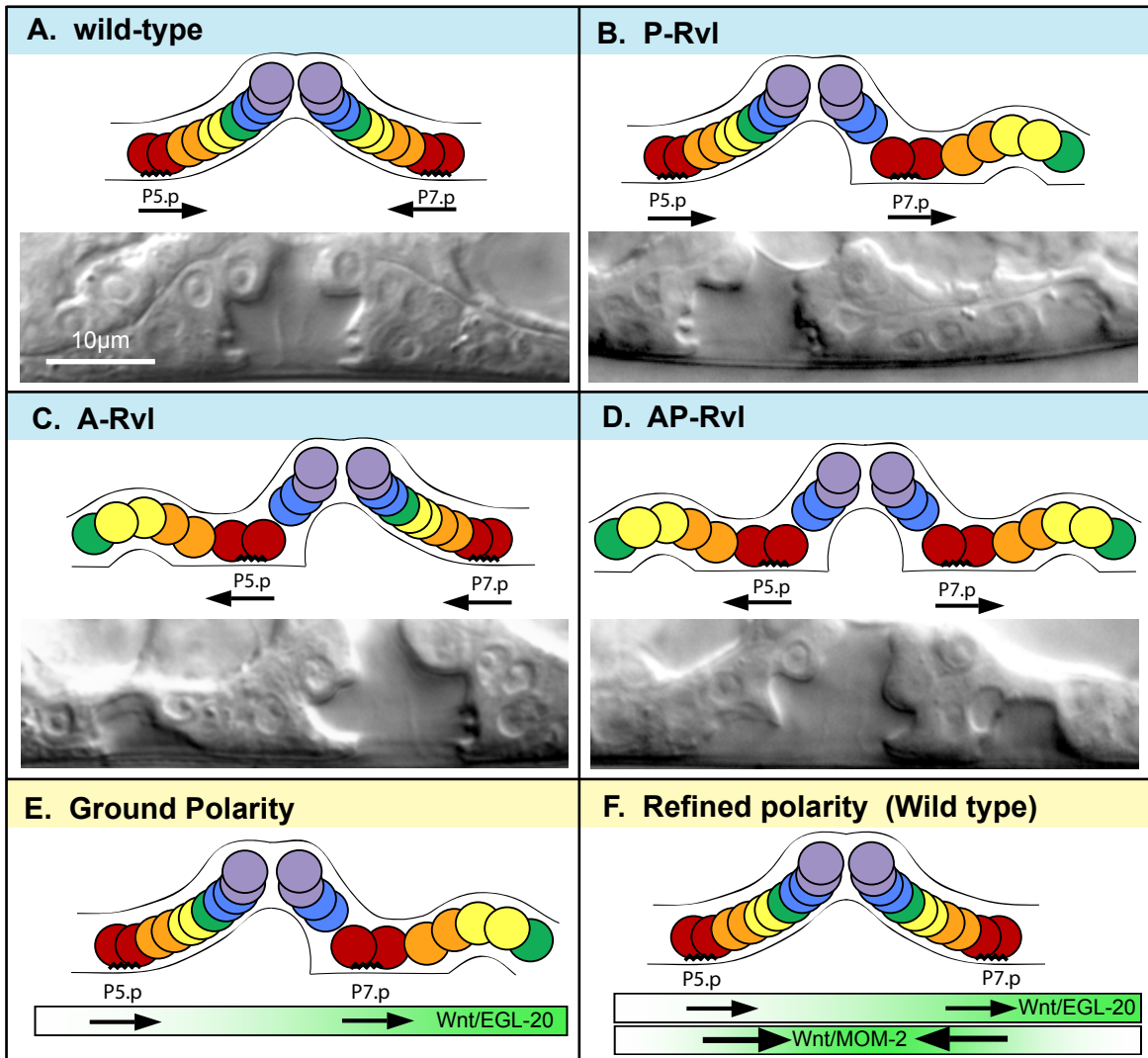
^Temperature sensitive allele; L1 worms were raised at 25C.

*Homozygous progeny from heterozygous mothers.

Figure 1. *C. elegans* vulva development



A) Schematic of vulval induction; anterior-left, dorsal-up. B) lineage trees of the VPC progeny, P5.p-left, P6.p-center, P7.p-right. C) Schematic arrangement (top) of the 1° and 2° vulval lineages along a proximal-distal axis. The cells located anterior or posterior to the axis of symmetry (dashed line) display opposite orientations. The jagged lines represent adherence to the cuticle. At the bottom is a Nomarski image of a wild-type vulva at the L4 stage.

Figure 2. Vulval lineage orientations and layered polarity model

Schematic arrangements of vulval lineages (top) and an example Nomarski image (bottom) for the four possible orientation combinations of P5.p and P7.p. Anterior-left. A) Wild-type, P5.p faces posteriorly and P7.p faces anteriorly. B) P-Rvl, both P5.p and P7.p face posteriorly. C) A-Rvl, both P5.p and P7.p face anteriorly. D) AP-Rvl, P5.p faces anteriorly and P7.p faces posteriorly. E) EGL-20, expressed from the posterior, promotes both P5.p and P7.p to face posteriorly. F) MOM-2, expressed in the centrally located anchor cell, orients both P5.p and P7.p toward the center. MOM-2 reverses P7.p polarity so that it faces anteriorly and reinforces the posterior-facing orientation of P5.p.

Figure 3. SYS-1, BAR-1 and VANG-1 expression in VPC progeny

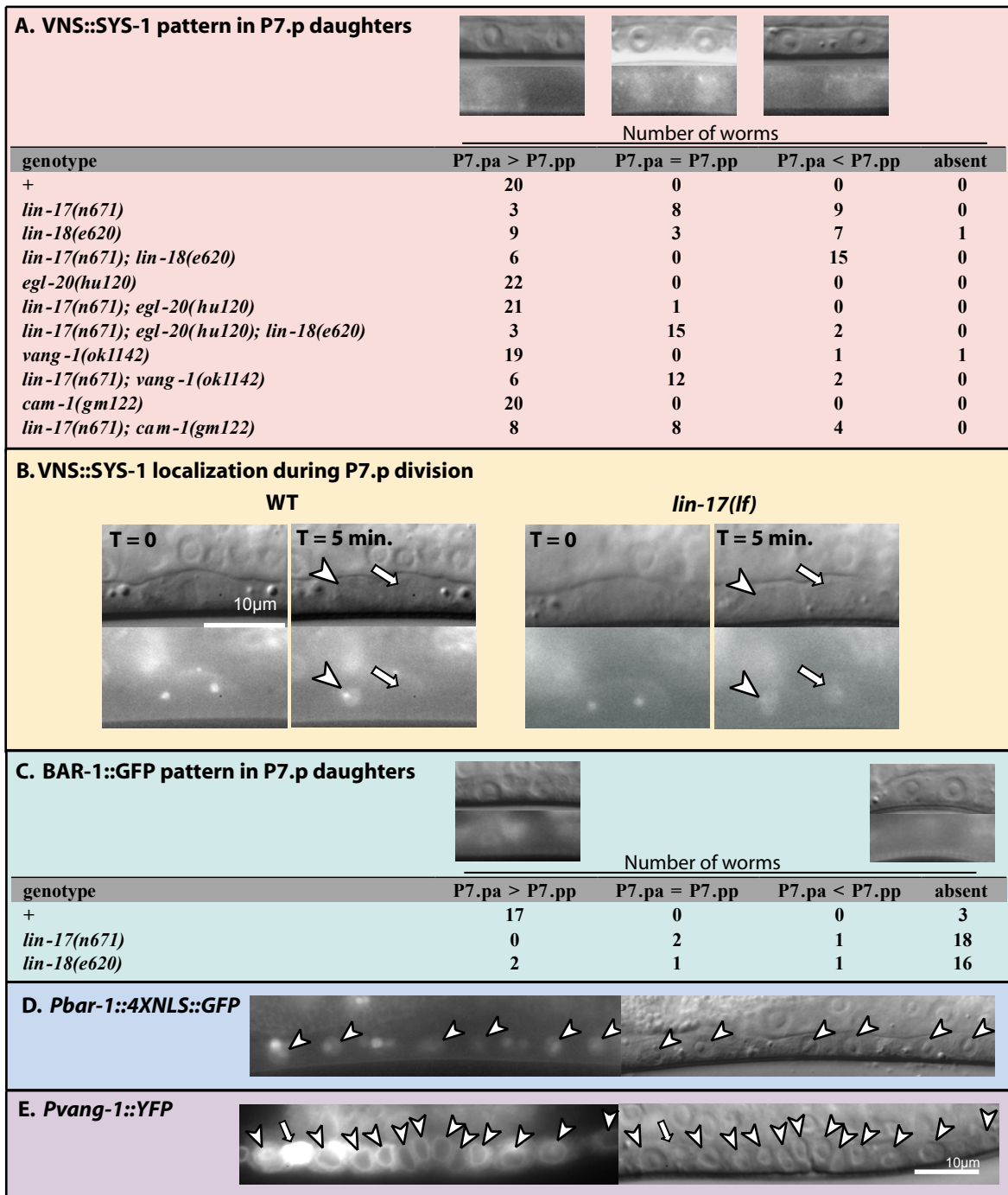
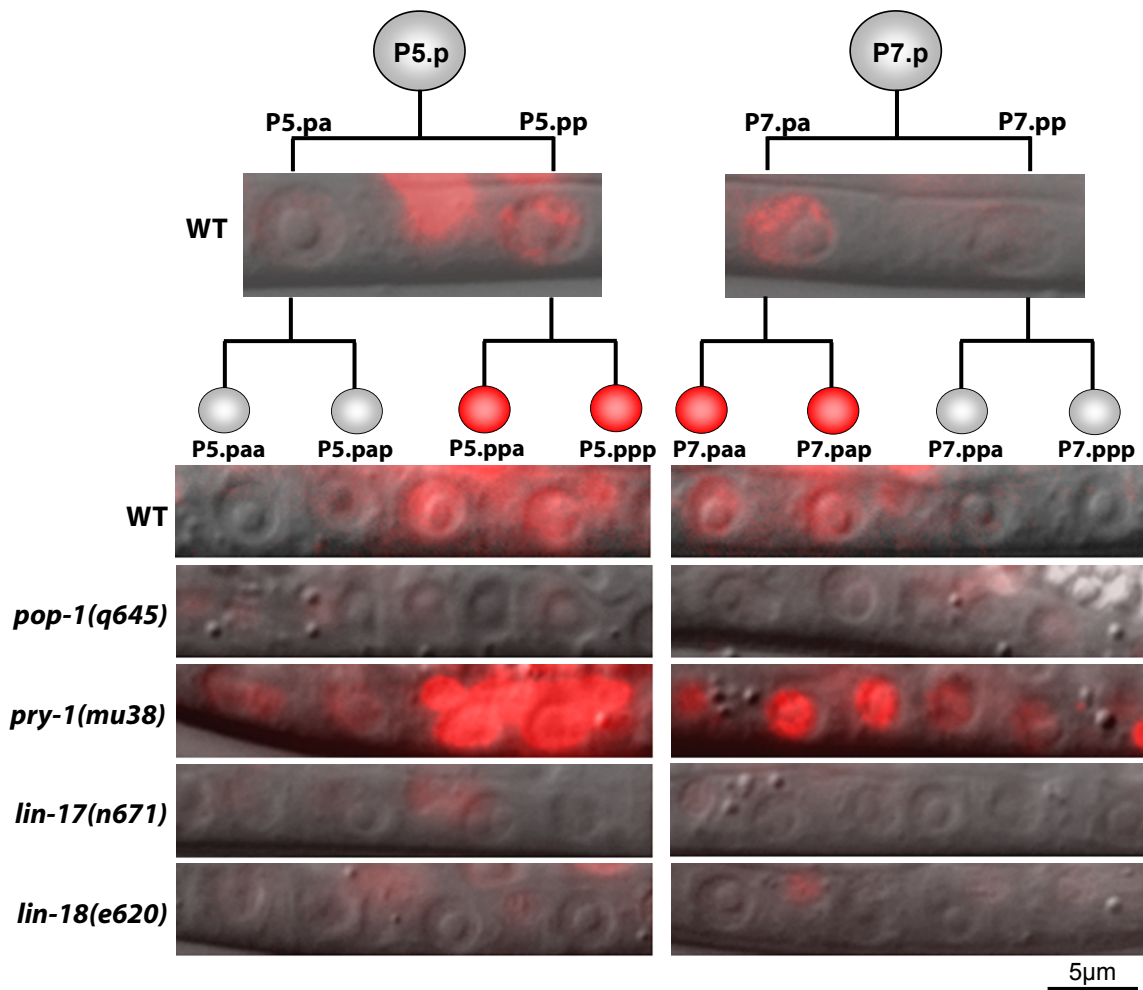


Figure 3. SYS-1, BAR-1 and VANG-1 expression in VPC progeny

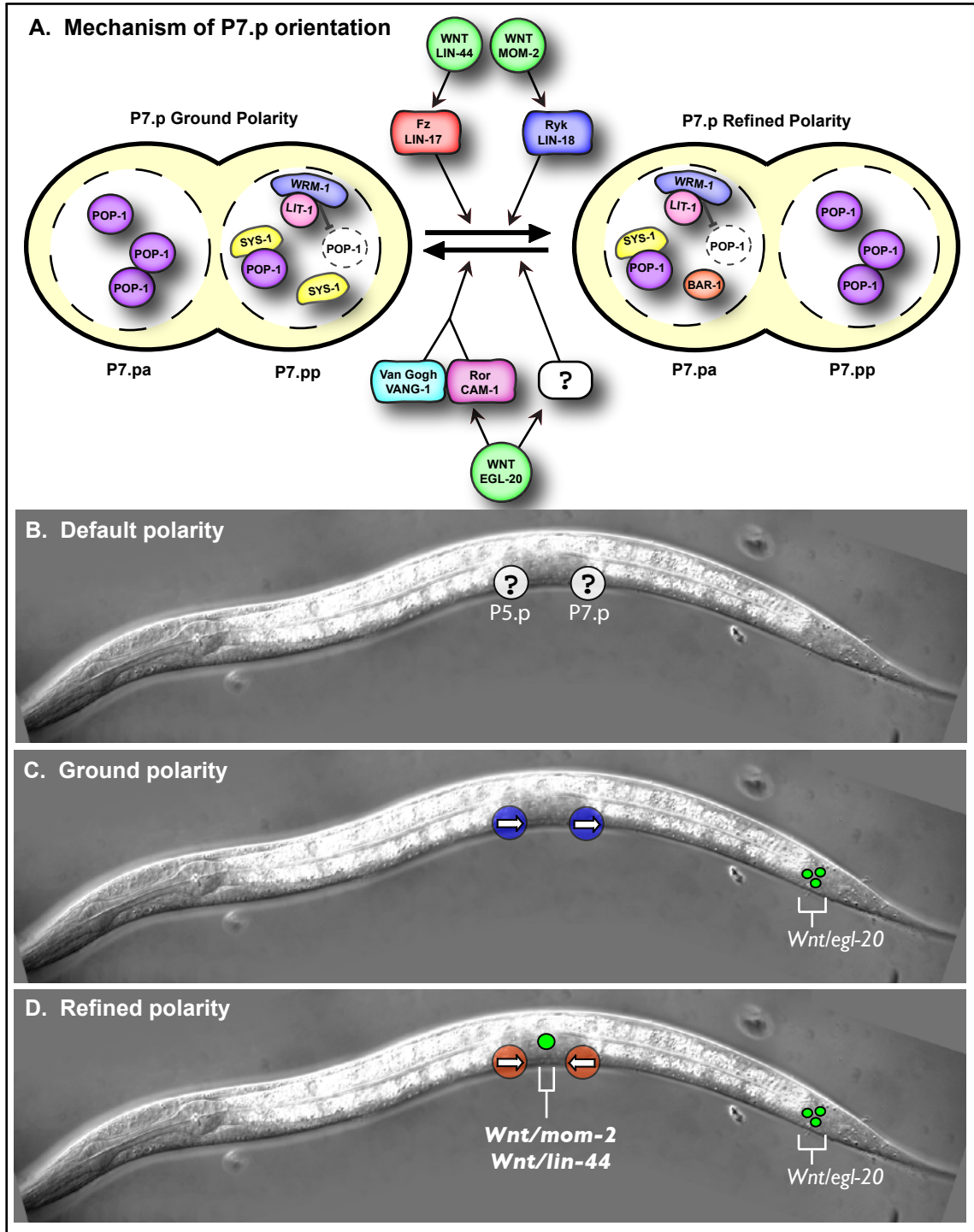
A) Subcellular localization of *qIs95*, a VNS::SYS-1 translational fusion. *qIs95* is expressed at very low levels. To characterize the localization, we captured a still fluorescence image using a long exposure time (8 sec.) and then applied the “Auto Contrast” function of Adobe Photoshop CS2. The resulting localization pattern was readily classifiable by eye into one of the three categories: SYS-1 was enriched in the anterior P7.p daughter nucleus (P7.pa > P7.pp), SYS-1 was present at similar levels in both P7.p daughter nuclei (P7.pa = P7.pp), or SYS-1 was enriched in the posterior P7.p daughter nucleus (P7.pa < P7.pp). A representative image is shown above each category and the number of worms in each category is listed. The VNS::SYS-1 localization pattern in P5.p daughters was unaffected in all of the genotypes examined, with the exception of symmetric distribution in a single *lin-17(lf); egl-20(lf)* double mutant worm and in two *lin-17(lf); egl-20(lf); lin-18(lf)* triple mutants. B) Nomarski (above) and fluorescence images (below) show VNS::SYS-1 localization during cell division. For wild type and *lin-17(lf)* mutants, the images on the right were taken 5 minutes after the images on the left. The two spots seen in the fluorescent images on the left are putative centrosomes. Arrowheads point to anterior daughter nuclei and arrows point to posterior daughter nuclei. C) BAR-1::GFP translation fusion; display is the same as in (A). D) A *bar-1::GFP* reporter that contains 5.1kb of the *bar-1* 5' regulatory region driving expression of nucleolus/nuclear localized GFP. This promoter region is the same as in panel C (Eisenmann et al., 1998). E) *vang-1::YFP* reporter is expressed in the VPC progeny (arrowheads). The bright *vang-1::YFP* expressing cell (arrow) is a ventral cord neuron.

Figure 4. POPTOP expression in VPC progeny

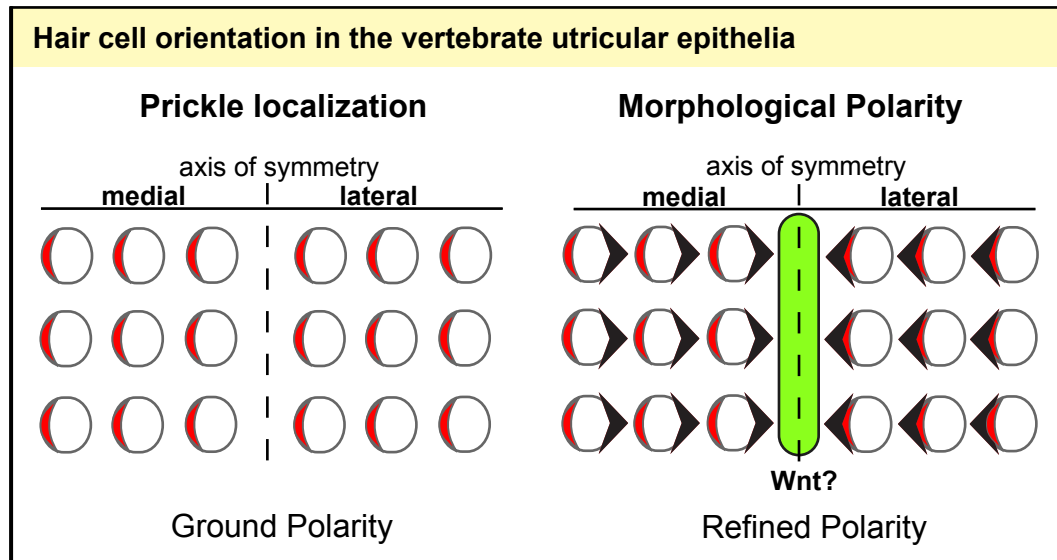


Overlay of Nomarski and fluorescence (red) images showing POPTOP expression in the VPC progeny. Representative images are shown. Fluorescent images of the VPC granddaughters were each exposed for 1 second except for *pry-1(mu38)*, which was exposed for 0.5 seconds. The fluorescence remaining in *lin-17(lf)* and *lin-18(lf)* mutants is in ventral cord neurons, where POPTOP is also expressed.

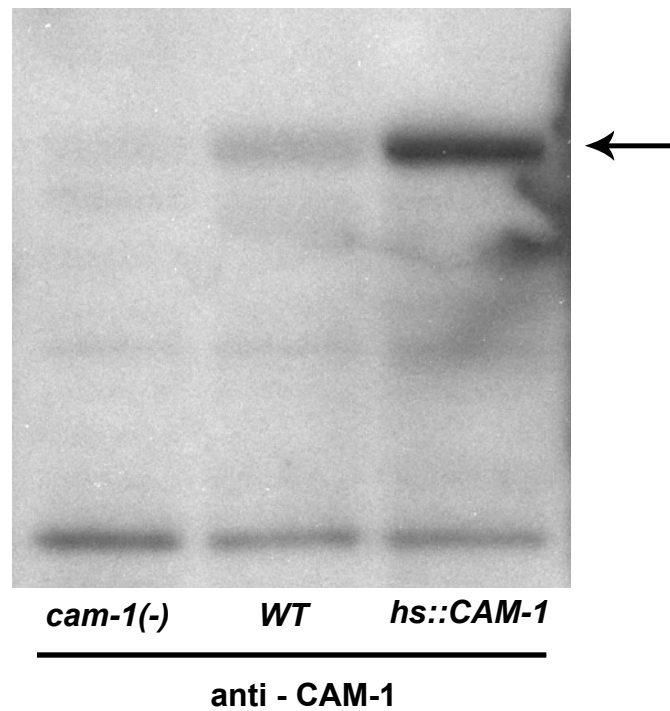
Figure 5. Model of VPC Orientation



A) Illustration of the genetic interactions contributing to the orientation of P7.p and the nuclear localization of POP-1, WRM-1, LIT-1, SYS-1 and BAR-1 in ground and refined polarity. We have examined WRM-1 and LIT-1 localization in refined polarity, but WRM-1 and LIT-1 localization in ground polarity is inferred from POP-1 localization, which was previously described (Deshpande et al., 2005). Localization of SYS-1 and BAR-1 in ground and refined polarity was described here. B-D) Schematics of default, ground and refined polarity. B) In the absence of Wnts, the orientation of P5.p and P7.p (white circles) is random (represented by a question mark). C) *egl-20/Wnt* is expressed in the tail (green circles) and establishes ground polarity in which both P5.p and P7.p (blue circles) face posteriorly (arrows). D) Wnts *mom-2* and *lin-44* are expressed in the AC (big green circle) and instruct P5.p and P7.p (red circles) to face the center (arrows).

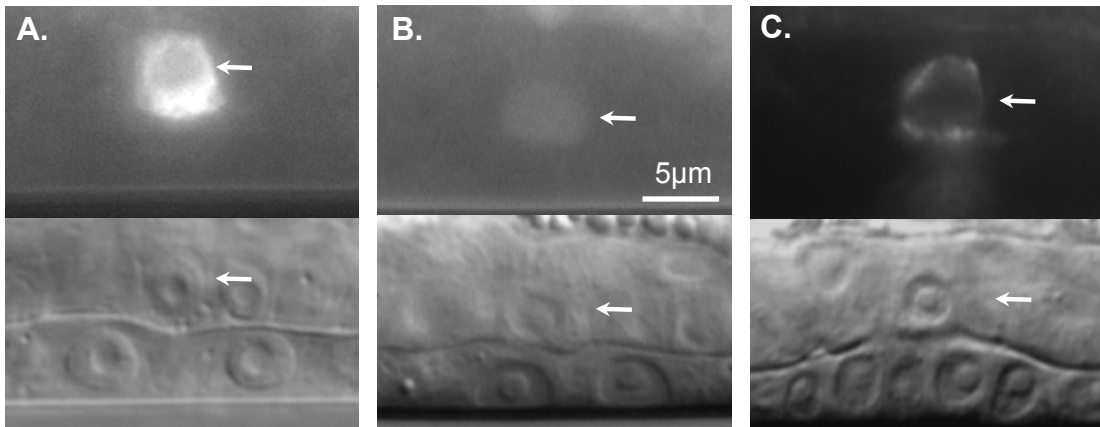
Figure 6. Ground and refined polarity in vertebrates

Schematic of proposed ground and refined polarity in the utricular epithelia of the vertebrate inner ear. Prickle (red crescent) is asymmetrically localized to the medial side of hair cells on both side of the axis of symmetry. Despite uniform prickle asymmetry, hair cells on either side of the axis of symmetry display opposite morphological polarity (black arrowhead). An additional patterning event is thought to determine the final morphological orientation (refined polarity) of these cells. This could be achieved by a local source of Wnt (green bar).

Figure S1. *hs::CAM-1* western blot

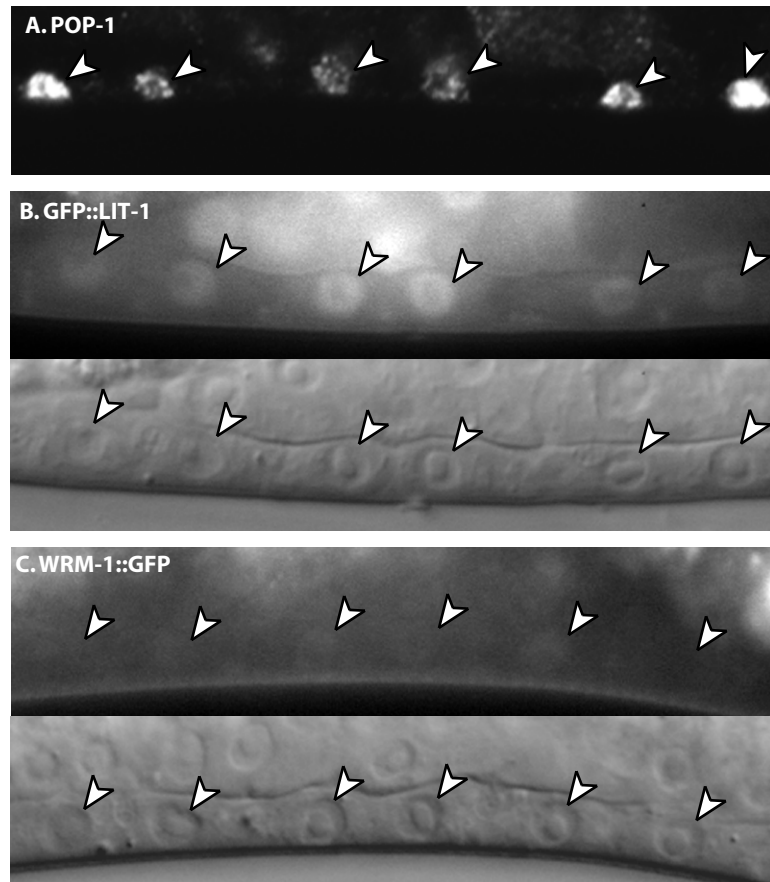
Worms carrying *syEx710[hs::CAM-1]* were heat-shocked for 45 min. at 33°C. This resulted in elevated CAM-1 levels (arrow) compared to wild type and *cam-1(lf)* mutants. Total worm lysates were probed with an anti-CAM-1 polyclonal antibody.

Figure S2. Anchor cell expression of *egl-20*, *lin-44* and *cam-1*.



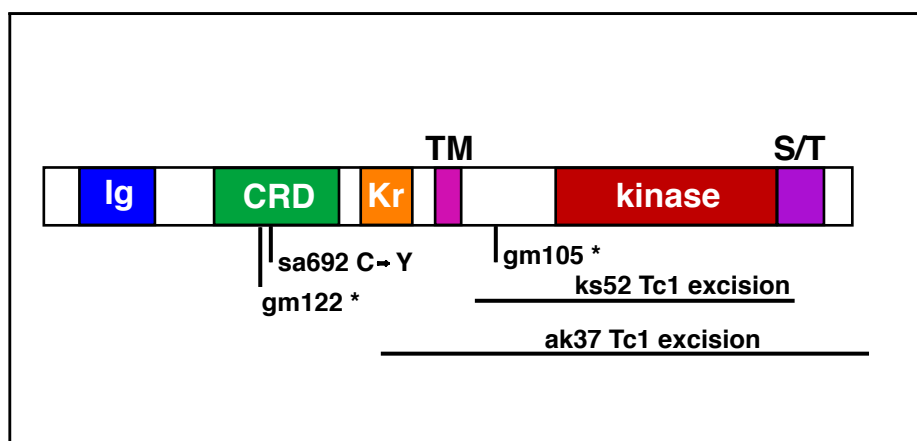
Fluorescence (top) and Nomarski (bottom) images of A) *Pfos-1a::EGL-20::GFP*, B) *Plin-44::GFP* and B) *Pfos-1a::CAM-1::GFP* transgenes expressed in the AC (arrow).

Figure S3. Localization of POP-1, GFP::LIT-1 and WRM-1::GFP in VC progeny



A) POP-1 expression in VPC daughter nuclei (arrowheads). POP-1 antibody staining was performed as described (Deshpande et al., 2005). B) GFP::LIT-1 (Rocheleau et al., 1999) was consistently observed in the VPC daughter nuclei (arrowheads). Asymmetric localization of GFP::LIT-1 among the secondary daughter nuclei was subtle and often not detectable by eye. To analyze the expression pattern we captured still images and used Openlab software to measure the mean pixel intensity of each nucleus. If the difference between two secondary sisters was greater than two Standard Deviations of the mean difference between the primary sisters, the pair was classified as unequal. In 16/22 wild type worms, GFP::LIT-1 levels were higher in the proximal daughters nucleus of P5.p and were equal between P5.p daughter nuclei in 6/22 worms. GFP::LIT-1 levels were higher in the proximal daughters nucleus of P7.p in 19/22 wild type worms, were equal between the P7.p daughter nuclei in 2/22 worms, and were higher in the distal daughter nucleus in 1/22 worms. C) WRM-1::GFP (*osEx158*, (Takeshita and Sawa, 2005)), is expressed in the VPC daughter nuclei (arrowheads) at extremely low levels. The fluorescence image shown here was exposed for 10 sec. and represents one of the rare cases expression was detectable. In each of the few cases where expression was detectable, it appeared higher in the proximal daughter nuclei of P5.p and P7.p.

Figure S4. ROR/CAM-1 structure and molecular lesions of mutations



CAM-1 protein structure depicting Ig (Immunoglobulin) domain, CRD (cysteine-rich domain), Kr (kringle domain), TM (transmembrane) domain, kinase domain and S/T (serine/threonine-rich) domain. Amino terminus is to the left. Molecular nature of *cam-1* mutant alleles is given below

IV-1

CHAPTER 4

Concluding Remarks

This thesis illustrates two mechanisms by which ROR proteins interact with Wnt signaling during intracellular communication. That ROR proteins can sequester Wnts was suspected since 2003 (Kim and Forrester, 2003) and is consistent with results from other studies (Billiard et al., 2005; Forrester et al., 2004; Hikasa et al., 2002). We showed, in Chapter 2, that expression of the membrane-tethered ROR/CAM-1 ECD between the site of Wnt expression and the recipient tissue behaves as a barrier and limits the amount of Wnt reaching that tissue. While this chapter served as confirmation of a previously suspected ROR function, it was extremely important because it allowed us to use ROR/CAM-1 over-expression as tool to inhibit Wnt signaling in our proceeding study.

CAM-1 over-expression enabled us to observe, in Chapter 3, VPC polarity in a background with reduced Wnt activity, which would otherwise be impossible due to the Vulvaless phenotype of Wnt mutants. By doing so, we found that unsignaled VPCs randomly face anterior or posterior and that Wnt/EGL-20 establishes a ground polarity where both VPCs face the posterior. We showed that CAM-1 acts as a receptor for EGL-20 during VPC orientation and that it functions in the same pathway as Van Gogh/VANG-1, a core component of the Planar Cell Polarity (PCP) pathway. While our study of Wnt sequestration by CAM-1 is complete, the interaction between CAM-1 and Wnt signaling during cellular orientation is just the tip of the iceberg.

There is an entire field devoted to the study of Planar Cell Polarity, which is the polarization of cells along the plane of the epithelium (reviewed by Seifert and Mlodzik, 2007; Zallen, 2007). PCP, the process, is regulated by PCP, the pathway, which involves the core components Frizzled, Van Gogh, Flamingo, Dishevelled, Prickle, and Diego, that are asymmetrically localized during cellular orientation. Established models of PCP

include the orientation of photoreceptors of the *Drosophila* eye and the orientation of hair cells of several systems; the *Drosophila* wing, mouse fur, and mouse inner ear.

Involvement of Frizzled and Van Gogh/VANG-1 in VPC orientation suggests that the PCP pathway might pattern the VPCs. As this would be the first description of PCP in *C. elegans*, it will be important to confirm or deny whether VPC orientation is similar to established models of PCP.

Many studies of PCP in other systems have focused on the subcellular localization of PCP pathway components, which are often localized to particular regions of the plasma membrane. Therefore, similar analysis should be performed in the VPCs. While, in other systems, these analyses are usually performed by antibody staining, our efforts here were limited to examination of fluorescent fusion proteins (data not shown: LIN-17::GFP and VANG-1::GFP). However, these transgenes were overexpressed and appeared bright on all surfaces of the cell, making any differences that may exist undetectable. Although antibody staining is impractical in *C. elegans*, fluorescence recovery after photobleaching, (FRAP), has been used successfully to detect subcellular localization differences of transgenes in *C. elegans* (Takeshita and Sawa, 2005). Therefore, this method, or others, should be used to analyze the localization of PCP pathway components in the VPCs. Involvement of the other core PCP pathway components in VPC orientation should also be investigated. Domain analysis of Dishevelled, which mediates different Wnt signaling pathways via different protein domains (reviewed by Wharton, 2003), is often used to distinguish the PCP pathway. Therefore, pathway-specific Dishevelled reagents should be constructed and tested for

their involvement in ground polarity. These results would enable stronger arguments for (or against) VPC orientation as a model of PCP in *C. elegans*.

Should the above experiments point toward VPC orientation as a PCP model, future studies will potentially lend great insight into the mechanisms of PCP. Although ground polarity has the disadvantage that it cannot be observed in the presence of refined polarity, there remain several advantages over other PCP model systems. First, the system can be reduced to two (or three) cells, creating great simplicity. Next, the individual cells involved can be observed and manipulated in live animals. Finally, and perhaps most importantly, we have identified the directional input (EGL-20) and are able to move its source.

The ability to perform genetic screens is one of the most powerful advantages of using a model organism like *C. elegans*. Because ground polarity is not observed in the presence of refined polarity, it would have been impossible to pick up ground polarity components in previous screens for VPC orientation. This is no longer a limitation. A genetic screen for defective VPC orientation should be performed in *Fz/lin-17* mutants that express EGL-20 in the anchor cell. Mutations that prevent EGL-20 from orienting P7.p toward the anchor cell (wild-type vulva) are likely to function in the ground polarity pathway. In contrast, a screen for suppressors of the *lin-17* mutant phenotype is expected to pick up both ground polarity pathway components and genes that act negatively downstream of *lin-17*. We advise against an RNAi screen because, in our experience, RNAi is not efficient in the VPCs. Since our results indicate that CAM-1 functions in the ground polarity pathway, the screen described above is also expected to pick up

components that act downstream of CAM-1. Therefore, our results set the stage for further investigations of CAM-1 signaling.

- Billiard, J., Way, D. S., Seestaller-Wehr, L. M., Moran, R. A., Mangine, A. and Bodine, P. V.** (2005). The orphan receptor tyrosine kinase Ror2 modulates canonical Wnt signaling in osteoblastic cells. *Mol Endocrinol* **19**, 90-101.
- Forrester, W. C., Kim, C. and Garriga, G.** (2004). The Caenorhabditis elegans Ror RTK CAM-1 inhibits EGL-20/Wnt signaling in cell migration. *Genetics* **168**, 1951-62.
- Hikasa, H., Shibata, M., Hiratani, I. and Taira, M.** (2002). The Xenopus receptor tyrosine kinase Xror2 modulates morphogenetic movements of the axial mesoderm and neuroectoderm via Wnt signaling. *Development* **129**, 5227-39.
- Kim, C. and Forrester, W. C.** (2003). Functional analysis of the domains of the C elegans Ror receptor tyrosine kinase CAM-1. *Dev Biol* **264**, 376-90.
- Seifert, J. R. and Mlodzik, M.** (2007). Frizzled/PCP signalling: a conserved mechanism regulating cell polarity and directed motility. *Nat Rev Genet* **8**, 126-38.
- Takeshita, H. and Sawa, H.** (2005). Asymmetric cortical and nuclear localizations of WRM-1/beta-catenin during asymmetric cell division in C. elegans. *Genes Dev* **19**, 1743-8.
- Wharton, K. A., Jr.** (2003). Runnin' with the Dvl: proteins that associate with Dsh/Dvl and their significance to Wnt signal transduction. *Dev Biol* **253**, 1-17.
- Zallen, J. A.** (2007). Planar polarity and tissue morphogenesis. *Cell* **129**, 1051-63.